October 16, 1965

Reference: Contract NAS 8-4012

SUBJECT: NAS 8-4012 Eleventh Quarterly Report

Dear Mr. Wood:

1. Current Status of Technical Work

This report outlines the progress made in the period July 15, 1965 through October 1, 1965 on NASA 8-4012 - "Design Criteria for Zero Leakage Connectors for Launch Vehicles". As in the previous quarter, efforts have been directed toward completion of four specific tasks:

a) Computerization of the design procedures for flanged and threaded tube connectors.

b) Advancement of the mathematical model for study of the interface sealing phenomenon.

c) Design, construction, and utilization of a leakage apparatus for experimental study of seals at high and low temperatures.

d) Design of a threaded tube connector incorporating the super-finish sealing surface principle.

The attached technical progress report explains in detail the extent of completion of each task. Briefly, programming of the flanged connector design procedure is approximately 50 percent completed; work has started (ahead of schedule) toward computerization of the threaded tube connector design. With regard to the mathematical model for the interface, efforts have been directed toward utilization of the newly expanded computer program and assessment as to whether the current area of contact/displacement curves gained from the program can be easily correlated with area of contact versus load curves gained from the literature. The leakage apparatus for experimental seal study has been completed, checked out, and used satisfactorily for three tests. The feasibility study toward use of the super-finished sealing principal has recently yielded an encouraging result in that electron beam welding of the flanges and unions to tubes has not caused excessive warpage of the sealing surface.

Digital computer programming of the flange connector design procedure is being accomplished by R. E. Smith, assisted by E. J. Le Clerc. Computer programming of the threaded connector design procedure is being accomplished by M. Ray. Advancement of the mathematical model for interface sealing investigations is being done by F. O. Rathbun, Jr., and H. Moore. Mr. J. Lanewski, assisted by Mr. R. White, is responsible for experimental

evaluation of seals at high and low temperatures. Design of the super finish sealing threaded tube connector is being accomplished by Mr. B. Weichbrodt.

2. Finances

Expenditures and commitments through September 26, 1965 were 41 percent of the authorization for the contract. Man hours expended through June 30, 1965 were 3378.2.

Very truly yours,

F.O. Rathbun, Jr.
Mechanical Engineer
Mechanical Technology Branch
Mechanical Engineering Laboratory
Research and Development Center
Building 37
Room 680
Tel. 374-2211 - Ext. 5-4972

TABLE OF CONTENTS

1. Computerization of Connector Design Procedures

1.1 Flange Check Design

1.1.1. Introduction

The purpose of this subtask is to provide a check design for flange connectors previously designed under conventional procedures and presently being used by NASA. These check designs will make use of the design procedures in the Separable Connector Design Handbook, Chapter 2, with any modification or addenda that may result from the utilization of other wrenching or bolting techniques. The size, type of service, and other information pertaining to operating conditions has been furnished by NASA, so that a comparison with the existing designs will be possible.

Since the flanged connector computer programs are in various stages of completion as indicated in section 1.2 of this report, the analysis sections of the computer program that have been written and debugged will be used wherever possible in the check designs.

1.1.2. Design Addenda

The designer of flange connectors is concerned with several parameters before proceeding with the detailed design. Some of these parameters may be of practical consideration, such as the type of nuts and bolts, wrenching techniques, or perhaps a more stingent requirement of weight minimization. The Design Handbook, Chapter 2, has optimized the design of flanged connectors for launch vehicles based on utilizing hardware (nuts and bolts) per specification ASA B18.2 and using box type wrenches the torquing tool. The sizes of the nuts and bolts, and the clearance requirement for the wrenching tool are input parameters used to make up Table 2.1 on page 2-15 of the Design Handbook. As mentioned in the footnote to this table, other wrenching techniques should be investigated. These other techniques may result in an appreciable size weight reduction of the connector.

To provide the designer with the above choices, additional tables have been derived based on other wrenching techniques. Table 1.1 was derived using hardware per specification ASA B18.2 (same as Table 2.1 page 2-15) and a hexagonal socket wrench per MS16581 as the torquing tool. Table 1.2 was obtained using internal wrenching nuts (12 point socket) and bolts thus providing a more compact design since the requirement of wrench clearance is eliminated. To appreciate the weight reduction that was obtained, flange connectors were designed using the various tables. The design procedures established in the Design Handbook were utilized and the connectors designed for the following conditions: (preliminary layouts only):

$p_{max\ oper}$ = 140 psi
Design Temp = $-297^{o}F$
Pipe size = 8.0 O.D. x 0.062 wall
Gasket thickness = 0.062 inch
Gasket width = 0.25 inch
σ yield (Flange Material) = 30,000 psi
σ yield (Bolts) = 40,000 psi
Effective seating stress for gasket = 1850 psi
Gasket stress for effective seating = 925 psi

Using the above parameters and the tables (Table 2.1 of Design Handbook, Table 1.1 and Table 1.2 of this report) three connector designs were obtained. These designs are shown in Figures 1.1 - 1.3 with their calculated weights. The results of the three designs are tabulated below.

Design	Weight	% Weight Savings over Design 1	Comments
1. Handbook	13.6#	--	Using Table 2.1 of Design Handbook (box wrench)
2. First Modification	11.0#	19	Using Table 1.1 (socket wrench)
3. Second Modification	7.4#	45	Using Table 1.2 (Internal wrenching Hardware)

As indicated, use of the internal wrenching hardware resulted in a weight savings of 45 percent. If a design requirement is the reduction of weight, the internal wrenching hardware can provide this and still utilize hardware which is available and not considered special.

Figure 1.2 shows that some additional savings are possible because unnecessary clearance exists between the nut and the bolt of the flange. An additional two percent savings can be obtained (47% total) by the perturbation of Second Modification (elimination of tolerance buildup).

The results obtained used the preliminary design section of Chapter 2 of the Design Handbook. Before the weight reduction is fully realized, it is necessary to perform the detailed stress analysis to confirm that the design is satisfactory.

1.1.3. Check Designs

The design addendum has shown that to realize appreciable minimization of weight, the internal wrenching hardware should be used. In the check

designs this hardware will be used (Table 1.2 of this report will be used instead of Table 2.1 page 2-15 of Design Handbook) so that weight optimization is achieved.

The check design inputs received from NASA indicate the use of a Naflex seal as the sealing mechanism. The use of this seal normally dictates the use of an integral flange with contact outside the bolt circle. Since the analysis section of the computor program for this type of flange has not yet been debugged, a trial check design will be done using no contact outside the bolt circle.

Two versions of this design will be examined. (See Figures 1.4 and 1.5.) The flange projections outside the gasket circle in Figure 1.5 are to retain the seal and not to provide an additional load path. As can be seen from the two figures, the resultant configuration will evolve from both stress considerations and seal space envelope considerations.

1.2 Computer Programs for Flanged and Threaded Connectors

1.2.1 Computer Program for Flanged Connector Design

1.2.1.1 Introduction

The digital computer program currently being written to optimize the design of flanged connectors can be broken up into five logical sections, interconnected as shown in Figure 1.6.

The entire effort during the second quarter has been directed toward the analysis section in an effort to obtain a working stress analysis program. This effort has been partially successful in that an operating program to analyse integral flanges with no contact outside the bolt circle has been obtained. The additions necessary to handle integral flanges with contact outside the bolt circle have been written but not completely checked out.

1.2.1.2 Integral Flanges - No Contact Outside the Bolt Circle

The portion of the analysis section which deals with flanges having no contact outside the bolt circle was checked out using the numerical example in the handbook on page 2-81. Considerable difficulty was encountered in trying to match the results presented, and a recheck of the handbook calculations uncovered some numerical errors in the sample problem solution. An errata sheet covering these correction will be prepared at a later date.

The checked out partial program for integral flanges is presently being used to obtain the stresses for the check designs in Task 1.1.

1.2.1.3 Integral Flanges - Contact Outside the Bolt Circle

The subroutines necessary to handle this type of flange have been written but have not been completely checked out. Specifically these subroutines are INIT 2 and FORCE 2. (See Figure 1.7.)

1.2.1.4 Loose Flanges

In order to obtain a complete working program for the integral flange type of connector in the shortest period of time, the programming of the subroutines applicable to the loose flanges has been postponed until after the integral flange program is completed and checked out.

1.2.1.5 Schedule

The estimated completion dates for various activities within this task are shown below. These can be considered as replacing the milestones as originally set up since the sub-tasks have been redefined.

Task		Begin	Finish
1.2.1	Flanged Connector Design Program	May 1, 1965	Feb. 11, 1966
1.2.1.1.1	Programming of Analysis for Integral Flanges Only	May 1, 1965	Oct. 15, 1965
1.2.1.1.2	Programming of Analysis for Loose Flanges Only	Jan. 10, 1966	Feb. 11, 1966
1.2.1.2	Programming of Design & Design Revision Section	Oct. 15, 1965	Dec. 24, 1965
1.2.1.3	Programming of Input & Output & Assembly of Entire Integral Flange Program	Dec. 13, 1965	Jan. 14, 1966
1.2.1.4	Documentation	Jan. 24, 1966	Feb. 11, 1966

There is no separate task for debugging as originally indicated, since the debugging of each subroutine or task is included in the time periods shown.

1.2.2 Computer Program for Threaded Connector Design

Since this entire threaded connector design is represented by combinations of equations, the greatest effort to date has been put into breaking the combinations down into logical sections and programming these sections as subroutines. Each subroutine can then be thoroughly checked using the example included in the Handbook design. One subroutine has already been written to solve the linear simultaneous equations and is now being checked. The

subroutine to evaluate the K_i constants has been written and is also being checked. The C_i coefficients are being analyzed for repetition of groups of variables so that computer running time can be reduced.

Figure 1.8 shows the presently planned flow chart for the threaded connector design program.

Subroutines Written -

SØEQU: - The coefficient matrix and the constant vector are reduced to upper triangular form and the dependent variables are solved for by back substitution. Each element is tested for zero before being operated on the save computing time. Time is further saved by having the matrix in common storage so addresses will not be set up each time the subroutine is used.

CALC: - To evaluate the K_i constants. Again computing time has been saved by use of common for the variables. Further more, the equations have checked for any repetition of groups of variables and these are calculated only once.

TABLE 1.1

Estimation of Bolt Size and Number of Bolts*

(1) (Total Bolt Area) (Bolt Circle Radius)			(2)	(3) Root Area			(4)	(4a)	(5)	(6)	(7) Flange Thickness Factor		
Fine	Coarse	8 Thread	Bolt Size	Fine	Coarse	8 Thread	Bolt Spacing**	Tolerance on (4) Including Bolt Head +0.050	Radial Eccen.	Edge Distance	Fine	Coarse	8 Thread
(in)	(in)	(in)	(in)	(in^2)	(in^2)	(in^2)	(in)		(in)	(in)	(in)	(in)	(in)
0.297	0.245	---	1/4	0.0326	0.0269	---	0.69	-0.06	0.40	0.35	0.150	0.136	---
0.416	0.361	---	5/16	0.0524	0.0454	---	0.79	-0.06	0.47	0.40	0.193	0.180	---
0.570	0.478	---	3/8	0.0809	0.0678	---	0.89	-0.06	0.50	0.45	0.233	0.213	---
0.692	0.605	---	7/16	0.1090	0.0953	---	0.99	-0.06	0.55	0.50	0.270	0.251	---
0.855	0.725	---	1/2	0.1486	0.126	---	1.09	-0.07	0.60	0.55	0.313	0.288	---
1.082	0.910	---	5/8	0.2400	0.202	---	1.39	-0.08	0.78	0.70	0.400	0.367	---
1.388	1.119	---	3/4	0.3513	0.302	---	1.59	-0.08	0.87	0.80	0.480	0.419	---
1.518	1.320	---	7/8	0.4805	0.419	---	1.99	-0.08	1.15	1.00	0.578	0.539	---
1.785	1.580	1.580	1	0.6245	0.551	0.551	2.19	-0.09	1.25	1.10	0.652	0.613	0.613
2.115	1.805	1.895	1-1/8	0.8118	0.693	0.728	2.41	-0.09	1.37	1.20	0.741	0.688	0.704
2.465	2.140	2.230	1-1/4	1.024	0.890	0.929	2.61	-0.10	1.47	1.30	0.830	0.774	0.790
2.78	2.320	2.545	1-3/8	1.260	1.054	1.155	2.85	-0.10	1.60	1.40	0.920	0.842	0.881
3.14	2.670	2.890	1-1/2	1.521	1.294	1.405	3.05	-0.11	1.69	1.50	1.007	0.927	0.964

* Table based on using nuts and bolts per specification ASA B18.2 and socket wrenches per MS16581.

** This spacing can be reduced with internal wrenching bolts or by use of special thin-wall wrenches. When this is done, an appreciable reduction in flange weight is possible since the bolt size can be reduced one or two sizes.

TABLE 1.2

Estimation of Bolt Size and Number of Bolts*

(1) (Total Bolt Area) / (Bolt Circle Radius)			(2)	(3) Root Area			(4)	(5)	(6)	(7) Flange Thickness Factor	
Fine	Coarse	8 Thread	Bolt Size	Fine	Coarse	8 Thread	Bolt Spacing**	Radial Eccen.	Edge Distance	Fine	Coarse
(in)	(in)	(in)	(in)	(in^2)	(in^2)	(in^2)	(in)	(in)	(in)	(in)	(in)
0.426	0.352	---	1/4	0.0326	0.0269	---	0.48	0.29	0.24	0.153	0.127
0.567	0.492	---	5/16	0.0524	0.0454	---	0.58	0.34	0.29	0.192	0.178
0.756	0.636	---	3/8	0.0809	0.0678	---	0.67	0.39	0.34	0.238	0.217
0.865	0.757	---	7/16	0.1090	0.0953	---	0.79	0.45	0.40	0.273	0.255
1.048	0.889	---	1/2	0.1486	0.126	---	0.89	0.50	0.45	0.317	0.291
1.380	1.162	---	5/8	0.2400	0.202	---	1.09	0.60	0.55	0.397	0.364
1.749	1.502	---	3/4	0.3513	0.302	---	1.26	0.68	0.63	0.477	0.442
2.040	1.771	---	7/8	0.4805	0.419	---	1.48	0.79	0.74	0.537	0.517
2.340	2.075	---	1	0.6245	0.551	0.551	1.67	0.89	0.84	0.630	0.593
2.445	2.080	---	1-1/8	0.8118	0.693	0.728	2.09	1.09	1.04	0.674	0.658
3.080	2.670	---	1-1/4	1.024	0.890	0.929	2.09	1.09	1.04	0.800	0.746
3.200	2.680	---	1-3/8	1.260	1.054	1.155	2.47	1.28	1.23	0.885	0.810
3.870	3.290	---	1-1/2	1.521	1.294	1.405	2.47	1.28	1.23	0.970	0.886

* Table based on using internal wrenching hardware (nuts and bolts).

** This spacing can be reduced with internal wrenching bolts or by use of special thin-wall wrenches. When this is done, an appreciable reduction in flange weight is possible since the bolt size can be reduced one or two sizes.

HANDBOOK DESIGN UTILIZING TABLE 2.1 Page 2-15

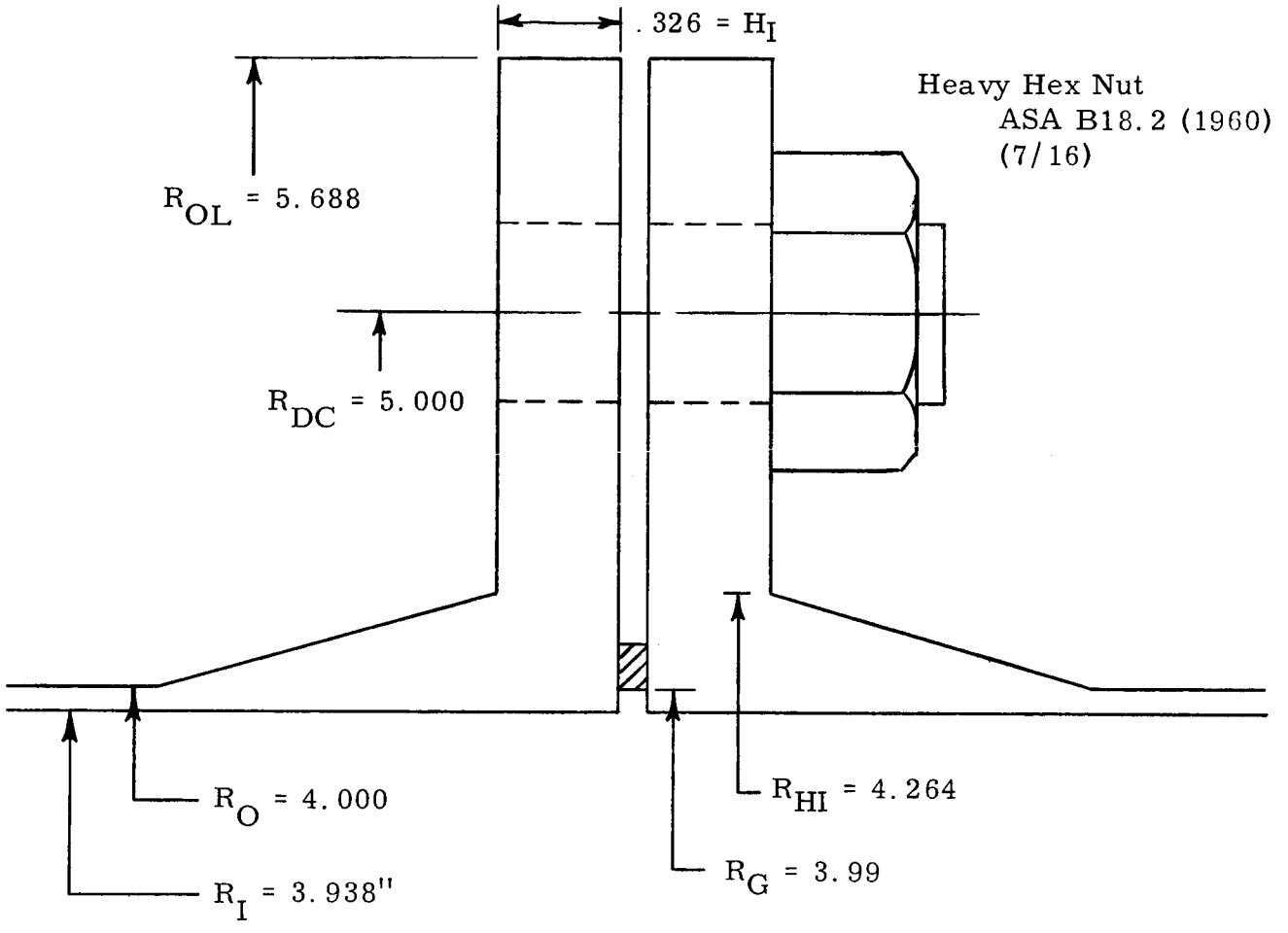

Weight - 13.6
Scale - 2:1

Figure 1.1

FLANGE DESIGN UTILIZING TABLE 1.1

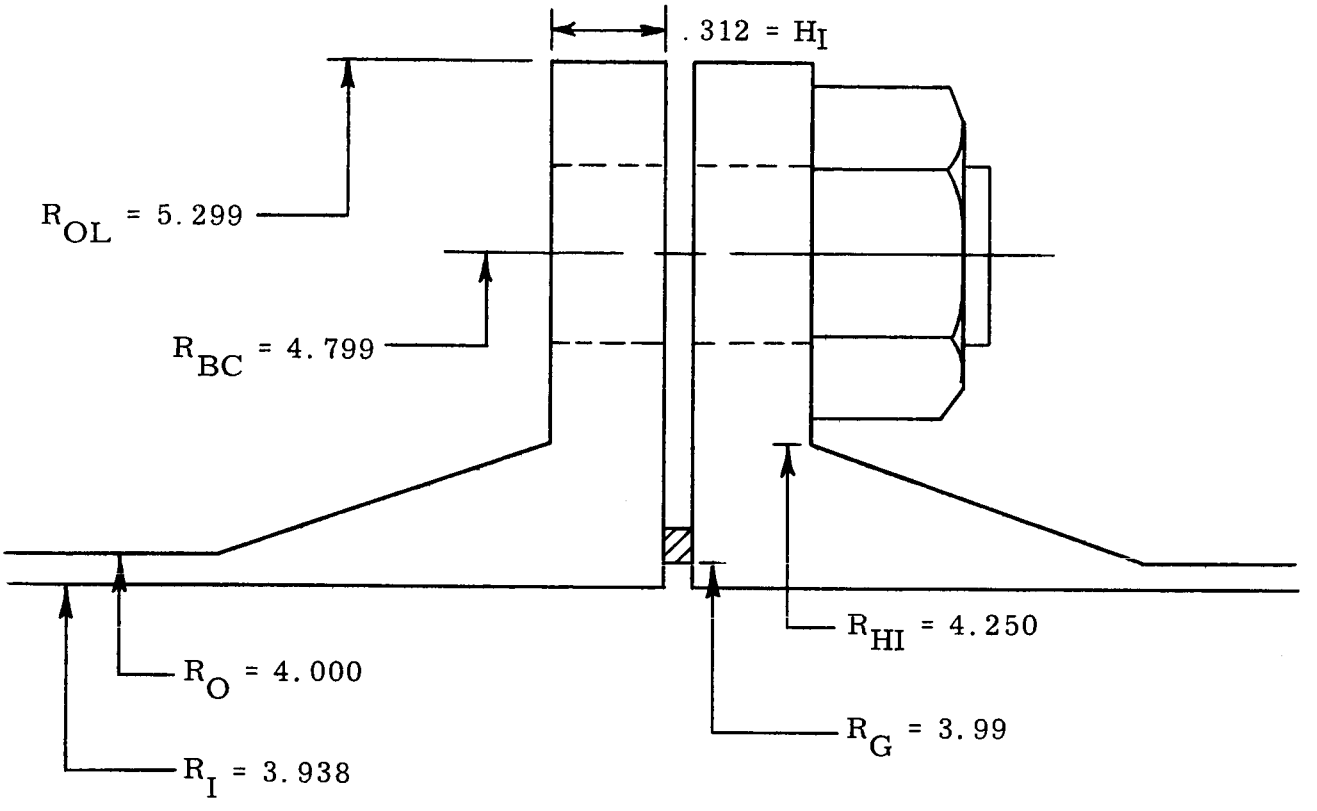

Weight - 11.03
Scale - 2:1

Figure 1.2

FLANGE DESIGN UTILIZING TABLE 1.2

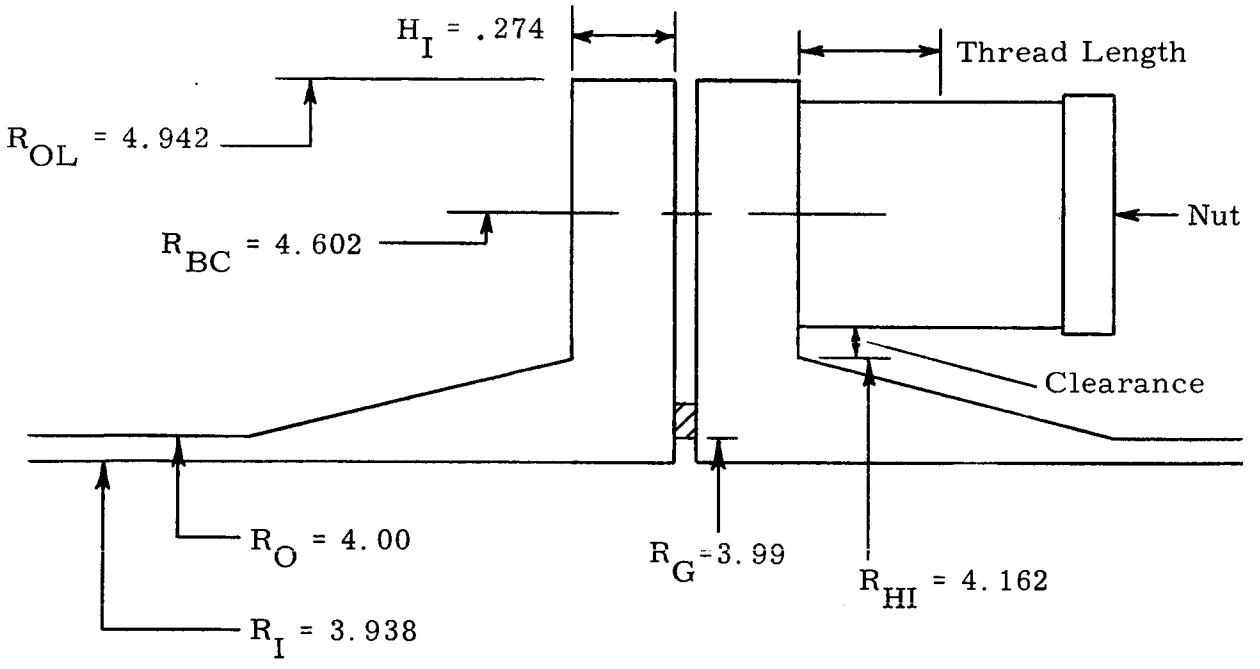

Figure 1.3

CHECK DESIGN "A" NAFLEX SEAL INSIDE SECONDARY LOAD PATH

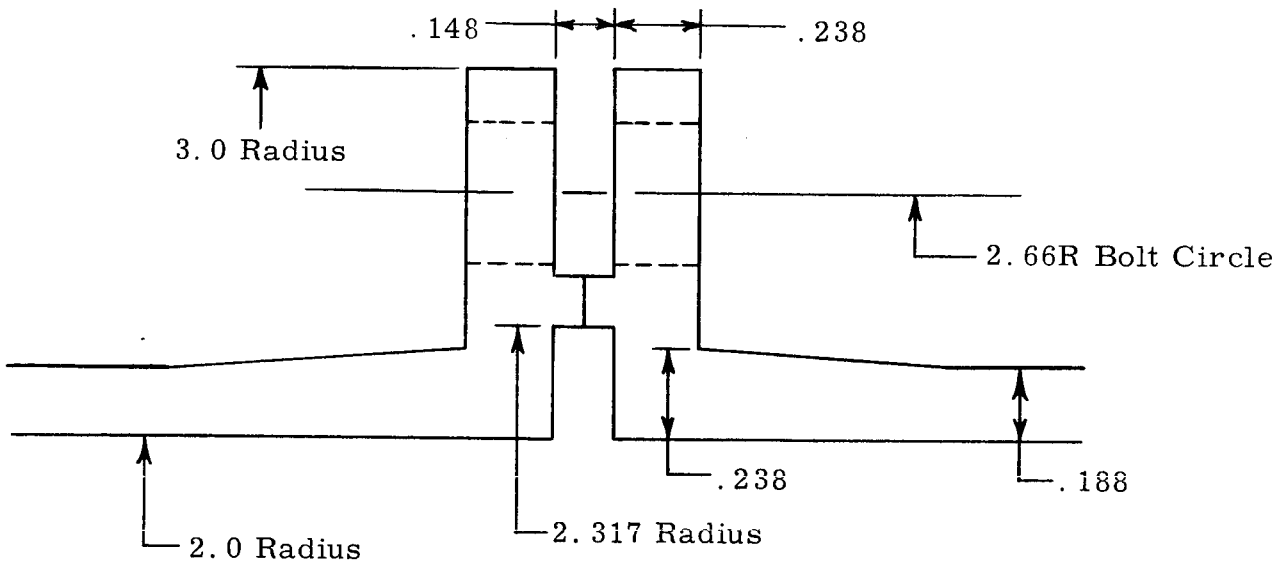

Scale - 2:1

Figure 1.4

CHECK DESIGN "B" NAFLEX SEAL OUTSIDE SECONDARY LOAD PATH

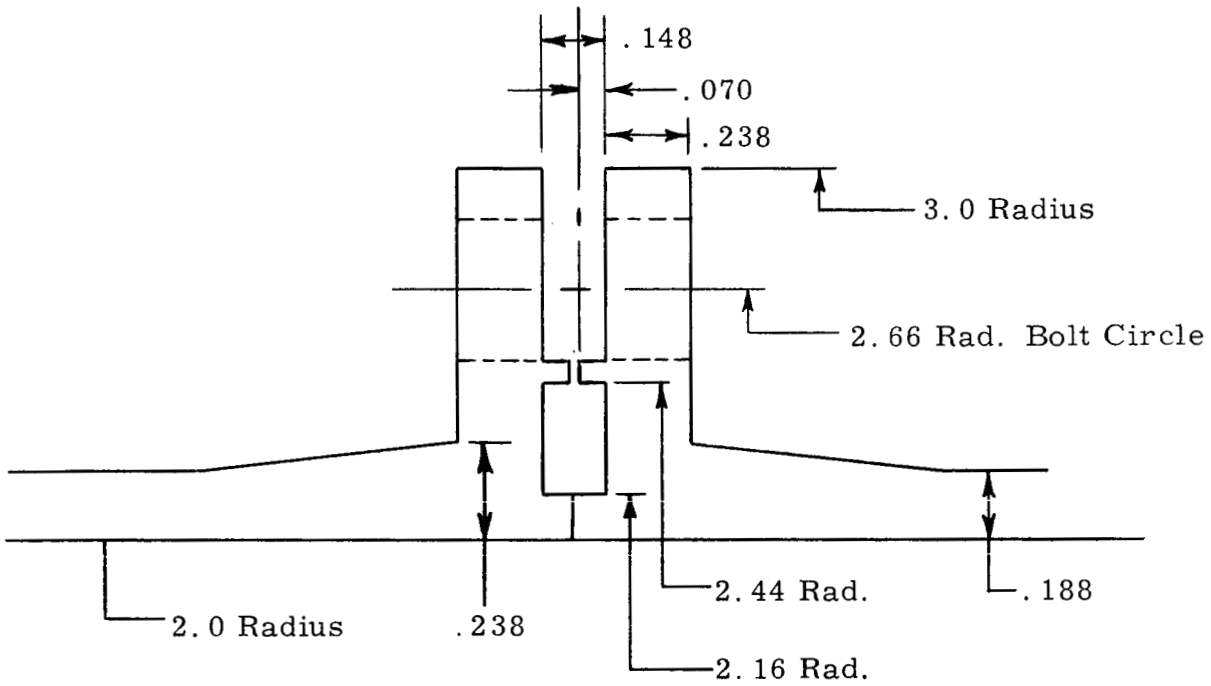

Scale 2 : 1

Figure 1.5

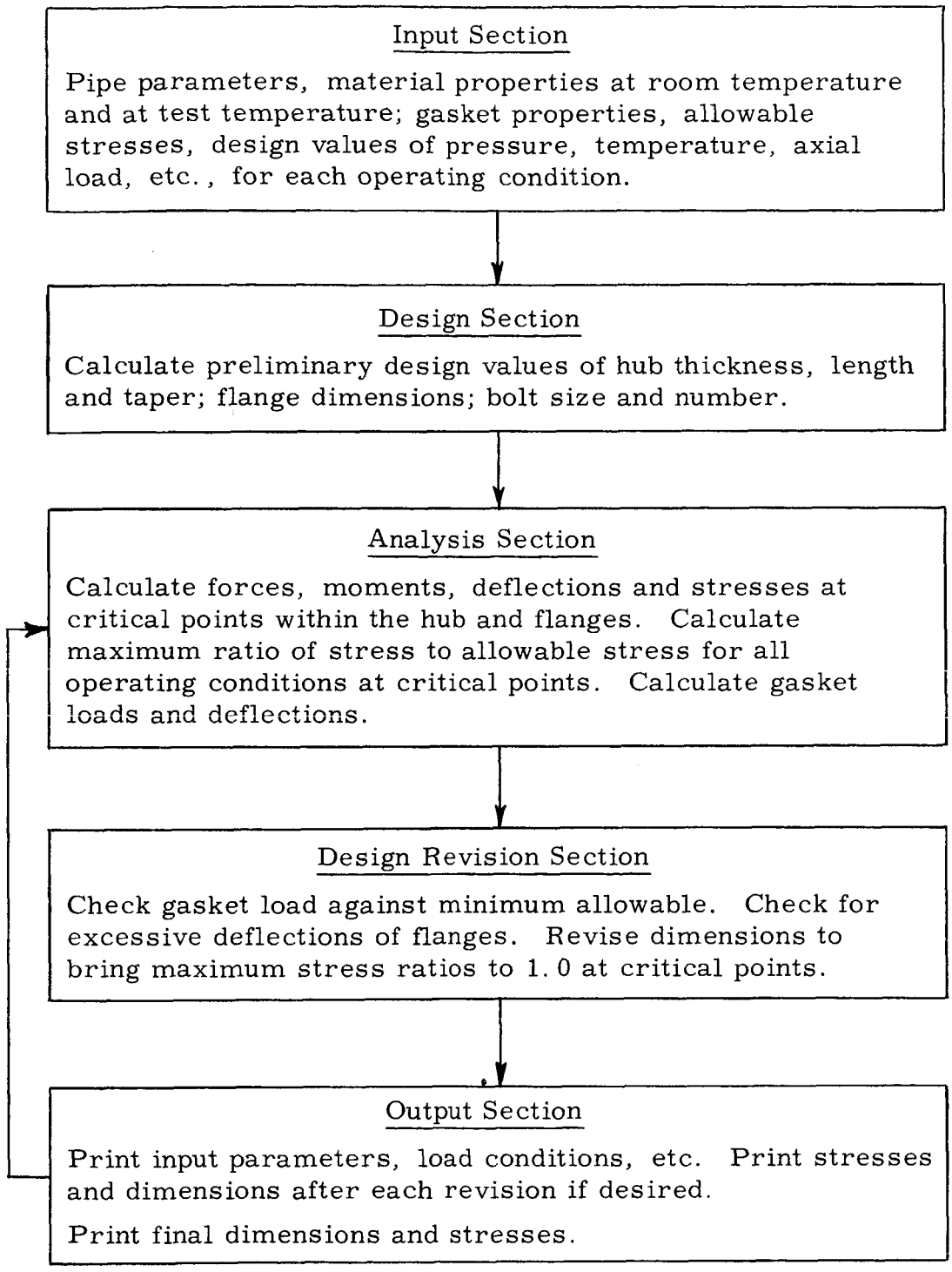

LOGICAL DIVISIONS OF FLANGED CONNECTOR PROGRAM

Figure 1.6

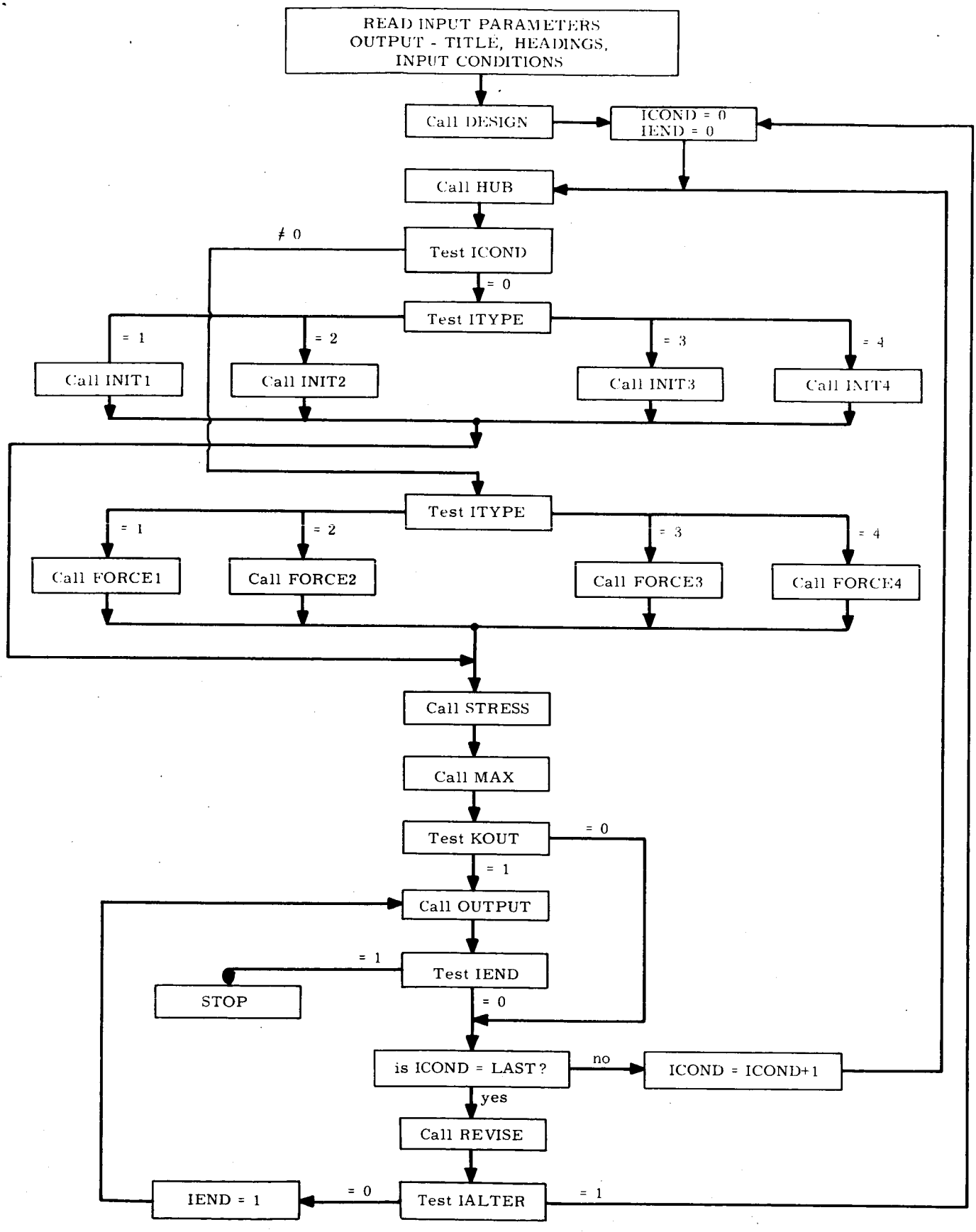
READ INPUT PARAMETERS
OUTPUT - TITLE, HEADINGS,
INPUT CONDITIONS
Call DESIGN
ICOND = 0
IEND = 0
Call HUB
≠ 0
Test ICOND
= 0
Test ITYPE
= 1
= 2
= 3
= 4
Call INIT1
Call INIT2
Call INIT3
Call INIT4
Test ITYPE
= 1
= 2
= 3
= 4
Call FORCE1
Call FORCE2
Call FORCE3
Call FORCE4
Call STRESS
Call MAX
Test KOUT
= 0
= 1
Call OUTPUT
= 1
Test IEND
STOP
= 0
is ICOND = LAST?
no
ICOND = ICOND+1
yes
Call REVISE
IEND = 1
= 0
Test IALTER
= 1

Figure 1.7

THREADED CONNECTOR DESIGN PROGRAM

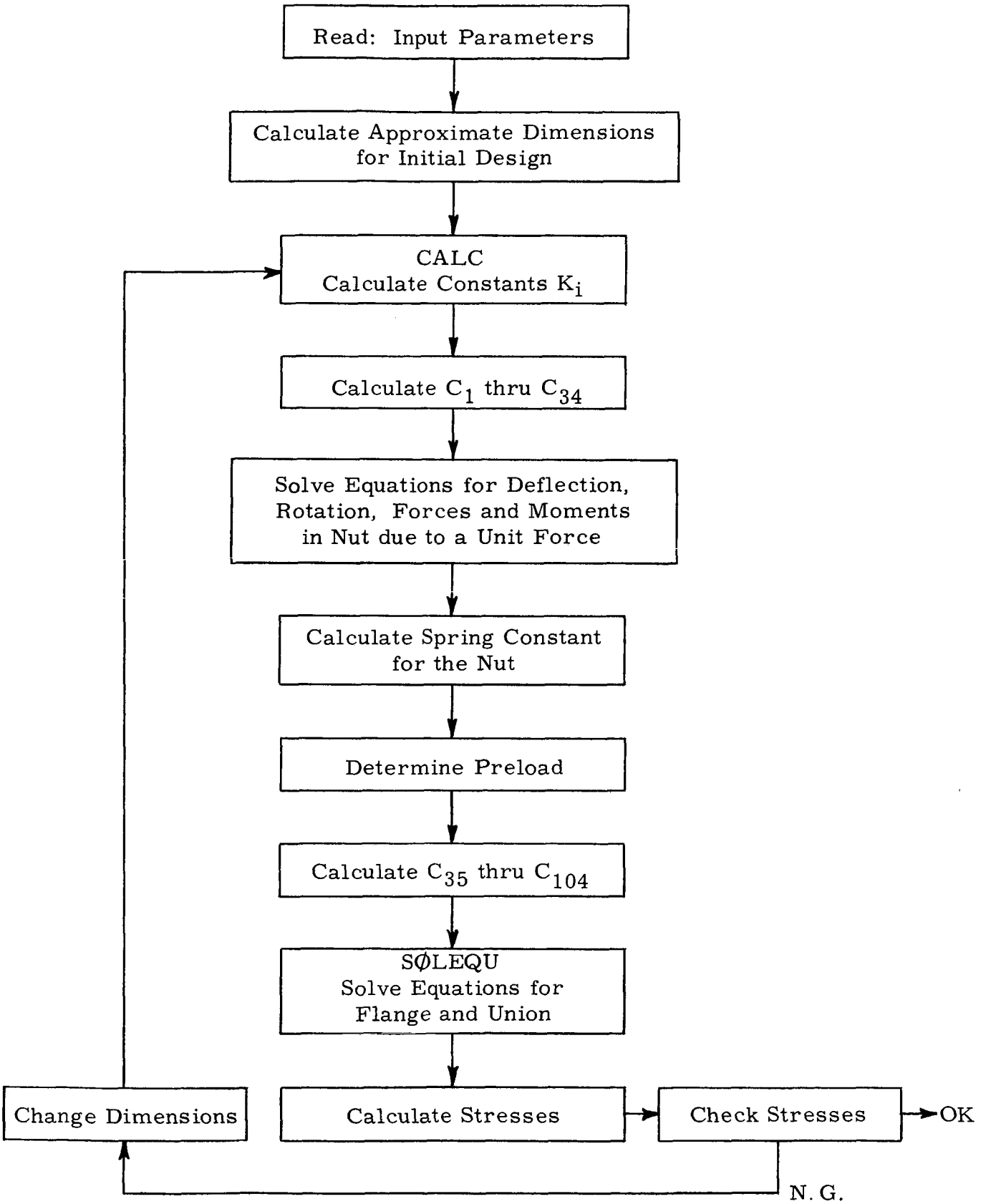

Figure 1.8

2. Mathematical model of interphase sealing phenomenon

2.1 Introduction

In the last quarterly report (quarterly report No. 10, July 15, 1965), several modifications to the computer program existing at the end of Phase III were stated as being necessary for use of the computer concept in a realistic fashion. Those modifications, six in number, have been successfully added to the program and have been used during this reporting period. Briefly, the modifications are:

a) Addition of a periodic or arbitrary nature to the asperity distribution in a direction perpendicular to the potential leak path direction.

b) Addition of a periodic or arbitrary nature to the surface in a direction parallel to the potential leakage flow.

c) Addition of an arbitrary or periodic nature to the surface at some angle other than parallel or perpendicular to the natural leak flow direction.

d) Mating of such a generated surface with another generated surface (rather than merely with a flat plate).

e) Addition of a larger number of possible height increments to the surface, namely extending the computer programming from 22 increments to 120 increments.

f) Increase in the plane area of the surface from 50 by 100 to 100 by 200 units.

With these modifications successfully included in the computer program, efforts have been directed towards evaluation of the computer program with regard to realistic growth of area of contact and assessment of the area of contact-displacement curves gained with an eye toward extending this relationship to an area of contact—load relationship.

2.2 Review of computer program concept

The goal of the present effort is to describe adequately in a digital computer system two surfaces comparing favorably to surfaces manufactured by real machining or grinding techniques, to mathematically force the two surfaces into contact, to realistically cause the asperities to deform and the leakage paths to become reduced, and to assess the probability of leakage existing in such a system. Where possible, probability techniques will be called upon to accomplish the total program. A use of the resultant program will be to establish the effect, by repetitive use of the mathematics, of the effective width, surface finish, material properties, and other parameters on

the sealing phenomenon. It is intended that the computer program will replace extremely large amounts of testing of sealing surfaces.

At the present time, mathematical surfaces having the same probability distribution of asperity heights found in real surfaces have been generated. Non-random surface properties have been added, but to date, not used in a realistic fashion. By mating such surfaces together, utilizing the Abbott's bearing assumption, it has been possible to "watch" the growth of areas of contact and the diminution of possible leak paths. By use of a maze threader, the point at which leakage is quelled is noted. To date, the surfaces have been put together incrementally, without consideration of the loads required. As yet, material properties have not entered the calculations.

It is intended that, upon accomplishment of realistic surface generation and the mating thereof, leakage calculations through resulting passages will be done allowing the entire material deformation-leakage problem to be solved via computer techniques. It is possible, however, should the metal asperity deformation problem be solved, that leakage calculations may not have to be accomplished in order to gain beneficial results from the program. It may be possible, with use only of the present maze threader, to produce graphs relating the various seal parameters to probability of leakage.

To date, the major concerns are the realism of the present computer program and the incorporation of material properties into the system.

2.3 Calculated surfaces mated

To evaluate the modifications made in the computer program, six different combinations of sealing surfaces have been mated together. Using ten increments of height for a random distribution of asperities as gained from the inputs necessary for lapped surface generation, and superimposing on this a periodic function utilizing six increments of height, it has been possible to generate surfaces having the possibility of 16 increments of height. Such a surface by no means exhausts the capabilities of the computer program, but it is adequate for evaluating the modifications. The periodic function used is that of a wedged shaped wave form utilizing a 1 to 1 height-lateral distance relationship. The resultant wave form is shown in Figure 2.1. Basically, this periodic function is put into the computer program such that the ridges caused by this function run perpendicular to the leak flow direction.

The final surface asperity distribution as viewed in a direction perpendicular to leak flow direction does not necessarily resemble the wedge shape shown in Figure 2.1 since 10 increments of height are used for the random distribution. (The total fraction of possible asperity heights utilized for the periodic wave form is only a bit over 1/3 of the total.) Thus, the resultant form should hint at periodicity but be dominated by the random nature.

Using the above described basic surface generation, six separate matings have been accomplished. To describe the six uses, the simplest technique is to ignore, for the moment, the random nature of the surfaces. Showing only the wedge shaped characteristic of the surface, the first three matings are described in Figure 2.2.

It is to be noted that the lower surface has been generated to a width of 80 units. The upper surface with which it is to be mated is 50 units wide. This disparity in width allows the upper surface to be displaced laterally up to 30 units. In the cases shown herein, it would be meaningful to utilize only six possible displacements (one unit at a time) in that further displacement would produce repetitive cases. Herein, cases 1, 2, 3 are displacements of zero, three, and six units. The resultant matings allow:

1) direct peak to peak mating,
2) a partial peak to peak mating,
3) completely out of phase mating such that the resultant surfaces, when mated, exhibit only their random characteristic.

Cases 4, 5, and 6 utilize the same asperity characteristics on both surfaces if viewed in any plane perpendicular to the leak flow direction. The cases employ the same three translations of the top surface to the bottom. However, in order to assess a case where the asperities are not exactly parallel (as for two machine surfaces, each having a lead) the top surface has been modified so that its asperities run (in a digital manner) at an angle to the periodic asperities on the lower surface. Figure 2.3 illustrates the surface generation used. As can be noted, the upper surface has, with regard to its periodic asperities, a 3 to 1 slope with respect to the lower surface asperities. Because of the digital nature of the surfaces, the entire asperity ridge cannot be rotated at an angle. Rather, it is necessary to advance parallel for three units, then to translate the next three units to the right "one", and the following three units again to the right "one". In this manner, the general trend of asperity peaks are not parallel but cross at an angle, in this case that angle indicated by a 3 to 1 slope of the upper surface. In this case, where the actual interface surface is only 100 by 80 units, the digital nature of the surface generation would be considered serious. However, should 200 by 300, or even larger areas be used, then this deviation from realism is not considered to be too serious.

For each case, both the upper surface and the lower surface are printed out individually on computer sheets. Figure 2.4 illustrates the system for height representation. Each number on the print out sheet represents, for the original surfaces, a height from a reference line which is placed one unit above the peak asperity height. The heights for the original surfaces are so specified that no rotation or inversion of the surfaces is necessary to place one surface upon the other. The initial mating print out places one surface upon the other and subtracts from the sum of the heights the two units representing

the reference line distances. Generally, the initial print outs should evidence extremely few areas of contact. Thereafter, the surfaces are brought together, one unit at a time, and the resultant number represents the sum of the original two heights as measured from the reference lines minus two minus X, X being the number of units through which the top surface has been displaced toward the bottom. At any location on the surface, should the value of the digit listed be either zero or negative, it is not printed and the omission indicates contact between the two surfaces.

In that, for the first mating print out, a possibility of 28 heights exist (and only 10 numerical digits exist) letters are used for indications of heights. Figure 2.5 shows the scheme used. It is to be noted that there is a difference in the printing of a zero and the letter O. The zero symbol has vertical sides, whereas the O is somewhat rounder in configuration.

In that a surface having 100 by 80 units takes two computer sheets to describe, herein only half of each surface or gap distribution is shown, namely the 50 x 50 area. A surface as illustrated herein has a leakage path running across the page and the tangential direction running vertically (as the numbers are read). In that a total description of all six cases entails the use of 160 different illustrations, only selected samples are shown in this report. The original surfaces, being completely numbered, are somewhat uninteresting in that the significant aspect of the computer sheets is the visual representation of areas of contact. Figures 2.6 through 2.11 show the gap distribution and areas of contact for case 1 in the conditions of displacements 1, 3, 5, 7, 9, and 10. In the latter case, sealing is yet to be affected. Only the lower half of each total surface is displayed. At the bottom of each illustration, the statement "there are XX.XXXX% zeros" indicates a per cent area of contact existing at the degree of mating. The remaining symbols "I = , J = , N = , M = ", indicate the size of the array and the point to which leakage has advanced.

To illustrate the effect of slipping the top surface over three units with respect to the bottom surface (therefore mating the surfaces in a manner other than peak to peak), Figures 2.12 through 2.16 show the gap and area of contact distribution for the fourth, sixth, eighth, tenth, and twelfth levels of displacement. Even at the twelfth displacement, sealing has not yet been effected, being effected at the thirteenth displacement.

Figure 2.17 shows the third set of surfaces in the eleventh displacement, displayed only to show the randomness of the area of contact distribution.

The results of mating the fourth set of surfaces, those involving the periodicity of the surfaces at an angle rather than parallel, are shown in Figures 2.18 through 2.24, the second, fourth, sixth, eighth, tenth, twelfth, and thirteenth displacement respectively. The thirteenth displacement resulted in the leakage being quelled.

As one might expect, when the two periodic parts of the surfaces are at an angle other than zero, slipping one surface three units with respect to the other should not result in a significant change in either the growth of area of contacts or the point at which leakage is quelled. Statistically, the two results should be very much the same. As it turned out, the results were almost identical the leakage being quelled at the fourteenth displacement in test Number 5 as opposed to the thirteenth in test Number 4. When the growth of areas of contact with displacement were plotted, the two tests were identical.

While Case 6 is not illustrated herein either, one would expect that it also would be very similar to the fourth and fifth test. Leakage was stopped at the thirteenth displacement in Case 6. Only a small change in the area of contact-displacement curve from cases 4 and 5 resulted.

2.4 Theoretical area of contact considerations

The computer program, thus far, yields area of contact as a function of distance between two reference lines, one imbedded under each surface. The area of contact can be plotted as a function of the number of increments used in bringing the surfaces closer together. While it may be assumed that each increment is an equal length, such is not necessary. Nothing in the computer programming necessitates the increments being equal. In fact, in earlier, non-periodic tests, the increments were chosen to be other than equal.

It is ultimately necessary to relate the area of contact as a function of load rather than space between reference lines under each surface. Load, or stress, can be measured and is applied to a real seal. The distance between two reference lines under the surfaces is related to load through the compliance or stiffness of the surfaces. Such, generally, will not be known due to the complexity of the problem, although some studies for particular surface finishes have been made.

It is of interest, however, to test the area of contact-displacement curves which might be gained from these computer runs with possible area of contact-load curves. In order to accomplish this, one can assume that the displacement increments are equal, and that each increment of displacement is caused by the same increment of load increase. Prior to accomplishing this, however, let us review what might be expected with regard to area of contact-load response.

For two rough surfaces in contact, the area of contact increase with load is caused by two separate phenomena, first the increase in number of contacts and secondly the increase in area of contacts already attained. For two surfaces with several contact points between them, and the local stresses at each asperity being in the plastic range, area of contact is generally believed to increase linearly with load. Based on a nominal area, the area of contact

can then be considered to be linear with applied stress. Hence, we can expect, at least initially (above the elastic stress range on each single encounter), that our area of contact would increase linearly with load. This is tantamount to saying that, once the assumption is made that distance increment is caused by equal increments of load, the area of contact would grow linearly with displacement increment on the computer sheets.

However, it is acknowledged experimentally that for large loads, where the true area of contact becomes nearly the same as the nominal area of contact, a linear relationship between area of contact and load would not be realistic. One would expect naturally that the area of contact would be approached asymptotically with increase in load. Even at extremely high loads, certainly some portions of the surface would not mate together absolutely. Such has been shown to exist experimentally in tests conducted on real seals under this program. It has been suggested by Finne and Shaw (The Friction Process In Metal Cutting, Transactions of the ASME, November 1956, pp. 1649-1653) that the area of contact versus load curve follows an exponential curve given by:

$$\frac{A_r}{A} = 1 - e^{-BN} \qquad (1)$$

where A_r is the real area, A is the nominal area, e is the Naperian base, B is a constant, and N is the load. While small loads would yield nonlinear area of contact versus load curves, the deviation from linearity would be small and such an equation would allow an asymptotic approach to one of the ratio A_r/A.

Hence, two possible curves might be expected, linearity over the lower range of load, and an asymptotic approach to 100 percent area of contact for high loads, which might be represented by equation (1).

2.5 Results of area of contact--load-displacement relationships investigation

If the growth in area of contact is plotted versus increments of displacement for all of six test cases, the curves shown in Figure 2.25 and 2.26 result. In both figures, it will be noted that the curves are anything but linear for very low increments of displacement, say up to approximately eight units. However, from approximately eight to 14 units, the curves are exactly linear, then followed by an asymptotic approach to 100 percent area of contact. Of course, with a digital representation, a true asymptotic finality to the curves is impossible; at some particular level of displacement, 100 percent area of contact is achieved.

At this point, it is judicious to question the validity of the mathematical model at early stages of displacement. For the first few increments of displacement, very few actual contact areas have been produced, as is shown in the computer print outs displayed herein. Thus, it is certainly unrealistic to expect that a load increment equal to one producing a displacement, say between

12 and 13, would be equal to the displacement, say between four and five. Thus, it is fitting to rule out the early part of the data and test the results merely from the point of linearity forward. In Figures 2.25 and 2.26, the linear portions of the curve have been extended downward until they intersect the zero area of contact line. In this condition, however, it is difficult to compare the curves one against the other. Thus, all six curves have been replotted in Figure 2.27. In Figure 2.27, all curves are then linear at the outset and all respondseemingly asymptotically towards 100 percent area of contact for high increments of displacement.

It is interesting to note the similarities and differences among the six curves. For example, as the tests progressed from one to two to three, it became easier and easier to build up areas of contact per unit displaced. One would expect this. When the two periodic functions are exactly opposite one another, then the lowest points in the surfaces would be immediately opposite one another, and initially the greatest gap height would exist. Hence, more increments of displacement would be required to bring those final points into contact. Comparing curves 4, 5, and 6, it is noticed that 4 and 5 yield identical curves, too close to be plotted separately. Curve 6 is so close that it makes separate plotting almost impossible. Thus, we have further confirmation, in the case of the angled periodicity, that sliding of the surfaces makes absolutely no difference as far as growth of area of contact.

With regard to leakage, the following observation can be made. In general, the area of contact necessary for the angled periodicity cases, 4, 5, and 6, is greater than for the parallel cases, 1, 2, and 3. The location on each curve where leakage was quelled is marked by an X in Figures 2.24, 2.25, and 2.26.

Table 2.1 tabulates the various displacement/area of contact relationships. It can be noted that five of the six cases, 1, 2, 4, 5, and 6 all sealed at approximately the same displacement (load) with only case 3 sealing at a much lower load (incidentally, the test which had no periodic nature to it). Were increment of displacement to be proportional to load, then one would expect that the load for sealing in cases 1, 2, 4, 5, and 6 would be approximately the same, although the area of contact associated with leakage stoppage in each case would be different. This fact is not completely compatable with logic.

In order to assess whether the load/area of contact curve as described by an exponential curve is reasonable, Figure 2.28 has been plotted, showing the results from test 3 along with an exponential curve, matching the computer curve at an area of contact of 78 percent. In that only one constant is present in the exponential equation, closer relationships between the two curves cannot be expected. In that the exponential curve is an approximation anyway, and has nothing to do with the physical situation, this agreement is considered reasonable.

Of the two comparisons, the linearity found in the computer curves is much more encouraging than the proximity between the computer data and an exponential curve.

From Table 2.1, the extent of the actual linearity existing in the computer data can be seen from column 8. The number in parentheses is the percentage of area of contact which exhibited linearity. It can be seen that over 40 percent of each curve was linear with respect to displacement in each case. The range of linearity, the per cent area of contact at which linearity began and which it ended, is also plotted in the same column. Column 7 in Table 2.1, the slope of the lines, defined here as the per cent area of contact divided by the digital increments required to attain that per cent area of contact, is akin to the compliance or stiffness of the surface. The steeper the slope, the easier to attain mating. It is noted that case 3 yielded the steepest slope, with test 1 yielding the lowest slope. It can also be noted, as can be seen from the graphs, that the slopes in tests 4, 5, and 6 are nearly identical. Physically, this is quite plausible. It would be much easier to produce complete mating on two surfaces that are generally flat with low relief scratches (as in the lapped case) rather than two surfaces having asperity distribution such as wedges.

2.6 Future plans

At present, it is planned to continue with the experimental computer programming as has been described herein in order to make as realistic as possible the mating phenomenon in a mathematical sense. The question as to the excess material which is presently "thrown away" by use of the Abbott's bearing curve will be attacked. A means of bringing material properties into the program will be explored. No major attempts at calculation of flow in the gaps existing in any of these surfaces will be made until it is assured that the mating of surfaces is satisfactorily realistic.

Also, efforts are being undertaken to generate surfaces directly from Talysurf traces rather than development of surfaces via probablistic or periodic function techniques. Through use of a Talysurf programmed to move longitudinally and displace laterally, coupled with a digital accumulation of data which can be stored on punched tape and later committed to a digital computer, it should be possible to accomplish all that has been accomplished to date with regard to mating on surfaces gained directly from pieces of metal rather than mathematics. The adaptation of a Talysurf to such use has been accomplished by the Burndy Corporation of Norwalk, Connecticut. Attempts at utilization of this equipment are being made.

TABLE 2.1

RESPONSE OF SIX COMPUTER SEALING SURFACE COMBINATIONS

(1) Combination of Sealing Surfaces	(2) Displacement To Seal	(3) Area of Contact To Seal %	(4) Displacement To 100 % Area of Contact	(5) Corrected Displacement To Seal	(6) Corrected Displacement To 100 % Area of Contact	(7) Slope (% area of contact) / (digital increments)	(8) Range of % Area of Contact of Linear Slope (approximately)
1	12	55.38	27	7.35	22.4	7.5	27-73, (46)
2	13	66.8	25	6.9	18.9	9.68	23-65, (42)
3	11	44.68	22	3.2	14.2	13.95	17-73, (56)
4	13	68.62	24	6.4	17.4	10.7	28-72, (44)
5	14	77.06	25	7.25	18.4	10.7	28-72, (44)
6	13	65.92	25	6.25	18.2	10.52	31-73, (42)

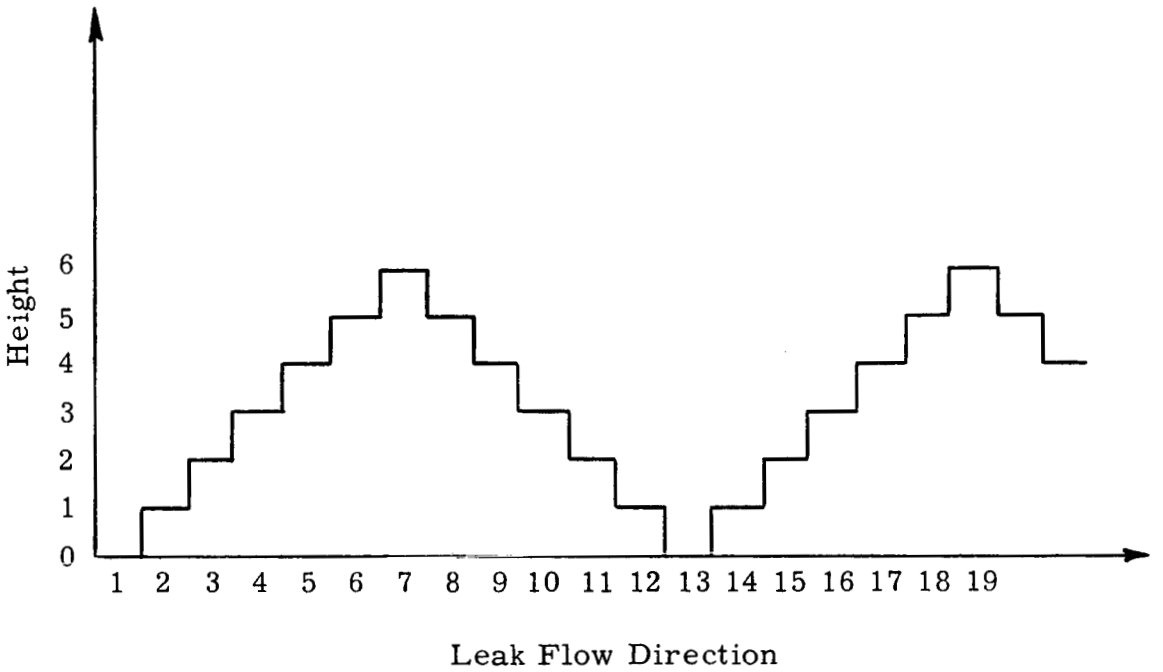

Figure 2.1. Periodic wave form used.

1) Peaks "in Phase"

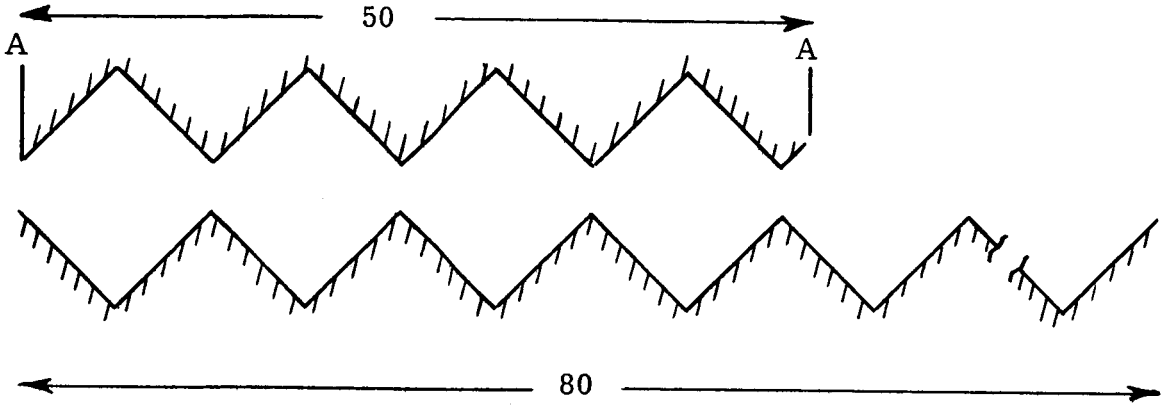

2) Peaks Translated 3 Units out of Phase

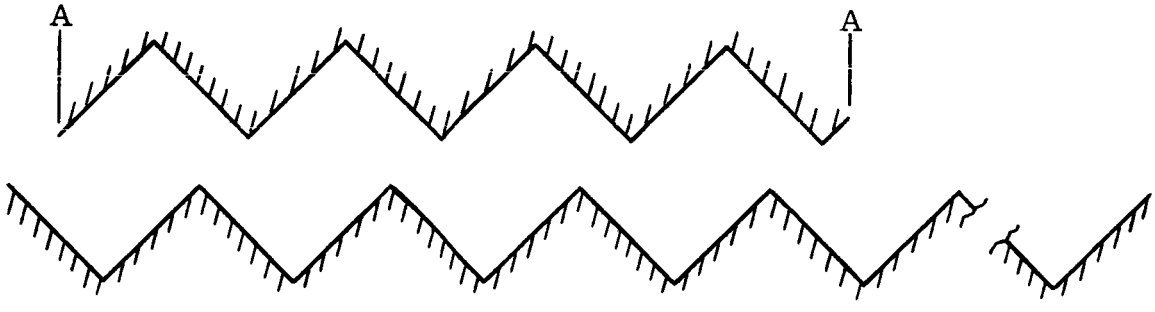

3) Peaks "out of Phase" - Purely Random

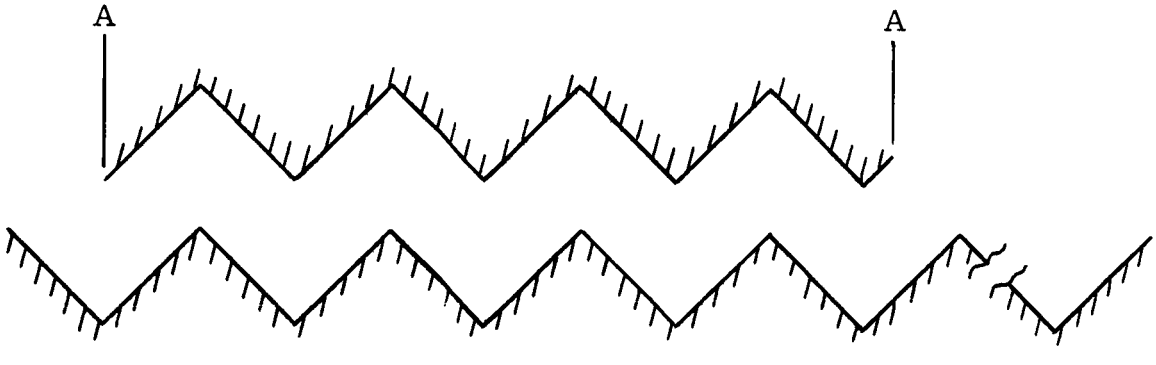

Figure 2.2. Cases 1, 2, 3 - Parallel Periodic Patterns Perpendicular to Leak Flow Direction.

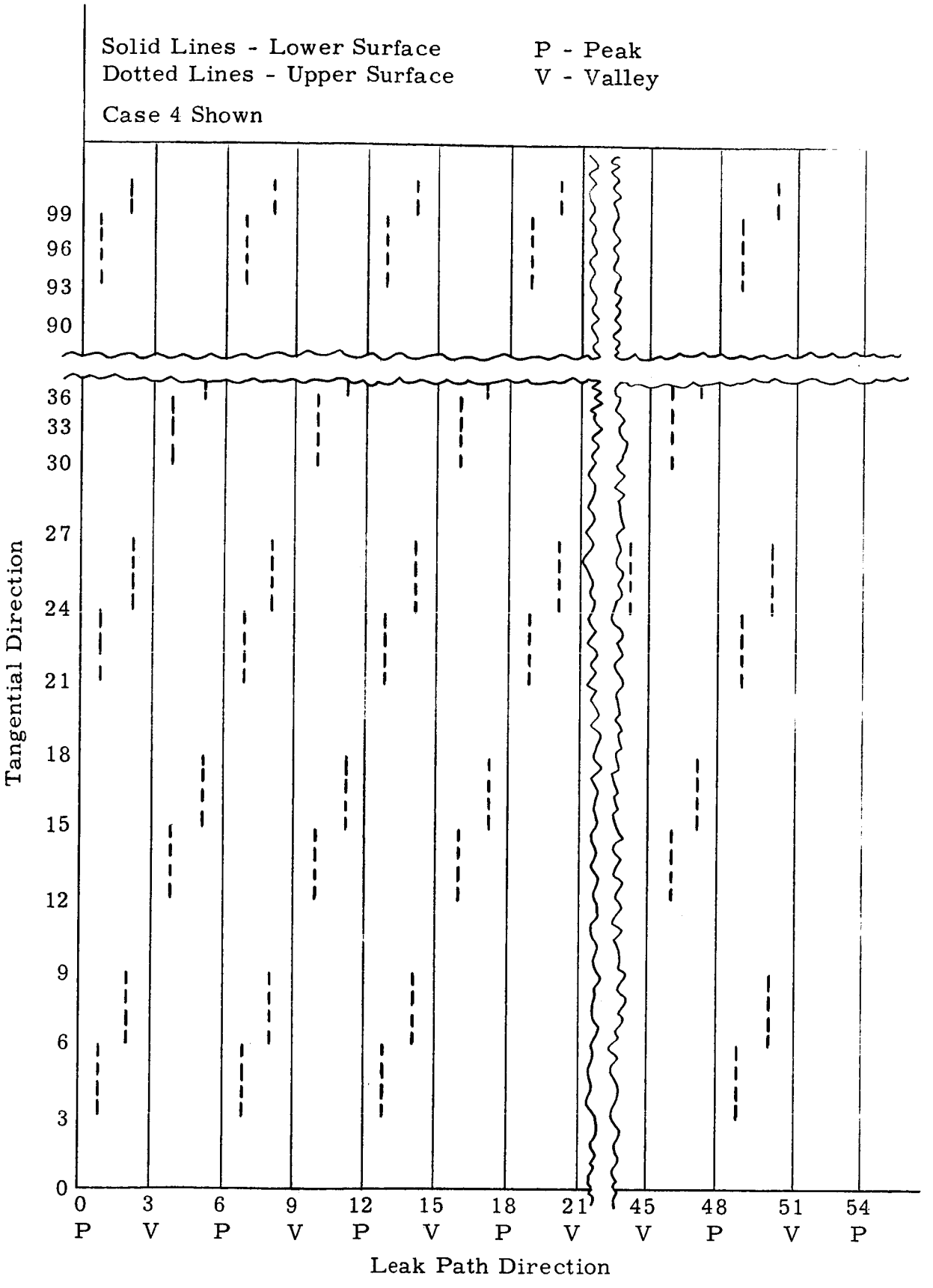

Figure 2.3. Periodic Surfaces at an Angle, Cases 4, 5, 6.

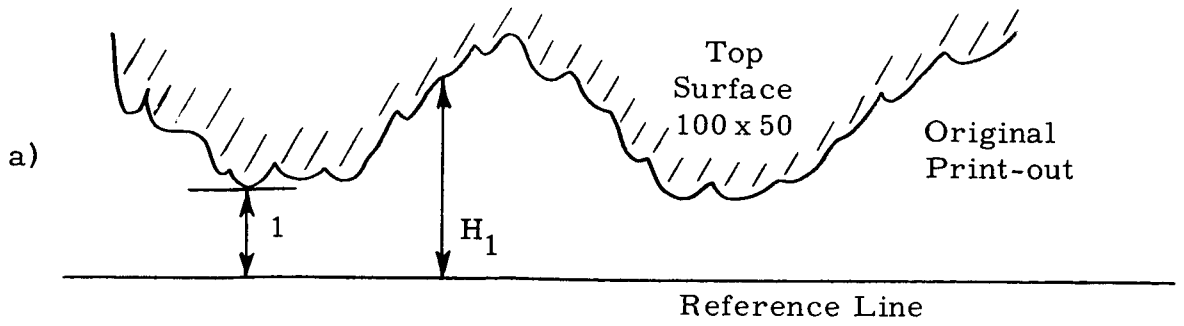

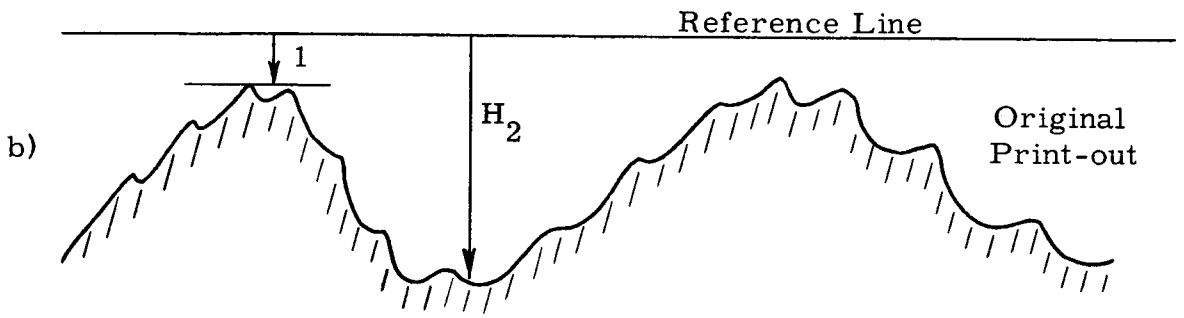

c) Firt Mating Print-out

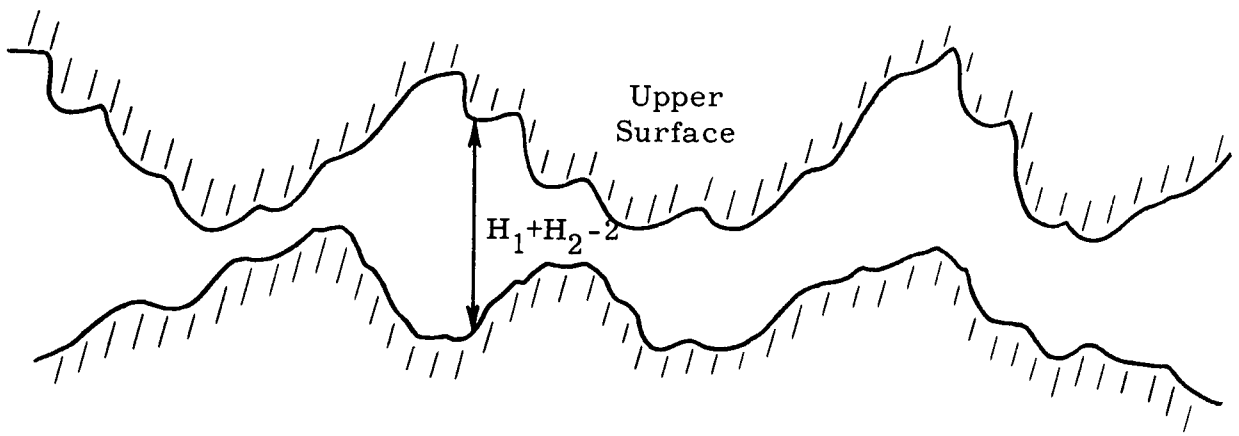

d) Later Mating Print-outs

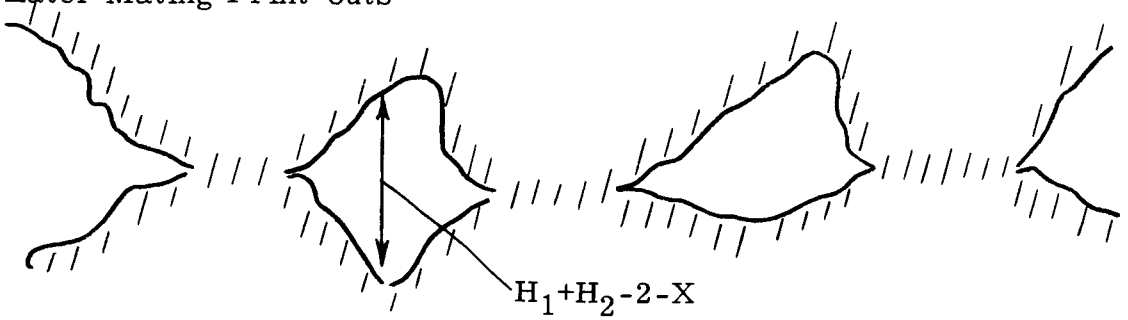

Figure 2.4. System of Height Representation

Actual	30	29	28	27	26	25	24	23	22	21
Listed	T	S	R	Q	P	O	N	M	L	K

Actual	20	19	18	17	16	15	14	13	12	11
Listed	J	I	H	G	F	E	D	C	B	A

Actual	10	9	8	7	6	5	4	3	2	1
Listed	0	9	8	7	6	5	4	3	2	1

Figure 2.5. Gap Height Description.

```
 57 /809DCFHFB9545569FFECA758899DFFFDBB986B00DEGCB80646
 58 /788CCHIGC9544560EEDB96464550ACDB0076300ADEGBA90635
 59 /788CCGHHEB97568AEEDB0757678BDFFDBA88490BDDFBA90646
 60 /688DCFGHDC0765780CDCBB978787BDDDB08551679BCE0977313
 61 /477BBCEHEA986780DFEFD088898BDFEDAA97390BEFIDB962 2
 62 /25600AFGDA096780DGFFDA776769ADCA8997500BEEFB097313
 63 / 4600AEGD0985670CDDDB9665658ADCA9997488BEEFB097313
 64 / 47AABGFB9974569EHHFEB987870BEDCDCD0899CIJIIFC9557
 65 /360BBCJIFDE05680FKJHHD976760BFEEGEFEAA9BFFFFC96224
 66 /80BCDFLJEDFA778BGKKIHE07576ABGGGHFCA866BEEEDB97557
 67 /ABEHHLNLFCC9678BFHHFEB97566ABFGGGEA95450CDDC075447
 68 /BCHKGKMICA07468AFFGFFA97588DCFGFGEA73349ABCA874336
 69 /BAEFEILHCA863479EFGEE974257BADFDDC9511389ACB986436
 70 /AABCCFGFBB08469AEEFEE975369BAFIHGGC0558BCCDC097326
 71 /00BBBEFECB075680EEGFD00869ACCGJIGIC84470AABA875227
 72 /90BAAEEDBA964468BACDC98869ADEHJHEF06225900AA097549
 73 /88CBBEEDA0865579BADHD09867CEEGJGGGB8669BCCDFDDA079
 74 /88BBCFFEBA98889DEEGIDD0878CDEGJGDB842370BBCEDBA946
 75 /898CBDDC0976456ACBDEA775460BBEIHED065690CCDFDA0836
 76 /789A0BCB9976356ACDGFB988680BBELIED95450ADCDBB98758
 77 /777CBFHGDDDC0A0EGILLHFD980ABBELKGE06459CGEFBA87647
 78 /878DBGHFBBA7688CFILLIEA96790ADKJGFA7579ADCD0965425
 79 /869DBGHEAC06477AEGHHDA863600AFLJFGB860ACFFGCCA9857
 80 /790EBDFC0B952660DDEGCA9957AABHMJIG0759AAEEFCCA0A88
 81 /577BACFC0AA7476BEEGJGBAA80BBCFJHEA655888BBDCCAA078
 82 /35500DFC0095255BDDFGDA0A0CCBCEHGFA654777A0CBB00956
 83 /24389CEB9984144BEFFHDB009AABCEJIIC875557A0CBB00956
 84 /13380CDA8873 34CEEFGCA97689ABDIFEA764457A0CCA98744
 85 / 2380CDC9984145ACDFGCDC8689BCEKHGB063457AADDB99855
 86 / 239BFGEAAA6379DGHIIDFD8660BDEKIGB9523770ADCA89844
 87 / 239BFFEA0A8390CEEFGCE94379BDGLHGA8412670ADB079622
 88 /1349BFECAAC0489BCCDE0B73268ABFKHGA841389ABECA89623
 89 /2459BFDBCBB9478ACBDD0C95488BCHNLLEA84680ABECA8A855
 90 /3348ADBABAB0490BDCFEAB84277ABGLIHA962468ABEDCAC845
 91 /446ABFEBCAA8389UAACB9062 4590DIFE974 247ABFDA90844
 92 /33400CC0B0084998900A07962 469AFHCB752 358BCGFDCB956
 93 /33489BB0B0A96AA0ABCB9085479BBIICC863259ADDGDBBA856
 94 /22380CCADAB96A090ABB9085468AAGGAA741 380DDEDCCCA88
 95 /1248AEEDFDCA7BAABCFEBCA869ADFLMEEB9636CCFHIJIGGB09
 96 / 368BFFEEBAA7B99ACFEBCA86ACGHMLFDA9535CBEEEFDBB867
 97 / 38ACGGFEBA95080CEJIGGC86ABEGIKHGEB966AADBCECA0656
 98 /150CDHGFEDC94960EILHEEA750CBCFIFFE00559AEFFFDA0544
 99 /26ABDHGEEC07386AEIKECB9449DAADGFEC794489CFGEB09433
100 /37AAEHGFDA84 549CHIFCB7359ECCEGGEC0A6600CFGDA07433
101 /46A0CEEDA851 55AFHGEBB7468DBCFHFEB99660ADFGEBA8556

  THERE ARE  0.7600 PERCENT ZEROS
I=  51 J=   3 N=  51 M= 102
```

Figure 2.6. Case 1 - Parallel Periodicity in Phase Area of Contact/Gap Distribution After 1 Increment of Displacement.

```
 56 /699ECGHFB9534369GFFECA88799CBCD090763A99ACE09562 2
 57 /687BADFD07323347DDCA9536677BDDDB00764088BCEA068424
 58 /566AAFGEA7322348CCB0742423389AB088541869BCE0978413
 59 /566AAEFFC0753469CCB0853554560BDDB0966278OBBD0978424
 60 /466BADEFB8543568ABA00756565OBBB08633 4570AC87551 1
 61 /25500ACFC9764568BDCDB8666760BDCB99751750CDGB074
 62 / 34889DEB9874568BEDDB9554547 9BA967753880CCD08751 1
 63 / 24889CEB8763458ABBB07443436 9BA977752660CCD08751 1
 64 / 2599UED07752347CFFDCC7656580CBABAB8677AGHGGDA7335
 65 /14800AHGDBC8346BDIHFFB7545480DCCECDC9970DDDDA74  2
 66 /680ABDJHCBD95560EIIGFC8535490EEEFDA96440CCCB075335
 67 /90CFFJLJDAA74560DFFDC07534490DEEEC973238ABBA853225
 68 /0AFIEIKGA9852469DDEDD975366BADEDEC95112790A9652114
 69 /09CDCGJFA9641257CDECC752 3509BDBBA73  1679A0764214
 70 /990AADED00862479CCDCC7531470 9DGFEEA83360AABA8751 4
 71 /880U0CDCA0853468CCEDBH86479AAEHGEGA622589909653  5
 72 /78099CCB0974224609ABA766479BCFHFCD84  378899875327
 73 /66A00CCB9864335709BFB87645ACCEHEEE064470AABDBB9857
 74 /6600ADDC0976667BCCEGB88656ABCEHEB062 15800ACB09724
 75 /670A0BBA87542349A0BC955324800CGFCB843478AABDB98614
 76 /567980A07754134 9ABEDU76646800CJGCB732389BAB0076536
 77 /555A0DFEBBBA898CEGJJFDB768900CJIEC84237AECD0965425
 78 /656B0EFD0095466ADGJJGC9745789BIHED953579BAB87432 3
 79 /647B0EFC9A842559CEFFB96414889DJHDE06489ADDEAA97635
 80 /578C0BDA8073 448BBCEA97735990FKHGE853799CCDAA98966
 81 /35509ADA89952540CCEHE0996800ADHFC943366600BAA99856
 82 /13388BDA8873 330BBDEB9898AA0ACFED943255598A0088734
 83 / 2167AC07762 220CDDFB0887990ACHGGA65333598A0088734
 84 / 1168AB96651 12ACCDEA9754679 0BGDC954223598AA976522
 85 /  168ABA7762 239ABDEABA64670ACIFE084123599BB077633
 86 /  170DEC9994157BEFGGBDB64680BCIGE073 15589BA967622
 87 /  170DDC9896178ACCDEAC721570BEJFE962  4589B08574
 88 / 1270DCA99A82670AABC8051 4690DIFE962 16790CA9674 1
 89 / 2370DB0A0072569A0BB8A732660AFLJJC96246890CA969633
 90 /11269B09090827 0BADC9062 5590EJGF974 24690CBA9A623
 91 /22490DCUA996167899A0784  2378BGDC752  2590DB978622
 92 /11288AA80886277678985 74  2479DFA053  1360AEDBA0734
 93 /112670080897499890A078632570 0GGAA641 379BBEB009634
 94 /  168AA9B907498789007863246 99EE9952  168BBCBAAA966
 95 /  269CCBDBA950990ADCUA96479BDJKCC07414AADFGHGEE087
 96 / 1460DDCC09950779ADCUA9649AEFKJDB97313A0CCCDB00645
 97 / 169AEEDC0973868ACHGEEA6490CEGIFEC074499B0ACA98434
 98 / 38ABFEDCBA72748CGJFCC9538A0ADGDDC883379CDDDB98322
 99 / 490BFECCA851649CGICA07227B99BEDCA572267ADEC087211
100 /1599CFEDB962 327AFGDA05137CAACEECA894488ADEB985211
101 /2498ACCB963  339DFECU05246B0ADFDC0774489BDEC096334

  THERE ARE  3.0600 PERCENT ZEROS
I=  51 J=   8 N=  51 M= 102
```

Figure 2.7. Case 1 - Parallel Periodicity in Phase Area of Contact/Gap Distribution After 3 Increments of Displacement.

```
 56 /477CAEFD07312147EDDCA966577A0AB8785419779AC8734
 57 /46509BDB851 1125BBA97314455OBBB0885428660AC98462 2
 58 /34499DEC951  126AA0852 2 11679086632 6670AC87562 1
 59 /34499CDDA8531247AA0863132348OBB08744 56800B87562 2
 60 /24409BCD0632134690988534343800086411 23589A6533
 61 / 33889ADA75423460BABU64445480BA07753 568ABEU852
 62 / 12667BC0765234eOCBBU733232570974553l668AAB8653
 63 /  2667AC0654123690008522121470975553 448AAB8653
 64 /  3778CB8553 125ADDBAB5434368A0909064559EFEEB95113
 65 / 26889FEBUA61246BGFDU05323268BAACABA7758BBBB952
 66 /46890BHFA0B73348CGGEDA6313278CCCDB974228AAAU853113
 67 /78ADDHJHB9952348BDDBA85312278BCCCA751 169009631  3
 68 /89DGCGIE9763 247BBCBB75314409BCBCA73   5789743   2
 69 /87ABAEHD9742  35ABCAA53  13870B00951   45798542  2
 70 /77899BCB8864 257AABAA531 2587BEDCC9611489909653  2
 71 /66888ABA9863124eAACBU66425799CFECE94  367787431  3
 72 /56877AA08752  248790954425?0ADFDAB62  1566776531 5
 73 /44988AA07642113587ODU654239AACFCCC842258990B007635
 74 /44889BBA87544450AACEU6643490ACFC084   36889A0875 2
 75 /458980096532 127980A7331 2688AEDA0621256990B0764 2
 76 /345768985532 12790CB854424688AHEA051 1670908854314
 77 /33398BDC0009676ACEHHDB0546788AHGCA62 159CAB87432 3
 78 /4340BCDB8873249BEHHEA75235670GFCB7313570906521  1
 79 /42508CDA7962 337ACDD0742 2667BHFBC842679BBC9975413
 80 /356A80B96851 22600AC975513778DIFEC631577AAB9976744
 81 /133879B96773 328AACFCB7746889BFDA72114448809977634
 82 / 11660B96651 11800BC076769989ADCB721 3337698866512
 83 /   459A8554    8ABBDUB6657789AFEE9431113769886512
 84 /   46907443    9AABC9753245780EBA732  1376997543
 85 /   46909554   1790BC909424589AGDC862  137700855411
 86 /   58BCA7772 350CDEEUB0424680AGEC851  3367097454
 87 /   58BBA7674 569AABC9A5  3580CHDC74   2367086352
 88 /   58BA97796 458990A683  2478BGDC74   4578A97452
 89 /  1588089885 34798Q06951 4489DJHHA74 24678A9747411
 90 /   470878786 56809BA784  3378CHED752  2478A09794 1
 91 /  278BA89774 4567798562   1560EBA53    378B07564
 92 /   669968664 5545676352   257BD9831   1489CB098512
 93 /   458868675277678985641 3588EE9942  15700C0887412
 94 /   469970785276567885641 2477CC773    4600A0999744
 95 /   47AA0B097387789BA89742570BHIAA852 299BDEFECC865
 96 /  248BBAA877385579BA8974279CDIHB0751 198AAAB088423
 97 /  479CCBA87516469AFECC94278ACEGDCA852277089A976212
 98 / 1690DCBA095 526AEHDAA7316989BEBBA661157ABBB0761
 99 / 2780DCAA963 427AEBA985  50770CBA935  459BCA865
100 / 377ADCB074  1 59DEB983 15A99ACCA96722669BC0763
101 / 2769AA0741  117BDCA883 24089BDBA85522670BCA874112

  THERE ARE  9.2200 PERCENT ZEROS
I=  51 J=   8 N=  51 M= 102
```

Figure 2.8. Case 1 - Parallel Periodicity in Phase. Area of Contact/Gap Distribution After 5 Increments of Displacement.

```
 57 /2438708063      3009751 2233800086632 64489A7624
 58 /12277BCA73      499863       45786441  44589A6534
 59 /12277ABB9631  25998641 1 12680086522 3468806534
 60 / 22870A8841  1247876631212168886421    136794311
 61 / 1166798B532 1248090842223268098553 1 34690C863
 62 /   4450A8543 1248A008511 1 358752331 4469906431
 63 /   4459A8432  14788863     258753331 2269906431
 64 /  1556A06331   39BB0963212146987878423 37CDCC073  1
 65 /  4667DC0894  240EDBB831 1 46099A9095536000073
 66 /246780FD9805112aAEECB941 1 56AAABU752  69998631  1
 67 /569BBFHF0773 1260BB09631   560AAA953   4788741   1
 68 /67BEAEGC7541  2500A00531 22870A0A951   3567521
 69 /65909CFB752   1390A9931   165808873    2357632
 70 /556770A06642  359909931   3650CBAA74  267787431
 71 /446669097641  2499A08442 3577ADCAC72  14556521   1
 72 /34655998653    265787322 3589BDB904    34455431  3
 73 /22766998542   13658B8432 1799ADAAA62  367780885413
 74 /226670096532223899AC844212789ADA862   1466798653
 75 /23676887431    57689511   4669CB984   3477808542
 76 /12354e76331    578A06322 24669FC983   4587866321 2
 77 /111760BA8887454 9ACFFB083245669FEA94   37A906521  1
 78 /21286AB06651 2270CFFC953 13458EDA051 13587843
 79 /2 386AB9574  1159ABB852   4450FD0A62 45700A77532 1
 80 /13496807463    4889A7533 1556BGDCA41 3559907754522
 81 / 11657074551 1 699ADA655246670DB95   2226687755412
 82 /   44807443    6880A8545477679BA05   11154766443
 83 /   23796332    6900B8644355679DCC721   154766443
 84 /   24785221    7990A7531 23568C0951    154775321
 85 /   24787332    5780A7872 23679EBA64    155886332
 86 /   360A9555  138ABCC8082 24689ECA63   1145875232
 87 /   360095452 347990A793  1368AFBA52    14586413
 88 /   360975574 2367789461   2560EBA52   235697523
 89 /   360867663 1257688473  2267BHFF952  2456975252
 90 /   258656564 3468709562  1156AFCB53    256987572
 91 /   560967552 234557634     348C0931    156085342
 92 /   447746442 332345413     350B761     267A08763
 93 /   236646453 5545676342  1366CC772    3588A86652
 94 /   247758563 5434566342   255AA551    248898777522
 95 /   2599808751656570967 52 3580FG9963   770BCDCAA643
 96 /   2600996551633570967 52 57ABGF0853   7699908662 1
 97 /  257AA09653 42479DCAA72 569ACEBA963  558679754
 98 /  478BA09873 3 49CFB9951 47670C00944  359000854
 99 /  568BA99741 2 59CE9763  38558A09713  2370A9643
100 / 1559BA0852    37BC0761  39779AA9745  4470A8541
101 /  54799852     50BA9661  28670B09633  4580A9652

  THERE ARE 19.4000 PERCENT ZEROS
I=  51 J=   9 N=  51 M= 102
```

Figure 2.9. Case 1 - Parallel Periodicity in Phase Area of Contact/Gap Distribution After 7 Increments of Displacement.

```
 56 / 3397A8063      3A009752213376784341   53357943
 57 / 216580841      188753     1168886441  42267954 2
 58 /   3504951      277641       2356422   2236794312
 59 /  55900741      377642       4688643   1246684312
 60 /   6589062     2565441        466642     145721
 61 /  44570731     2687862   1 46876331   12478A641
 62 /  223896321    2698863      13653 11   224778421
 63 /  22379621     2566641       3653111     4778421
 64 /  33498411     17008741    247656562  115ABAA851
 65 /  2445BA8672   28CB0061    248779787 3314888851
 66 / 24568DB7683   49CCA072    349990853    4777641
 67 /347U0DF08551   48008741    348999731     256652
 68 /450C9CEA532    38898831     65898973      13453
 69 /43787AD053      1789771      43686651       13541
 70 /33455898442    1377871     1438A09952     4556521
 71 /22444787542     27798622   13559BA9A5      23343
 72 /12433776431      435651    13670B0782     1223321    1
 73 /  54477632      14360021    5779B9994    1455686632 1
 74 /  445887431    16779A622     5679B964      244576431
 75 / 145466521      354473       2447A0762    125568632
 76 /  13245411      3569841      2447DA761     23656441
 77 /   5480966652327 9ADD0861  23447DC972      1597843
 78 /   64908443     58ADDA731   1236CB983      1365621
 79 /  164907352     3790063      2238DB894   2358895531
 80 / 1274685241     2667955 11   3340EBA92  13377855323
 81 /   43585233     477989433  24458B073        44655332
 82 /   22685221     4668963232 554570983        32544221
 83 /    157411     47880642213 3457BAA5        32544221
 84 /     2563       57789531    1346A873        325531
 85 /    256511      35689565    1457C0942       3366411
 86 /   14897333    1690AA686    2467CA941       23653 1
 87 /   14887323   12577895 71   1469D093        23642 1
 88 /   148753352   14556724      348C093       134753 1
 89 /   148645441    35466251     450FDD73      234753 3
 90 /    36434342  124658764      349DA031       3476535
 91 /   34874533    12335412      126A871        3486312
 92 /   22552422   11 1232 1      138054         45986541
 93 /    14424231  332345412     144AA55       136696443
 94 /    25536341  321234412      339933        266765553
 95 /    37768653  4334587453   1368DE7741    5580ABA99421
 96 /    48877433  4113587453   3590ED8631     547778644
 97 /   359987431  2 257BA995   3479AC09741    336457532
 98 /  2560987651  1 27AD0773   25458A88722    137888632
 99 /  346097752     37AC7541   163369875 1     15897421
100 /  33709863      150A854    17557997523    22589632
101 /  3257763       3809744     6458087411    23689743

  THERE ARE 32.8200 PERCENT ZEROS
I=  35 J= 102 N=  51 M= 102
```

Figure 2.10. Case 1 - Parallel Periodicity in Phase. Area of Contact/ Gap Distribution After 9 Increments of Displacement.

```
 56 / 22860A952      209986411 226567323    42246832
 57 / 1 247973        77642      5777533    31156843 1
 58 /   449084       16653       1245311    11256832 1
 59 /  4489963      266531       3577532     1355732 1
 60 /  2478951      145433        355531        3461
 61 /  3346962     1576751       3576522     1367053
 62 /  11278521    1587752         2542     11366731
 63 /  1126851     145553          2542       366731
 64 /   223873      699763     136545451     40A0074
 65 /  1334A07561   178A995   13766867622    377774
 66 / 13457CA6572   38BB0961    238889742    366653
 67 /23699CEC744    3799763      23788862    145541
 68 /3498B8D0421    2778772      54787862      2342
 69 /326760C942      67866       3257554       243
 70 /22344787331    266706      327098841    344541
 71 /11333676431   16687511    2448A0804     12232
 72 / 132266532      32454      2569A9671     11221
 73 /  43366521      32591      4668A8883    344575521
 74 /  33477632     56680511     4568A853     13346532
 75 /  3435541      243562       133609651    14457521
 76 /   21343       245876       1336C065     1254533
 77 /   437985554121680CC975    12336CB861     486732
 78 /  53897332     470CC062      125BA872      25451
 79 /  53896241     2689952      1127CA783   124778442
 80 /  16357413     1556842      2239DA081    2266744212
 81 /   32474122    3668A3322   13347A962       33544221
 82 /   1157411     355782121443469872          2143311
 83 /      463     367795311   22346A004       2143311
 84 /     1452      4667842      2350762        21442
 85 /     1454     24578454      346B9831       22553
 86 /    3786222   58900575     1356B083        12542
 87 /    3776212   14667646      358C982        12531
 88 /   37642241    3445613      237B982        23642
 89 /    3753433    2435514      349ECC62      123642 2
 90 /   25323231   13547623      238C092       2365424
 91 /   23763422    12243 1        15076        23752 1
 92 /   11441311       121         27943        3487543
 93 /     331312  2212343 1       330044       25585332
 94 /    1442523  21 1233 1       228822       155654442
 95 /   26657542 3223476342     257CD663     44790A08831
 96 /   37766322 3  2476342    2489DC752     436667533
 97 /   24887632  1 146A0884   2368089863    225346421
 98 /  145987654    160C9662   14347077611     26777521
 99 /  235986641     2608643     52258764       478631
100 /  22698752       490743    6446886412    11478521
101 /  2146652       2798653     53479763     12578632

THERE ARE 40.2200 PERCENT ZEROS
```

Figure 2.11. Case 1 - Parallel Periodicity in Phase Area of Contact/Gap Distribution After 10 Increments of Displacement.

```
 57 /7700A9B875211679B9858767BAACB0977898577 9B097526666
 58 /67AABAB874212679A874/432467987755467699AA907515444
 59 /57AAB0B006533790A9857544 69AA0997867867 70A907526787
 60 /68AAA9098444589900097865369998775634424 6997853 3674
 61 /3679C900956668 99BCA087657000990085777 579CC0053 2453
 62 /256899B096876800BCB97543478877997576578 0A8053 3444
 63 /256899A005766778 0AC864323677778874545760A8053 3655
 64 /2579C0C9747557 90BDCA865457888 90AA7759BCCGEC0745566
 65 /570AAAFC07A859CCCGEA865357777 00CE099BDAACC08412344
 66 /990BCDIFP9B770CDDGFB855366668BCBC976A090AB09634344
 67 /DCEFFIHE090669ABBDCA/43255668ACBB855887890874123 56
 68 /EBEGCFFC8786488ABDAC/433668 00BCAB853665778752 1 24
 69 /EBCDADEA7544267 0AC985211467 99AB99631323667631323 5
 70 /CB00CCDA866646690A886223469A0CFDC077767998874251 24
 71 /BA099BC0876535606BB00635679ABBDIFC065545776652 4357
 72 /AA088BB976431348986863467 9ACDEIEA7333236777653757 9
 73 /BAA99AA877542348A98A745877ADDFICO9776569B009099557
 74 /BBAU0BB98976667ACBAC8578760CDDE065332358A000056446
 75 /CB98800766543459A989>244459CACEC8865246 9B099946435
 76 /A07779065443245 9AAA06457679DCCGA77552470A986735679
 77 /B08BBDEB09A9880CEEHGU67780AFEDFA8754247BDA0662480C
 78 /C99BABC96685568BEFGEA667679CCCGA87653670A9844 29AC
 79 /C89ACAE854743460DDCA6234360CBEHC9086499BCCB88560AA
 80 /A88099D742632359DBAC745647ADDHHA0065390ABBA9067BB0
 81 /755788C96473457AEBBBA5788AACCED975233878AAA0067566
 82 /43689987425234 6ADAB994880CBBBEC97412275699099453 33
 83 /225788A63141235AECCAU4769A0CBEDA062347569909845322
 84 /235677052 31235BEBC08253688BADC975134756978763343 3
 85 /235709A631422350CAEC8364688CBEC076444756989873443 4
 86 /3579AAC9636469ACEBFD8464690ECDB075353545889762497 7
 87 /3579BBB983855669A0BA656458AGCEB073132435778651486 6
 88 /35780BCA0474455898094353460FCEB073243446889762464 5
 89 /35679DC994633558988054745 70GEHEBA766565788976269 89
 90 /24568BA904743669090C05364479FCEB0943326579 0A8748646
 91 /55799B078363257997073131146C0B0872111657879652575 6
 92 /3248808584743677769 62 31148A9A954   276890CA967635
 93 /1137808585965899980743644 6BC9A955222490A00C0867413
 94 / 1490B967497688898074353350A798441 1390990B0879634
 95 / 260CEB90708800AA0C075645AFGACB8854540EDDFGGA99757
 96 / 380DDA896876090000CA86867BGHDDB9743448CABBBB756678
 97 / 30CEEB99685488CDEGDA9A67ADFEEDA07444899AAA9435656
 98 /25ADEFB876954866DFHCU79446DDBCC80854260BDDB9434545
 99 /47BBCEA76563489CBDE0636337DCBBB607431508BBB07223434
100 /4700CEB9523 157ABDD0645458DCBBA7976647 0AAB06343324
101 /3589BB962 1 3780BBB0766678DCABA7954358ABBBA8566557

  THERE ARE  1.0600 PERCENT ZEROS
I=  51 J=   3 N=  51 M= 102
```

Figure 2.12. Case 2 - Parallel Periodicity Half Out of Phase Area of Contact/Gap Distribution After 4 Increments of Displacement.

```
 56 /77AUA9B675111668B99799877769A8785555527689874Z 2233
 57 /5586970653   4570763654569A08755676355708753 4444
 58 /4599090652   457965Z521 2457655332454779978S3 3222
 59 /3599080684311578976353224799877564564558978S3 4565
 60 /4699978762236778875643147776553412Z 24775631 1452
 61 /1457878873446770A9865435688778863553S7AA8831  231
 62 / 3467708746546860A07532125665577535435689683l 1222
 63 / 3467798735445568986421 14555566523235689683l 1433
 64 / 35788A7525335760BA964323566678995537OAAECA8523344
 65 /358999DA859637AAAEC964313555588AC8770B99AA862  122
 66 /7780ABGDC70556AEBED06331444460A0A754987690874121Z2
 67 /BACDDGFC8784479008A9521 334469A00633665678652  134
 68 /C0CEADDA65642669OB9852114668CA9063144355653     2
 69 /C0AB9BC95322 4589A763   24577907741 1 1445541 1 13
 70 /A0888AB9644424478966Z  124798ADBA855545776652 3  2
 71 /098770A8654313460008841345790OBGDA84332355443  2135
 72 /998660075421 126764641245794RCGC95111 145554315357
 73 /099779965532 1269769523655988DGA875543470887877335
 74 /00988007675444594096356548ABBC84311 1369888834224
 75 /A07668854432123797673 22237A9ACA6643 2470877724213
 76 /985557843221 2379998423545TBAAE95533 2589764513457
 77 /0860UBC0879766BACCFE8455669DCBD96532 250B9844 268A
 78 /A77U90A744633460CDEC9445457AAAE96543145897622  79A
 79 /A67989C63252124BBBA94 12148A0CFA78642770AA06634899
 80 /966877B52 41 137B09852345Z9BBFF9884317890097845008
 81 /533566A742512359C0009356699AACB753 116569998845344
 82 /214677052 3 1249B90772668A000CA752   5347787723111
 83 /  3566941 2  139CAA98254798A0CB984 1253477876231
 84 / 1345583  1  130C0A86 3146609BA753 125347565411211
 85 / 13587941 2  13EA9CA6142466A0CA8542225347676512212
 86 /135799A74142479AC0DB6242478CAB085313132366754 2755
 87 /135700076163344798094342369EAC0851 1 21355643 2644
 88 /135680A98252233676872131248DAC0851 2122466754 2423
 89 /13457BA772411336760863252358ECFC09544343566754 4767
 90 / 2346097825214478TA83142257DAC087211 4357896526424
 91 /335770856141 35775851 1  24A80865    43565743 3534
 92 /1 2668636252145554Z4  1  26979732    54678A9745413
 93 /  1568636374367776852142240A79733   276988A86452 1
 94 /  2780745275466676852131138957622   17877808657412
 95 /  48AC07858668899BA8534239DE9A06632328CBBDEE977535
 96 / 168BB967465487888A9646450EFBB07521226490000534656
 97 / 18ACC077463266ABCEB979459BDCCB9852226779997213434
 98 / 39BCD065473266OBDFA857226BB0AA68632 480BB07212323
 99 /2500AC954341267A0BC8414115BA00048521 3600085  1212
100 /2588AC073 1  3590BB8423236BA0095754425899084121l 2
101 /13670074    156800085444568A9095732136900096344335

  THERE ARE  6.2600 PERCENT ZEROS
I=  51 J=   3 N=  51 M= 102
```

Figure 2.13. Case 2 - Parallel Periodicity Half Out of Phase Area of Contact/Gap Distribution After 6 Increments of Displacement.

```
 56 /5598970653    4460775776556796563333 5467652     11
 57 /3366758431    2358541432347798653345413358653l 2222
 58 /237787843     235743 3     23543311 23255775631 1
 59 /13778686621   356754131   257765534234233675631 2343
 60 /247775654    14556653421 255543312     255341    23
 61 / 2356566512224558976432136665566413313599661     1
 62 / 124558652432466898531    3443355313213467461
 63 / 1245576513223346764z     23333443 1 13467461    211
 64 / 13566953 3113568097421 134445677331589CA963 1122
 65 /136777B96374159990A7421 13333669A65580779964
 66 /556890EB858336900CB6411 2222489895327656786 52
 67 /09ABBEDA6562257680973    1122479884114434564 3     12
 68 /A8AC98B94342 44780763    24466897841 22133431
 69 /A89070A731    23679541     235578552      22332      1
 70 /986669074222 22567442     25769B0963332355443   1
 71 /876558964321 12688662 12357880EB96211 133221     13
 72 /7764488532      454242  235790AEA73      233321 3135
 73 /87755774331     475473 1433700BE9653321258665655113
 74 /887668854532223798794134326900A621     147666612  2
 75 /98544663221    1575451     15979A94421   2586555 2  1
 76 /763335621      1577762 13235099C73311   3675423 1235
 77 /864880A865754469AADC6233467BA0B7431    3807622  469
 78 /955878952241124BABCA7223235999C74321 236754     579
 79 /945767A41 3    2600972     2698AD95642 5589984412677
 80 /74465503  2    1508763 12 3700DD76621 5678875623886
 81 /311344952 3  137A8887l3447799A0531    4347776623122
 82 /  245583  1    2707655 4469888A953     31255655 1
 83 /  134472       17A9976 3257698A0762    31255654 1
 84 /  123361       18A8964 1 2448709531    31253432
 85 /  136572       1697A94 2 24498A9632    31254543
 86 / 13577952 2 2579A8B04 2 256A908631 1 1 144532   533
 87 / 13588854 4112257687212 147C9A863       133421   422
 88 / 13468976 3  1145465  1  26B9A863       244532   2 1
 89 / 12350955 2  11454861 3 136CADA87322121344532 2545
 90 /  1248756 3  22565961 2  35B9A865     21356743 42 2
 91 /113558634 2  1355363       2968643     21343521 1312
 92 /   446414 3  2333252       475751      32456975232 1
 93 /   346414152145554633  2  28957511     5676696423
 94 /   568523 5324445463  1  167354       56556864352
 95 /  269A85636446677696312 17BC798441 1 6A00BCC755313
 96 /  460074524326566697424238CD00853     4978888312434
 97 /  69AA855241 4490AC07572370BAA0763    4557775   1212
 98 / 170AB843251 4480BD9635   4008994641   2680085    1 1
 99 / 3889A73212   45980A62 2   309888263    1688863
100 / 3669A851     13780062 1 140988735322 3677862
101 / 1458852      346888632223409787351  14788874122113

  THERE ARE 19.0600 PERCENT ZEROS
I=  51 J=  10 N=  51 M= 102
```

Figure 2.14. Case 2 - Parallel Periodicity Half Out of Phase Area of Contact/Gap Distribution After 8 Increments of Displacement.

```
 56 /3376758431    22485535543345743411111 324543
 57 /114453621      13632 21 1255764311232 1136431
 58 / 15565621      13521 1     13211     1 3355341
 59 / 15564644     134532 1    35543312 12 1145341    121
 60 / 25553432     23344312     333211        3312      1
 61 /  1343443     233675421  144433442 11 137744
 62 /   233643 21 24467631     12211331 1  124524
 63 /   233543 1  1124542       1111221    124524
 64 /  1344731 1  13468752     1222345511 3677A9741
 65 / 14555074152 3777A952     1111447943368557742
 66 /33467800636114786A062        2676731 54345643
 67 /87900CB9434  35668751        257662  22123421
 68 /969A7007212  22568541     224467562      1121
 69 /967858951     145732       1335633        11
 70 /764447852      34522       35470874111 133221
 71 /6543367421     46644     135668C074       11          1
 72 /554226631      232 2     135789C951        111    1 13
 73 /6553355211     253251  2115880C74311    36443433   1
 74 /66544663231   1576572 121 478894         254444
 75 /76322441       35323       37579722      364333
 76 /5411134        35554   1 13877A511      14532 1    13
 77 /64266896435322479988A4 112450980521     16854     247
 78 /73365673  2   2690A95   1 13777A521     14532     357
 79 /72354592  1     48875       476987342  33677622  455
 80 /52243381       386541     1588BB544    34566534 1664
 81 /1  12273  1   1596665 12255779831      21255544 1
 82 /   23361       585633 22476669731      1  33433
 83 /   1225        597754 1 354769854      1  33432
 84 /    114        696742     22658731     1  3121
 85 /   1435        475972     22769741     1  32321
 86 /  135573      35796082     34978641        2231    311
 87 /  1366632 2     35465       25A79641        112     2
 88 /  1246754 1     23245        4079641        2231
 89 /   138733       23264  1   14A9B9651      12231    323
 90 /    26534 1     34374      13079643       134521 2
 91 /  1336412      133141        746421       1213     1
 92 /   2242 2 1    111 3          25353       1 234753 1
 93 /   1242 2 3   2333241         67353       34544742 1
 94 /   3463 1 31  2223241         45132       3433464213
 95 /   47963414224455741        50A57622      49880AA5331 1
 96 /  2488523 21 43444752 2     16AB88631      27566661   212
 97 /  4799633 2  22789A8535    1580998541     2335553
 98 /  5890621 3  22680B7413     288677242      468863
 99 / 1667951      2376894       187666 41      466641
100 / 1447963       156884       287665131     145564
101 /  23663       12466641     128756513      2566652      1

  THERE ARE 36.9800 PERCENT ZEROS
I=  51 J=  21 N=  51 M= 102
```

Figure 2.15. Case 2 - Parallel Periodicity Half Out of Phase. Area of Contact/Gap Distribution After 10 Increments of Displacement.

```
 57 /  22314          141        335421    1     1421
 58 /  33434           13          1           113312
 59 /  3342422       1231        133211          2312
 60 /  333121       11221        111             11
 61 /   121221     114532       2221122         15522
 62 /    11421     224541            11         23 2
 63 /    11321       232                      23 2
 64 /   12251      124653           1233    14559752
 65 /  2333852 3  1555973           2257211 4633552
 66 /112456A8414  2566984          45451   32123421
 67 /65788A07212  1344653           3544        12
 68 /74795885       34632         224534
 69 /74563673        2351         113411
 70 /54222563         123          13258652      11
 71 /43211452        24422        13446A852
 72 /332  441          1          13567A73                  1
 73 /4331133          31 3        3668A521      14221211
 74 /44322441 1       35435        256672         32222
 75 /541  22          131 1        153575        142111
 76 /32   12          13332        165593        231         1
 77 /42 446742131   2577092       2387683        4632       25
 78 /51143451        478973        155593        231       135
 79 /5 13237         26653         25470512    114554      233
 80 /3  2116         16432         36600322    12344312    442
 81 /      51        374443       3355761         33322
 82 /    114         363411      25444751         11211
 83 /      3         375532     132547632         1121
 84 /      2          47452        43651          1
 85 /    213          25375        54752          1 1
 86 /   13351       1357486       1275642            1     1
 87 /   14441         13243        395742
 88 /    24532         1 21        285742            1
 89 /    16511         1 42        2970743           1     1 1
 90 /     4312        12152        1857421         123
 91 /   1142          11 2         5242              1
 92 /     2              1         3131            12531
 93 /     2     1     111 2        45131         1232252
 94 /   1241    1       1 2        23 1          1211242   1
 95 /   257412 2    2233252       389354        2766899311
 96 /   2663 1      2122253       4906641        534444
 97 /  2577411        56796513    36877632       113331
 98 /  36784    1     468052 1     66455 2       246641
 99 /  44573         154672        65444 2       24442
100 /  225741         34662        65443 1       23342
101 /   1441          24442        65343 1       34443

  THERE ARE 57.1400 PERCENT ZEROS
```

Figure 2.16. Case 2 - Parallel Periodicity Half Out of Phase. Area of Contact/Gap Distribution After 12 Increments of Displacement.

```
 56 / 31212623 2      2355675532131111122    3  1      1
 57 / 1     41          2426345331211133 3 1  2    1 2
 58 / 2   131           21                  231222  2
 59 / 2 1 1222 2        22  12311    1 24411     2   223333
 60 / 2      22 11 1111221 121          1             22
 61 /         331331221234412331 1 112 4431221        11
 62 /        343255222212222    1     121321             11
 63 /        243242      111           1   1            2 11
 64 /  11 14311542 113333    1     22  2465564342 231   11
 65 / 2431155430942542333 11       1412578777411    1
 66 /4445570845A853553323 2         3224875522122 2
 67 /8786590835852133321 1           22247532              12
 68 /746637873362  2121    1    1 21321474
 69 /9443 4531 2                    1 21 14                 1
 70 /65331543222                  12425546842        1     14
 71 /5432 342211      2  1  1224475665672              33
 72 /4431 33                     22448776444          2123355
 73 /5431 3411             3311222696574552     11213133323
 74 /6532 463231     1322641112134324111      122 1112324
 75 /441  231 1       1  2     1 35225531       11 11 1211
 76 /33   11          11231  24435116331       1   212444
 77 /76253665234522256346423368966114221      242  446788
 78 /74 3 232 121 113444652235545  42211       1   556576
 79 /62 4 121        132 2     23551475343  2234421676354
 80 /21 4            132 2  1235751573442  232452276535
 81 /       21  1  1 2321441435763 3411     321442211114
 82 /               322132 436883 22        1  22       1
 83 /               445142 316663 23121     1  21
 84 /               543 2  1 3342 23  1     1           1
 85 /               552 2  2 3341 13 133   1           1
 86 /   1121  242131662 2  3 5452  1 321          313453
 87 / 1 12512111     11  42332635311  2            314222
 88 /   24721            3 111535311  31           2 2
 89 /   2261         21  4 12265641333542          316554
 90 /   126          21  411225432 21 2 1          1 5322
 91 /     3          2        1          1             3421
 92 /     2          1                            1222 241
 93 /     2  1 2  212    1  131      *     2  1232232   2
 94 /   111  1 211312        1             2   221122  13
 95 /  2345123443453421 11  454232 21 32431 49874552 3431
 96 / 12134111123352322242356444433 1 212  1644112323441
 97 / 1444522112135465558567445654 42 112  1431      121
 98 / 25534   24323145767323123 74 32  121 1443      11
 99 / 25212   22221 333231   1484 32   11  21
100 / 13122          223243   1373 21  132112
101 /  1             1332553224262 2    2 2232112212321

  THERE ARE 44.6800 PERCENT ZEROS
I=   1 J= 102 N=  51 M= 102
```

Figure 2.17. Case 3 - Parallel Periodicity Out of Phase, Area of Contact/ Gap Distribution After 11 Increments of Displacement.

```
 56 /688997ACA08088H99CCAU8886700877979 9A0AA80ABAA08099
 57 /6889979A0B0088C90CB98778689D000B90AB90080AA9888098
 58 /699BCACCBE3BAAEAEGE0U997680C900A00BCCBBAAA08778099
 59 /577A00BBACAA99B790A766753580780009AA0000BBB0990CA0
 60 /599A09ABADBB90B90BDU889757AC070BBBDC0000CBB0990BAA
 61 /598998009A0077A990CAUBC9798C98ADDEDD0AAAC90879ABBB
 62 /487689AA0B09669778A09AA65780790CDECA7888B9009ACAA0
 63 /49979ABBACA088A0AABCABA6568967800AA085666B0BB0AA900
 64 /4786689A0B0988A980CCBCB6579067790098677680B80AA9A0
 65 /3675790BAC98779669CDBCA657886880AC097888BBDBEB000
 66 /36768ABDBC09888559CEBBU5468768800BA08889DCDDBD0987
 67 /3676800CAB89909660CFCDA768765780 0A086666AABB0B9776
 68 /25780CCGCB8988767ADGCA954647790DECB0789CGFHHFDB986
 69 /2577000CA07876567ACEA9843647790BCB974568BCFECAA854
 70 /2477999B007865467ADU0873253657 80A0754567BDGEDA0964
 71 /1388ABBFCB99888CDFHICCB9688A0ABDCB964570CEHFEC0A97
 72 /1399ABBFC077688DEEH1FDB0788A0BCDDC964570CDECAB0075
 73 /248900AFC855589CCDIHEB08356779ABBA753358CBECBB0A97
 74 /260ABBCFEA75578AACHGEB0848900BCB09532469DCHDC99746
 75 /36AACCDDB075600BBDJJGCB959A00BDBB9655468CCGCB89758
 76 /5609AABB0863367 89AGFD0A960CBABDBB0766458CCEAB90756
 77 /7808009075325 89BDEIDB99659BA0ABAA066879BFFGBC09568
 78 /79B9CCBC075480BEGGKFA87458000BDCAA8789BEFED0A76347
 79 /6807AAAB96438ABDGF!D965237990BECA076570DECB9066348
 80 /79A8D0AB8644890CFDGFA9755800AADB0867568AC099955459
 81 /7ADBGBBA7533999AFEHFA97557990ACA9658679BEBBBB8766B
 82 /70CAFBB097558880DBEC974348BBBBEC0758557BHFEDB76660
 83 /0BDDECCBA876000DDBDD086459DDCDGHC970668DDCBA968760
 84 /0BDEECDBA0A700AFFDECA84248ACBDFFB969668CCBA0856548
 85 /0BDFGDDCA9A6099EFDDA7632470A0ACED06079BFDDEEC0087A
 86 /ACEFGDCB99A6988CDCC8564458AAACGFEA8C90DFEFFECBCBAB
 87 /ACEEFCB06795888DCCA63422370AACFBA86A89CDEEEDCA099A
 88 /ACEHIDC07685900DDEF0809889CCDFJEB86068ACDBB0875680
 89 /BCDGHEEB0097008A0AB7799889AAACD0086A789ABAA9875689
 90 /BCDGHEEBBBA8AA9BBCD98ABA90BBADFBB08C999BDAB8767880
 91 /BBDIGCB0AA87AB0BCCH98AAA979970B998685668090776990A
 92 /CBCHFEDBBBA0DB9BA998790885775708875754580876658898
 93 /CBCHHDC09988A080988768977466579887575458087787AAA0
 94 /CA0CEBA98880BBACB00989099677680987 7CA9899655669997
 95 /BB0BECDA99809889980989097588788A099F07566467888B04
 96 /BB0BECDA009AA9890898909864897 9AA09AGA757758000BB04
 97 /BA0DECC0887986557577887644785799989C9657758000BA94
 98 /A08BCDDA9999987899AABA0755996ABCDCED077988ABBAD054
 99 /A87BCDB979999756779 9A99755986BCFDDFB8559980ABBD944
100 /A0790BA86887776699AACAA9790A9CCEDFEA855A090AAAC844
101 /8768ABB979755455U9AACA998B0B0DHFDEC07550A0ABCED467

  THERE ARE  0.3600 PERCENT ZEROS
I=  51 J=   2 N=  51 M= 102
```

Figure 2.18. Case_4 - Angled Periodicity Area of Contact/Gap Distribution After 2 Increments of Displacement.

```
 57 /46677579808866A78A07655646788880789078868997666876
 58 /477UA94A0C0099C9CEC887754684A7889880AA0099986556877
 59 /3559880094997705789544531368568887998868000878A98
 60 /37798790980078078OH866753594858000BA8888A008778099
 61 /37677688798855977784980A7570A769BBCBB8999A786579000
 62 /26546799808744755698879943568578ABCA95666078879A998
 63 /27757900994866988994A90943467456899863444080089978B
 64 /25644679808766976884AUA04357845578876455408008997 8
 65 /14535780 9A76557447ABUA9435664668 9A875666008B0C0888
 66 /1454690B0AB7666337ACU0832465466880986667BABB0B8765
 67 /1454688A90577874484DAB954654356889864444900807554
 68 / 3568AAEA0576654598EA9732425578BCA08567AEDFFDB0764
 69 / 355888A98565434594C976214255780A07523460ADCA99632
 70 / 255770885643245988B8651 3143568985323450BECB98742
 71 / 166900DA077666ABDFGAA074669890BA0742358ACFDCA6975
 72 / 17790 DA855466HCCFGDB08566980ABBA742358ABCA908853
 73 / 267889DA633367AABGFC0861345579009531136A0CA008975
 74 / 48900ADC95335699AFEC086267880A08731 247BAFBA77524
 75 /1499AABB0853488000BHHEA07379880B007433246AAEA067536
 76 /34879900864114567 9EDB89748A090B008544236AAC9078534
 77 /568688785 1 3670BCGBU7743709890998446570DDE0A87346
 78 /5707AA0A8532680CEEID96523688808A9965670CDCB8954125
 79 /4685999074216906EDGH743 157780CA9854358BCA07844126
 80 /5796B890642267 8ADBED9753368899B086453469A877733237
 81 /59B0E00953117779DCFD9753357789A974364570C000065440
 82 /58A9D0087533666BB0CA/521260000CA85363350FDCB054448
 83 /80BBCAA09654888BB0BB664237BBABEFA758446BBA09746548
 84 /80BCCAB09895889DDBCA962 269A0BDD0747446AA098634326
 85 /80BDEBBA9794877CDBH9541 258989ACB848570DBBCCA88659
 86 /9ACDEBA07794766ABAA634223699 9AEDC96A78BDCDDCA0A090
 87 /9ACCDA084573666BAA9412  15899AD0964967ABCCCBA98779
 88 /9ACFGBA8546378 8HBCD8687667AABDHC0648469AB008653468
 89 /0ABEFCC0887588698905577667999AB8864956790997653467
 90 /0ABEFCC0009699700AH7690978009BD0086A7770B906545668
 91 /00BGEA0899659080AA0769997577580776463446878554 789
 92 /A0AFDCB00098B0709776578663553586653532368654436676
 93 /A0AFFBA877669868766546755244357665353236865565 998
 94 /A98AC0976668009A088767877455468765 A976774334477 5
 95 /0080CAB977687667768767875366560 877D853442456600 2
 96 /0080CAB9887997678676787642675799879E95355368880082
 97 /098BCAA866576435535566542256357776 7A74355368880972
 98 /9860ABB977777656779909853377490ABACB8557669009B632
 99 /9650AB07577775345577977533764 0ADBBD063377689008722
100 /9857809646655544779 9A99757897AACBDC963398789 99A622
101 /6546900757533233879 9A97760808BFDBCA853389890ACB245

  THERE ARE  1.5600 PERCENT ZEROS
I=  51 J=   3 N=  51 M= 102
```

Figure 2.19. Case 4 - Angled Periodicity Area of Contact/Gap Distribution After 4 Increments of Displacement.

```
 56 /2445537976464485599764442366433535576774678776 4655
 57 /2445535768664492698543424506668567856646775444654
 58 /25589799BA8877A7ACA665532469566766899887776433 4655
 59 /133766887977558356732231 14634666577666688865569 76
 60 /155765787088568568045453137963688809666698865568 77
 61 /154554665766337556976895358954700A0067779564357888
 62 / 432457768652253347657721346356 90A9734448566579776
 63 / 553578879764476770978721245234677641222868867756 6
 64 / 342245768654475469968213562335665423328688677576
 65 / 231356879543352259089721344244679653444880 08A8666
 66 / 232478089654441159A3861 243244668764445090080654 3
 67 / 232466978455652269B907324321346676422227788685332
 68 / 134699C984544323700C9751 2 33560A9863459CBDDB08542
 69 / 13366697634321237 9A754  2 335689853 12489BA97741
 70 /  335558663421 23700643  1 213467631 12380CA07652
 71 /  44788B9855444908DE9952447678098 52 1369ADBA96753
 72 /  55788B96332440AADEB086344768900952 13690A9786631
 73 /  45667B9411145990EDA864 12335788731  1498A9886753
 74 / 2678898A7311347790CA864 4566898651   2509D09553 2
 75 / 27799008631266380FFC9851576680885211 2499C9845314
 76 /12657788642  23457CB0675269878088 6322 1499A7856312
 77 /3464665631  14540AE0855215876787762243588BC8965124
 78 /35859989631 468ACCGB743 14666809774345 8ABA06732  3
 79 /2463777852  478JCBE0921  35568A97632136 0A985622  4
 80 /3574067842  4569B0CB7531146677086423124796555 11 15
 81 /3708C88731  5557BABB7531135567975214235 8A888843228
 82 /3697B8865311444608A953   48888A963141138DBA0832226
 83 /6800A9987432666008006 42 150090CD95362240098752 4326
 84 /680AA90876736678B0A974   47980BB8525224998764121 4
 85 /680BC009757265 5AB00732   367679A0626358B00AA966437
 86 /79ABC0985572544909941 2  147779CBA749560BABBA989878
 87 /79AAB986235144409972     36779B874274590AAA0976557
 88 /79ADE0963241566 0UAB6465445990BFA842624790886431246
 89 /890CDAA866536647678355544577790664273457877543 1245
 90 /890CDAA888747758890547875688708886495558078432 3446
 91 /880EC986774378689985477753553685542412246563325567
 92 /989UBA088876085875545564413313 6443131 146432214454
 93 /989DD0965544764654432453 3 22135443131 146433437776
 94 /9769A875444688798665456552332465433975455211225553
 95 /8868A907554654455465456531443487655B63122 2344886
 96 /8868A907665775456454 6542 453577657C7313314666886
 97 /8760A996443542113133 432  341355545952133146668 75
 98 /764890075555543455778763115527890 9A06335447887061
 99 /743890853555531233557553115428980 0B8411554678805
100 /763568742443332255779775356759 9A0BA7411765677794
101 /4324788535311 116577975548686 0D80A963116767 89A0 23

  THERE ARE  6.2200 PERCENT ZEROS
I=  51 J=  14 N=  51 M= 102
```

Figure 2.20. Case 4 - Angled Periodicity Area of Contact/Gap Distribution After 6 Increments of Displacement.

```
 56 / 223315754242263377542222 144211313354552456554243 3
 57 / 223313546442273476321122 238444634563442455322243 2
 58 / 336757769665595A944331 247344544677665554211243 3
 59 / 1154466575533613451  1   241244435544446664334754
 60 / 335435658663463468422231 157414666874444766433465 5
 61 / 32332443544115334754673136732588988455573421356 66
 62 / 21 23554643  311254355  124134789751222634435755 4
 63 / 331356657542254558756 5   23 1245542    6466455344
 64 / 12  2354643225324776 76  134 1134432 11 6466455354
 65 /  1 13465732113  378675  122 224574312226688696444
 66 /  1 25686743222  379664   21 224465422238788684321
 67 /  1 24475623343  4707851 21  1244542    556646311
 68 /  12477A7623221 158A753    1134897641237A0BB08632
 69 /  11444754121   1579532    113467631   267097552
 70 /  1133364412    1588421      124541    168A98543
 71 /  225660763322278OBC7763 2254568763   147980974531
 72 /  3356607411 22899BC0864122546788 73   14789756441
 73 /  23445072   23778C89642   11356651    27697664531
 74 /  456670951  12557BA9642 234467643     387887331
 75 /  557788641  44668DUA763 354468663     277A76231 2
 76 /  43556642    1235A03453 4765686641    277956341
 77 /124244341    23689C8633  365456554  213600A6743  2
 78 /1363776741  2469AAE0521  24446875521236909845 1   1
 79 / 24155563   2568A0C83    1334697541  14897634    2
 80 /135284562   234708A0531  244558642 1  2574333    3
 81 /1586A6651   333509B0531  13345753  2 1369666621  6
 82 /1475066431  222486975 1  266669741 2  16809861   4
 83 /46389776521 4448868842   38878AB7314  2887653 21 4
 84 /468997865451445008972 2   257680063 3  2776542    2
 85 /4680A887535 433908851    145457984 413608899744215
 86 /5790A876335 32278772     25557A0952734809009767656
 87 /57990764 13 2228775      145570652 523789998754335
 88 /579BC8741 2 3448890424322377800962 4 257866421  24
 89 /678AB9964431442545611332235557844 2 51235655321  23
 90 /678AB9966652553667832565346658066427333685621 1224
 91 /668CA7645521564677632553133146332 2   243411 3345
 92 /767B0986665486365332134 22 11 14221 1   2421   2232
 93 /767BB8743322542432212 2311    13221 1   24211215554
 94 /754796532224665764432343 3 11 243211753233     3331
 95 /664697853324323234234231 221265433041     122664
 96 /6646978544355323423234 32  231355435A51 11 2444664
 97 /6548977422132   1 11221   12 13332373  11 2444653
 98 /542678853333321233556541  33 5678798411322566584
 99 /52167863133331  1133033 1  32 67088062  332456683
100 /54134652 22111  335575531345377980952  543455572
101 /21 25663131     435575332646488089741  45456798  1

  THERE ARE 17.4400 PERCENT ZEROS
I=  51 J=  15 N=  51 M= 102
```

Figure 2.21. Case 4 - Angled Periodicity Area of Contact/Gap Distribution After 8 Increments of Displacement.

```
 56 /    11 3532 2   4115532       22    1 113233 234332 211
 57 /    11 132422   512541        1622241234122 2331    21
 58 / 1145355474433737972211      251223224554433 2      211
 59 /  322443533114 123             2  22213322224442112532
 60 / 1132134364412412462  1      352 24446522225442112433
 61 / 1 11 221322  3112532451 1451 3667662333512  13444
 62 /     1332421  1   32133      2 1256753     4122135332
 63 / 11 13443532  323365343      1   2332      4244233122
 64 /      132421  31 255454     12   1221      4244233132
 65 /     124351   1  156453          23521     4466474222
 66 /     3464521      157442          22432    165664621
 67 /     22534 1121   258563          2232      3344241
 68 /    255954 1      369531        1267542   1598008641
 69 /    222532        35731         124541      4587533
 70 /    111422        3662            232       46976321
 71 /    34485411    3680A5541     32346541     2570875231
 72 /  11344852      6770A6642     32456651      256753422
 73 /   122385      1556A0742        13443       547544231
 74 /  23445873      33509742     12245421       16506511
 75 /  33556642    22446BB9541  132246441         55954 1
 76 /  2133442       13986231  254346442         5573412
 77 /  2 2212       1467A6411  143234332       148894521
 78 / 14155452     24799683      22246533     14787623
 79 /  2 33341     34098A01      11247532      2675412
 80 / 13 6234      125869831     2233642        352111      1
 81 / 3649443     1113870831     1123531       1474444      4
 82 / 25384421       264751      4444752        408764      2
 83 /246675543    222364662     166569051 2    665431      2
 84 /24677564323 223386733       35468841 1    55432
 85 /24689665313 21178663        23235762 2 1486677522   3
 86 /35789654113 1  3655          33359873 512687887545434
 87 /35778542  1     6553          2335843  3 1567776532113
 88 /3570A652     122667B2 21   15568874   2  356442       2
 89 /45690774221 22 3234  11   13335622   3  134331       1
 90 /45690774443 33144561 343124436844 2 51114634         2
 91 /446A954233  34245541 3331 11 2411         212    1123
 92 /5450876444326414311  12         2          2        1
 93 /5450065211  32 21      1         1          2      3332
 94 /53257431    244354221 1211       21    531 11      111
 95 /4424756311 21  11 21 121        4321182             442
 96 /442475632213312 1 121     1 13321393        222442
 97 /43267552    1                  111 151       222431
 98 /32 4566311111    1133432    11 34565762   1  344362
 99 /3  45641 1111      11311    1  4586684    11 234461
100 /32 1243           11335331 12315576873    32123335
101 /    3441 1        21335311 42426086752    23234576

  THERE ARE 35.7600 PERCENT ZEROS
I=  51 J=  16 N=  51 M= 102
```

Figure 2.22. Case 4 - Angled Periodicity Area of Contact/Gap Distribution After 10 Increments of Displacement.

```
 57 /        1 2     3  32          4    2  12      11
 58 /   2313325221151575          3    1  23322111
 59 /   1  221311   2   1                   11     222     31
 60 /   1  121422   2  24          13    22243     322     211
 61 /         1     1   31 23     23   144544 1113      1222
 62 /       11 2          1  11          34531     2     1311
 63 /      122131    1 1143121           11        2 22 11
 64 /        1 2     1   33232                     2 22 11 1
 65 /        213         34231           13        2244252
 66 /      12423         3522             21       434424
 67 /        312         30341            1        1122 2
 68 /      33732         14731           4532      37688642
 69 /        31          1351            232       2365311
 70 /        2           144              1        247541
 71 /     122632       34689332      1 12432       358653 1
 72 /     12263        45589642      1 23443       345312
 73 /       163        3349652          1221       325322 1
 74 /    1223651       1138752        232          43843
 75 /   1133442        22400732    1   2422        33732
 76 /     1122           1704 1    3212422        33512
 77 /                   245942     21 1211        266723
 78 /   2 3323         2577461        24311      25654 1
 79 /     1112       1247694          2531        4532
 80 /   1 4 12         364701         1142        13
 81 /  1427221         165861          131        252222     2
 82 /   31622           4253        222253        286542
 83 /  24453321        44244       4434783        44321
 84 /  24553421 1     1664531      1324662        3321
 85 /  24674431 1      56441        1 1354       2644553     1
 86 /13567432   1      3433        11137651 3   465665323212
 87 /1355632           4331         113621   1   34555431    1
 88 /1358943           4456        3346052       13422
 89 /23478552          1 12        11134     1    1211
 90 /234/8552221 11  2234   121   2214622   3    2412
 91 /2249732 11   12 2332   111       2                      1
 92 /32386542221 42 21
 93 /3238843       1                                        111
 94 /31 3521       22132                    31
 95 /22 25341                             21    6           22
 96 /22 25341    11                       11   171          22
 97 /21 4533                                    3           21
 98 /1   23441             1121          1234354        12214
 99 /1   2342                1           2364462         1224
100 /1     21              11311      1 3354651    1    1113
101 /      122             1131    2 2 486453       1 12354

  THERE ARE 58.2000 PERCENT ZEROS
I=    8 J= 102 N=  51 M= 102
```

Figure 2.23. Case 4 - Angled Periodicity. Area of Contact/Gap Distribution After 12 Increments of Displacement.

```
 57 /          1     2  21          3    1    1
 58 /   12 221411    4 464          2         12211
 59 /      11 2      1                                111      2
 60 /       1 311    1  13          2    11132      211      1
 61 /                   2  12    12    33433      2         111
 62 /          1                     .  2342      1       2
 63 /       11 2          32 1                     1 11
 64 /          1          22121                    1 11
 65 /       1 2           2312            2       1136141
 66 /       1312          2411            1       323313
 67 /       2 1           2523                      11 1
 68 /      22621          302             3421     26577531
 69 /        2            24              121       12542
 70 /        1            33                        13643
 71 /      11521        23578221          1321       247542
 72 /      1152         34476531         12332       2342 1
 73 /        52         2238741            11        214211
 74 /     11254           27041           121        32732
 75 /     22331        11399621           1311       22621
 76 /       11            653          21 1311       224 1
 77 /                   134831         1    1         155612
 78 /  1 2212          146605             132       14543
 79 /        1         136583             142        3421
 80 /     3  1          25365              31         2
 81 /  31611             5475              2         141111      1
 82 /  2 511             3142           111142       175431
 83 / 1334221           33133          3323672       3321
 84 / 1344231           55342           213551       221
 85 / 1356332           4533               243      1533442
 86 / 2456321           2322              2654   2  3545542121 1
 87 / 244521            322                251      2344432
 88 / 247832            5345           2235941       2311
 89 /12367441              1               23          1
 90 /1236744111         1123    1     11 3511   2    13 1
 91 /1138621         1 1221                1
 92 /2127543111   31 1
 93 /2127732
 94 /2  241       11 21                          2
 95 /11 1423                                 1    5              11
 96 /11 1423                                      6              11
 97 /1  3422                                      2              1
 98 /   1233                  1                  123243        11 3
 99 /   1231                                    1253351         113
100 /     1                   2                 224354            2
101 /     11                  2     1 1 375342                  1243

 THERE ARE 68.6200 PERCENT ZEROS
```

Figure 2.24. Case 4 - Angled Periodicity Area of Contact/Gap Distribution After 13 Increments of Displacement.

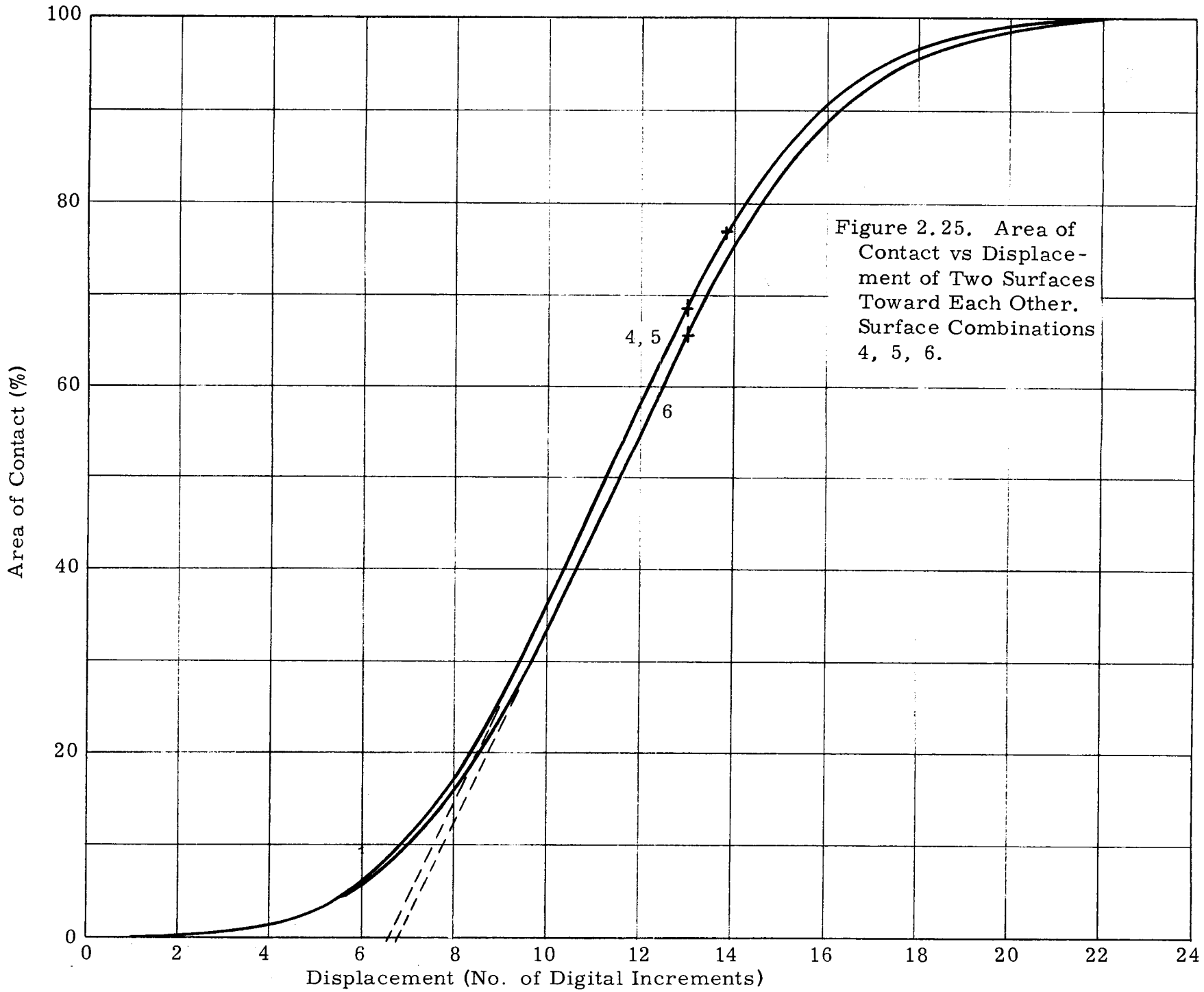

Figure 2.25. Area of Contact vs Displacement of Two Surfaces Toward Each Other. Surface Combinations 4, 5, 6.

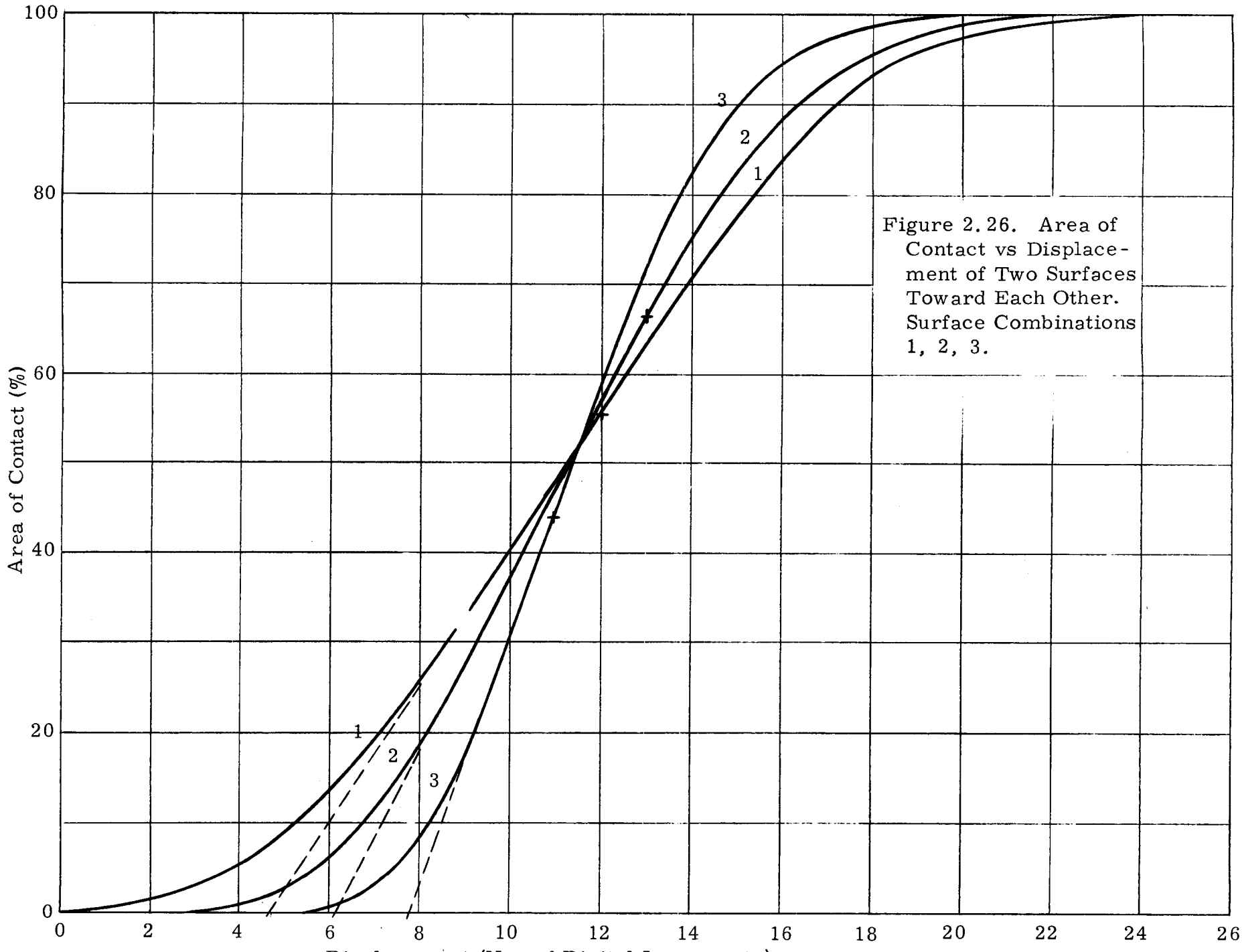

Figure 2.26. Area of Contact vs Displacement of Two Surfaces Toward Each Other. Surface Combinations 1, 2, 3.

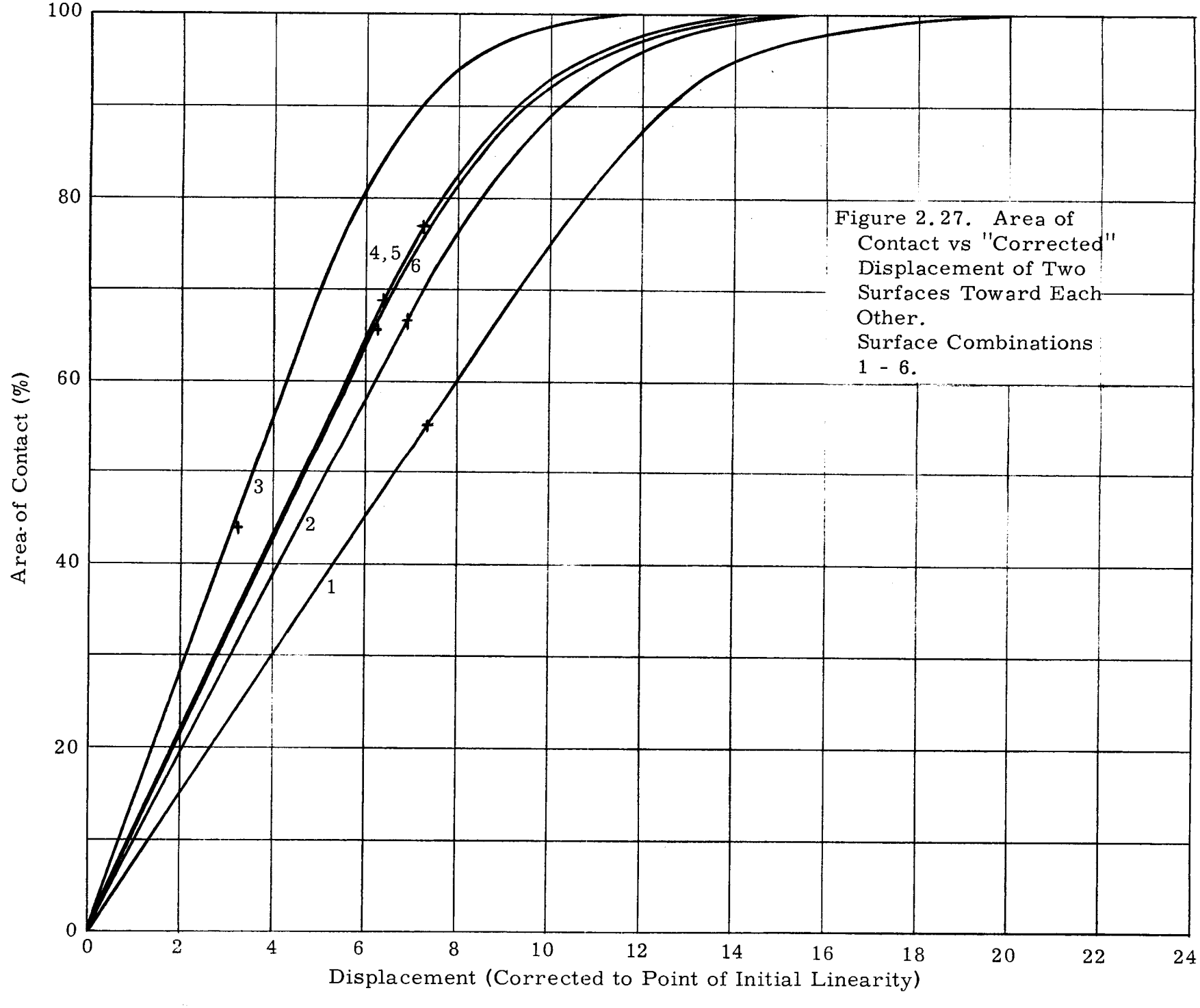

Figure 2.27. Area of Contact vs "Corrected" Displacement of Two Surfaces Toward Each Other.
Surface Combinations 1 - 6.

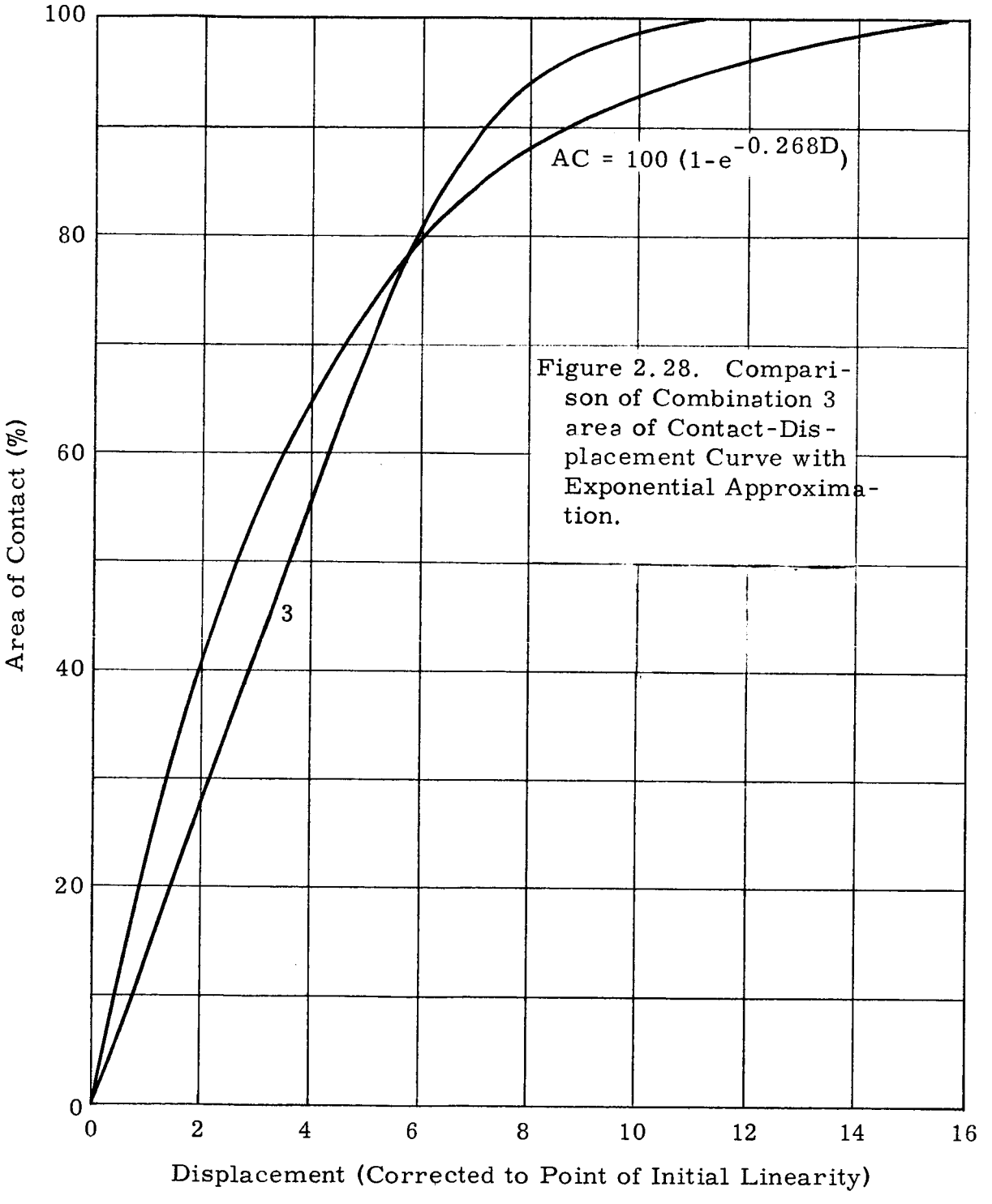

Figure 2.28. Comparison of Combination 3 area of Contact-Displacement Curve with Exponential Approximation.

3. Advanced Leakage Experiments

3.1 Introduction

As mentioned in the previous quarterly report, the purpose of this task is to broaden the scope of experimental information concerning various sealing systems by extending the capability of the experimental apparatus to operation in a -321°F to +700°F temperature range. The test fixture in its modified form was described and pictured. Since that time, a definite test program has evolved along with some preliminary test results. The accessory hot and cold parts were fabricated and successfully tested. This describes the proposed test program and then the test results obtained to date.

3.2 Proposed Test Program

Table 3.1 shows the proposed test program, illustrating the various sealing surface combinations. Basically, three categories will be investigated: elastomers, plastics and metals. The elastomers and plastics will be studied at the -321°F temperature. The metallic systems will be viewed both at this low temperature and at a temperature high enough to reduce the yield strength of the weaker component to 80 percent of its room temperature value. The last column of the table indicates the maximum temperature of each test, the limitation being the sensitivity of the metallic seal/gasket component with temperature. Various references were reviewed for the yield strength versus temperature information for the data shown in other figures herein.

A number of the proposed tests are similar to those made at ambient temperature in an earlier phase of this contract. The tests as well as the description of the surfaces in the column noted in Table 3.1 are described in Volume III of the Final Report for Phase I of this contract and the second contract period Final Report, June, 1964. The gasket surfaces will be approximately the same as those used for the previous tests. The tests made with elastomers and plastics employed a slightly different surface in past tests than the fine machined surfaces planned for future tests. Previous tests were made with a medium roughness circumferentially machined surface, slightly coarser than the surface to be used now.

Whenever two aluminum seal surfaces are to be used, 6061-T6 aluminum will be employed. This is necessitated by the requirement of welding the inlet tube to the lower half of the test sample. Aluminum of 2024-T4 grade is not readily weldable.

3.3 Progress to Date

All components of the test fixture have been fabricated, including the split oven and cryogenic enclosure. Figures 3.1 and 3.2 are indications of performance of the oven and cryogenic chamber. They are plots of temperature versus time

for a typical temperature test. The temperature is sensed by a thermocouple adjacent to the seal surface.

Three separate seal tests have been made, each with some measure of success. The first test was a gasket test employing 1100-0 aluminum as the gasket with stainless steel (type 347) as sealing surfaces. The fine machined profile was used in this test on the stainless surfaces. Phase I test data was taken as in past tests (Volume 3 final report) at room temperature. Phase II was accomplished, this time with the introduction of 6000 psi helium gas pressure. Phase III was accomplished by increasing the stress on the gasket until the leak was quelled. At this point in the test, the temperature was lowered to the liquid nitrogen temperature (-321°F). No further increase in leakage was recorded, and the stress was removed, thereby resulting in Phase IV, still at cryogenic temperature (Figure 3.3). A second part of this test resulted in repetition of the just described portion, using the same gasket but increasing the temperature to +700°F. These test results will not be illustrated because of the inability to reduce the data properly. At the conclusion of the hot test, the gasket was observed to be severely deformed and conclusive stress data could not be derived. The final gasket thickness was about 1/2 of the original, with the gasket area roughly 2.8 times that of the original.

Reduction of data for the first half of the test was made by utilizing load-deformation data of a similar material gasket and the same seal surfaces.

Especially notable is the large difference in stress for Phase III. At present the large increment of stress required for sealing at high pressure over that at one atmosphere is attributed to the higher 6000 psi pressure.

A second similar test, however, resulted in contrary results (Figure 3.4). This test was essentially a repeat of the first using an 1100-F aluminum gasket which had been annealed prior to machining to the 1100-0 state. The same stainless steel surfaces used for the first test were used here. The data were taken only at room temperature. The attempt to go to cryogenic temperature resulted in a leak occurring at the indiun vacuum seal, making further testing impossible. To be noted in this test, however, is the similarity of the Phase I with that of the first test. Phases II and III, however, are entirely different from the first test. An increase in internal pressure to 600 psi resulted in no greater leakage and hence no Phase III was required.

A third test (Figure 3.5) was a metal to metal test without a gasket. The seal surfaces were in high relief from the remaining structural mass by .030 inches. Aluminum 2024-T4 and type 347 stainless steel were the seal materials utilized, each with a fine circumferentially machined surface. Two attempts were made to complete Phase I for this test, the second immediately following the first without disturbing the test set-up. As can be noted, the leak was never quelled in the first attempt (Curve A) even though the normalized

stress was raised to 2.4 times the yield strength of the stainless steel(≈35,000 psi).

The normal load was removed and then reapplied without distrubing the test set-up. These data resulted in Curve B of Figure 3.5. With a stress of 2.4 times the yield strength of the stainless steel, measurable leakage still occurred. At this point, it was decided to disassemble the seal pieces for visual inspection. Nothing out of the ordinary was evidenced. A Talysurf profile test was made and showed both materials had yielded at the surface, the aluminum apparently more so than the stainless steel.

3.4 Future Work

Future work will involve attempts to resolve some of the questions raised by the just described tests. A non-uniformity of results was noticed and hopefully will be resolved (Tests #1M and #3M). The metal-to-metal test will be repeated going to higher loads before a conclusion can be made as to sealability.

Further work will be done to optimize or improve the sealing ability of the vacuum seal to enhance its reliability. A few seal tests were shortened by inability of the seal to operate properly at the low temperature. A spring loading feature is contemplated to overcome this difficulty without sacrifice of the liquid metal seal capability at the high temperatures.

TABLE 3.1

PROPOSED TEST SYSTEMS

Test Number	Seal Material	Seal Surface	Gasket	Temp. Range (^{o}F)
1	347S.S.	FM	1100-0 Al.	R.T. to -321 to +250
2	347S.S.	FM	Silicone Rubber	R.T. to -321
3	347S.S.	FM	Kel-F	R.T. to -321
4	347S.S.	FM	Teflon FEP	R.T. to -321
* 5	347S.S.	FM	Teflon TFE	R.T. to -321
* 6	347S.S.	FM	Viton A	R.T. to -321
* 7	347S.S.	FM	Neoprene	R.T. to -321
8	347S.S.	CM	Copper	R.T. to -321 to +400
9	347S.S.	CM	Nickel	R.T. to -321 to +400
10	347S.S.	RG	1100-0 Al.	R.T. to -321 to +250
11	347S.S.	RG	Copper	R.T. to -321 to +400
12	347S.S.	RG	Nickel	R.T. to -321 to +400
13	347S.S. & 2024-T4 Al	FM	---	R.T. to -321 to +300
14	6061-Al & 6061-Al	FM	1100-0 Al.	R.T. to -321 to +250
15	6061-Al & 6061-Al	FM	Copper	R.T. to -321 to +315
16	347S.S. & 2024-T4 Al	CM	---	R.T. to -321 to +300
17	6061-Al & 6061-Al	FM	Nickel	R.T. to -321 to +315
18	6061-Al & 6061-Al	CM	1100-0 Al.	R.T. to -321 to +250
19	347S.S. & 2024-T4 Al	RG	---	R.T. to -321 to +300
20	347S.S. & 347S.S.	RG	---	R.T. to -321 to +400
21	6061-Al to 6061-Al	FM	---	R.T. to -321 to +315
22	347S.S. & 347S.S.	FM	---	R.T. to -321 to +400
23	6061-Al & 6061-Al	CM	---	R.T. to -321 to +315
24	347S.S. to 347S.S.	CM	---	R.T. to -321 to +400
25	6061-Al to 6061-Al	RG	---	R.T. to -321 to +315

Code:

FM fine circumferential machining
CM coarse circumferential machining
RG radically ground

* Order determined by time of receipt of material.

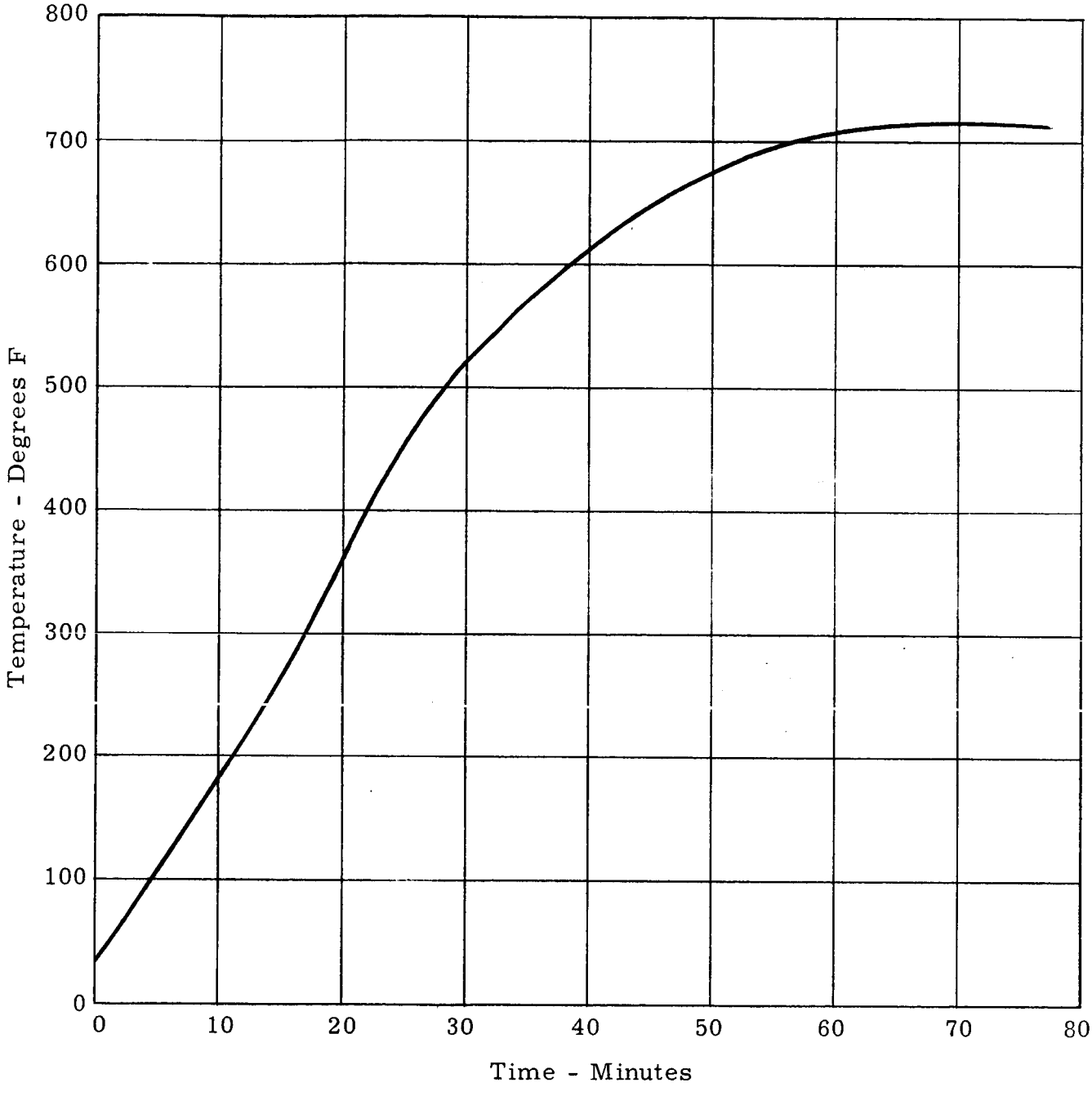

Figure 3.1. Seal temperature vs. time for a typical high temperature test.

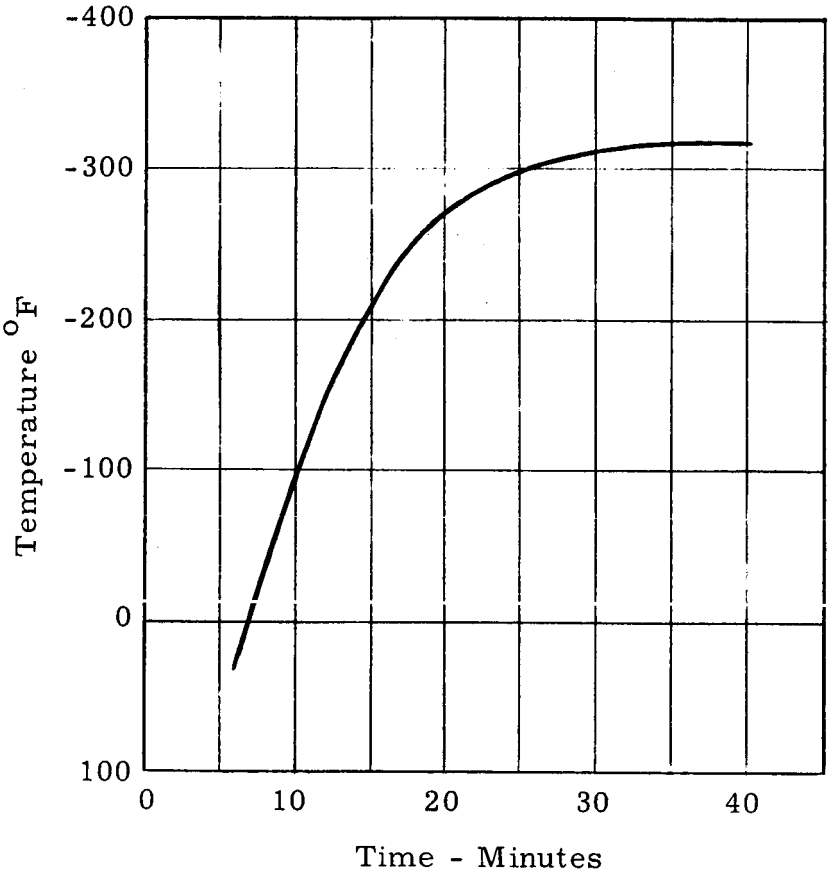

Figure 3.2. Seal temperature vs. time for a typical low temperature test.

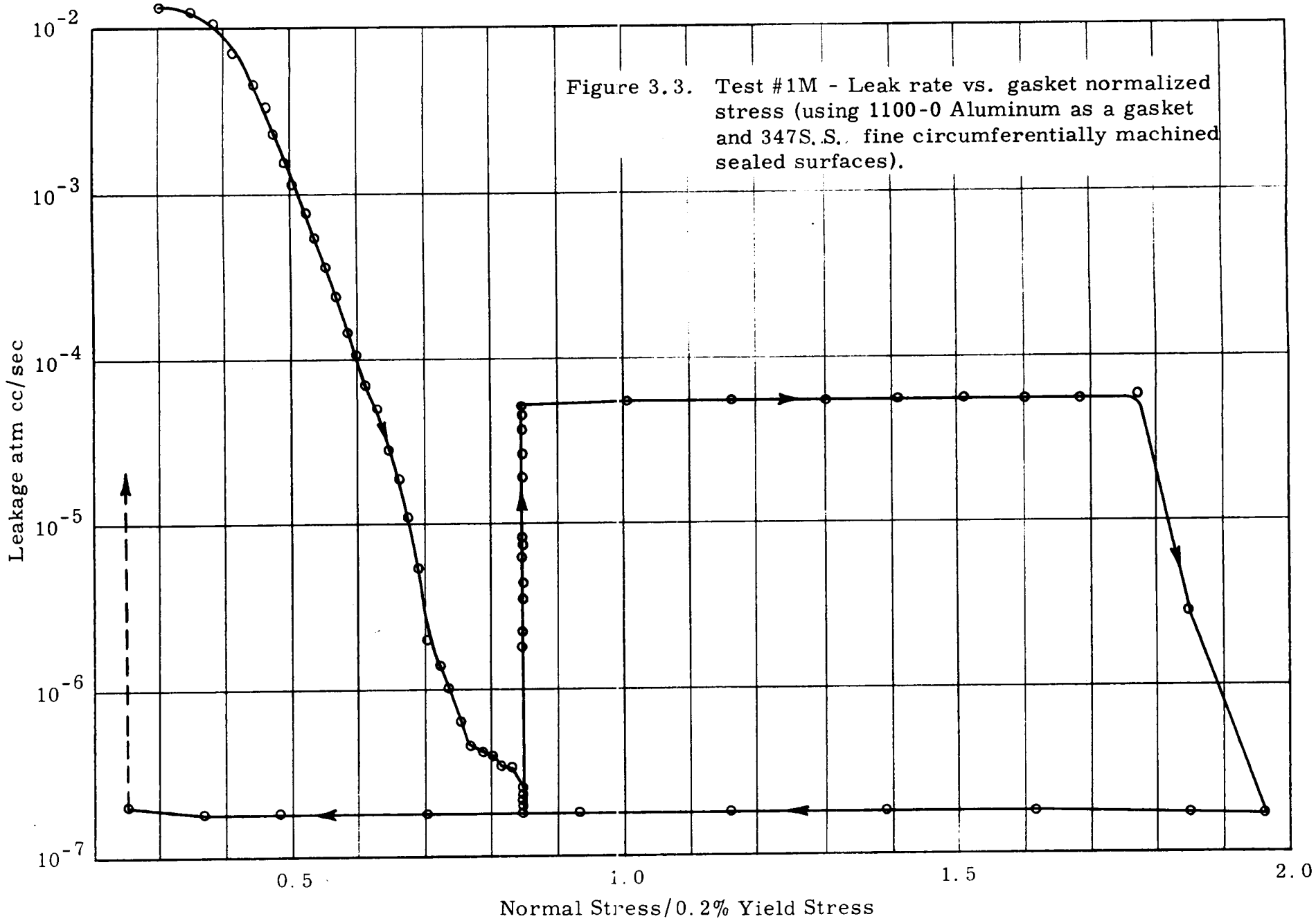

Figure 3.3. Test #1M - Leak rate vs. gasket normalized stress (using 1100-0 Aluminum as a gasket and 347S.S. fine circumferentially machined sealed surfaces).

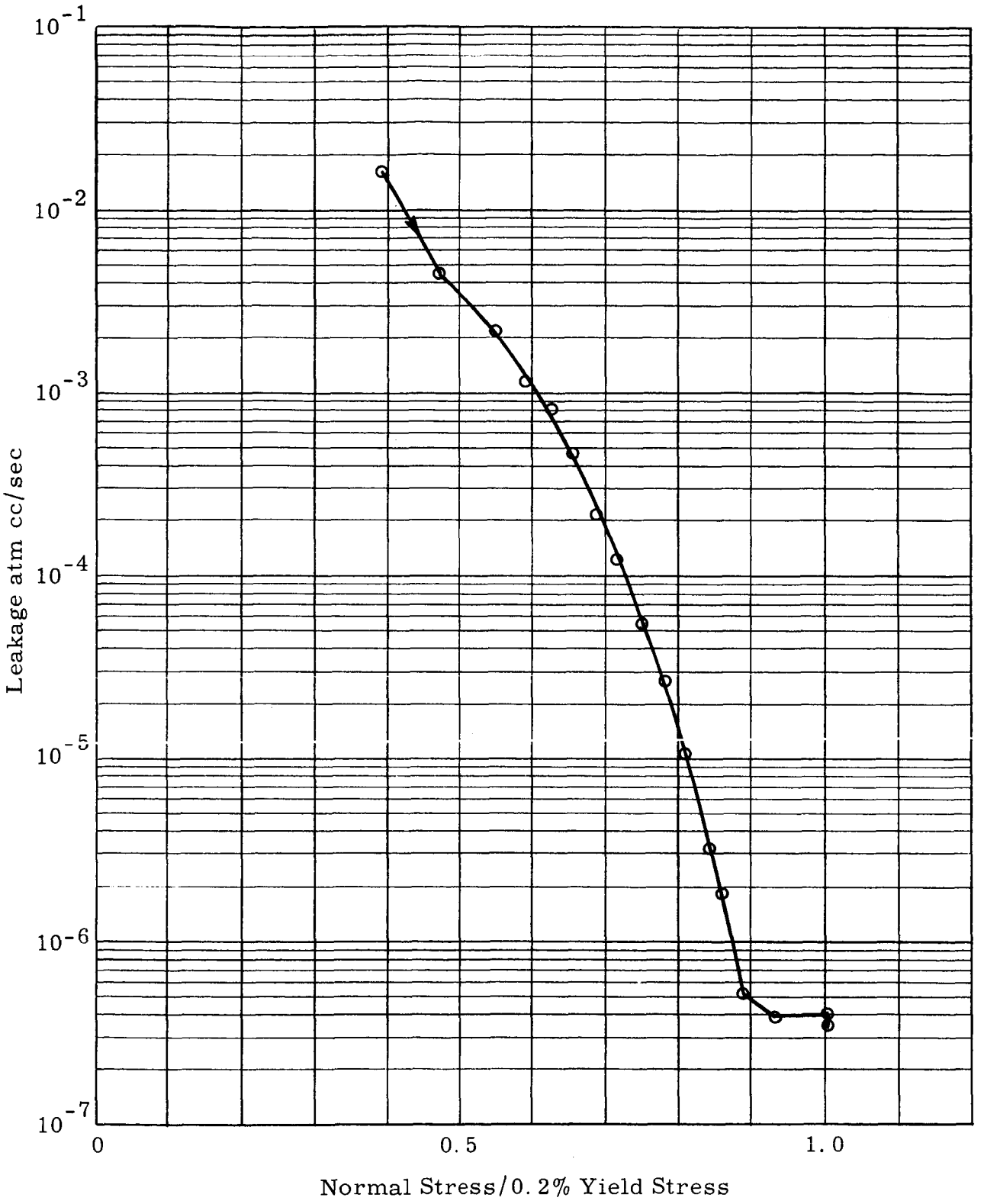

Figure 3.4. Test #3M - Leak vs. normalized stress for 1100-0 aluminum with 347S..S.. seal surfaces, fine circumferentially machined.

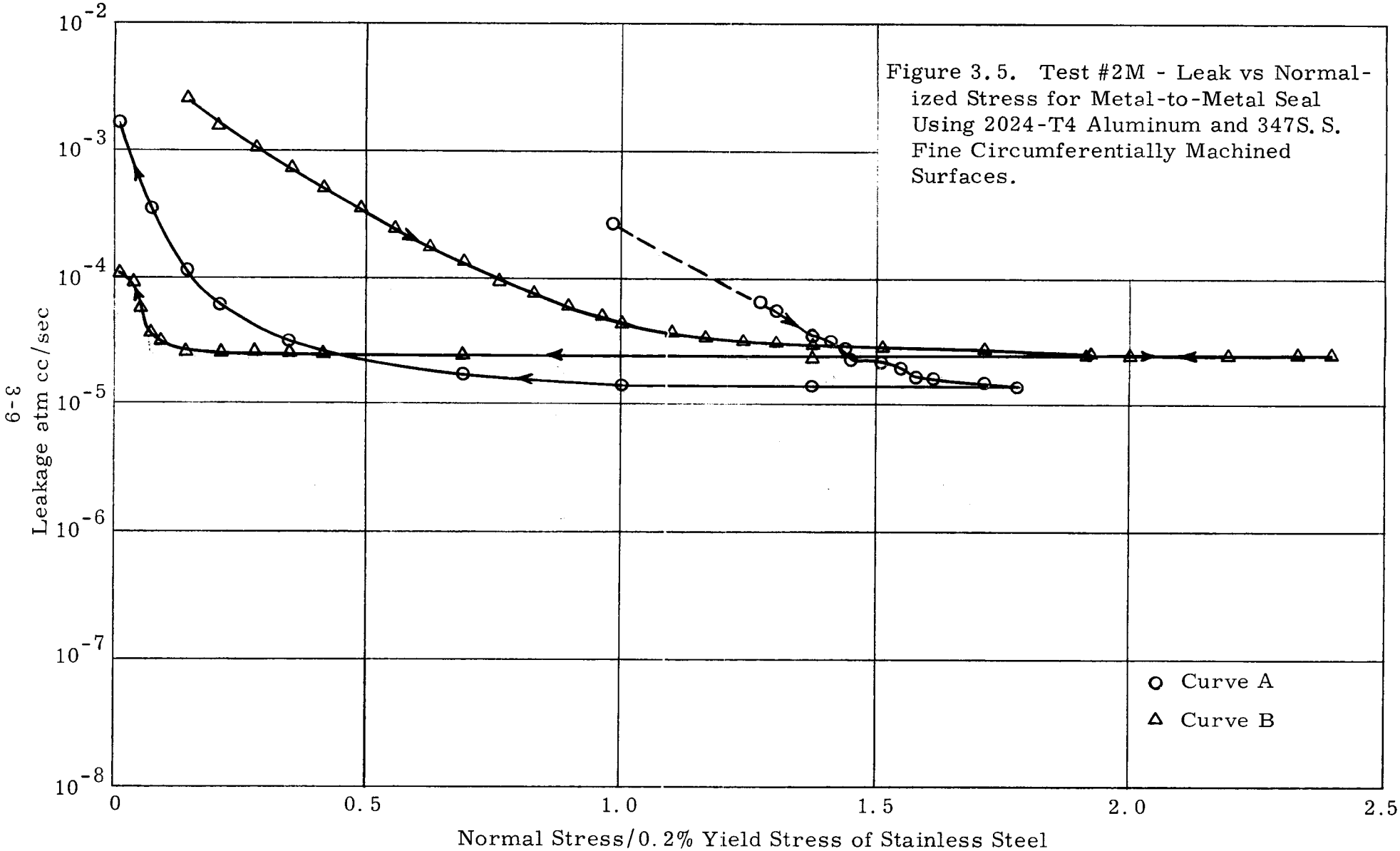

Figure 3.5. Test #2M - Leak vs Normalized Stress for Metal-to-Metal Seal Using 2024-T4 Aluminum and 347S.S. Fine Circumferentially Machined Surfaces.

4. Tube Connector Utilizing Superfinished Sealing Principle

4.1 Introduction

In the previous quarterly report, it was concluded that the connector will be made of either a regular stainless austenitic steel or the superalloy A-286. It was also found that several materials problems would make it necessary to complete a preliminary test program before the final design could be attained. This test program would aim at answering the questions:

1. Does welding of the connector to the tubing deform the superfinished surface?
2. Can heat effects during the welding be limited such that the cold drawn properties of the 316 steel tubing are not affected?
3. If A-286 is used, it must normally be welded in the annealed (soft) condition and then heat treated. Thus, the heat treatment must be be made after the superfinish has been applied to the seal surface. Does this procedure affect the quality of the surface?
4. Can an acceptable superfinish be applied at all to an A-286 surface?

The test program, designed to answer all those questions, was presented in Section 4.4.3 of the previous quarterly report. At the time when that report was written, three test pieces had been designed and manufactured, and were sent out for superfinishing.

During the last contract period, most of the tests according to the program, with minor modifications, have been accomplished. Results and conclusions will be discussed in the remainder of this report.

One more task has been undertaken during this period. In the previous quarterly report it was concluded that a connector designed for 6000 psi and made of regular stainless steel would have to utilize a seal interface with a secondary load path. The secondary load path alternative has later been ruled out due to manufacturing difficulties. It has therefore been investigated whether a reduction of the design pressure from 6000 psi to 4000 psi will make a single load path type connector made of regular stainless steel feasible.

4.2 Conclusions and Recommendations

The conclusions which can be drawn from the efforts during this period are summarized below.

1. A-286 can be given an acceptable superfinish by using the technique employed by Jones Optical Works.

2. Heat treatment for hardening of A-286 affects both flatness and surface finish of the seal surface to a degree where it can be suspected that the sealing ability is reduced.

3. Welding connector and tubing together with TIG-weld does not change the surface finish, but warps the seal surface seriously. The method can primarily be ruled out. (The welding itself presents no problems.)

4. Electron beam welding has been successfully used to weld a fully hardened connector to the tubing, and does not affect the flatness of the seal surface seriously. The optimized welding parameters have not been established yet, but it is believed that in EB-welding a practical and satisfactory solution to the problem has been found.

5. The feasibility study for a 4000 psi connector shows that it, from seal interface considerations, can be designed for regular stainless steel and single load path.

It now has to be determined whether the connector shall be designed for 6000 or 4000 psi. In both cases EB-weld has to be employed. The 6000 psi connector must be made of a superalloy like A-286, the 4000 psi connector can be made of regular stainless steel, at the expense of increased weight and volume. It appears to be advantageous to use A-286 for both design pressures.

We plan the following work during the next reporting period.

1. Complete the EB-weld study. It looks now like it will offer the possibility of welding fully hardened A-286 to tubing without warping the seal surface or producing cracks. (If hardened material is weldable, the superfinish can be applied after the hardening, and that part of the problem is removed.)

2. Simultaneously, begin the final design of a connector, assuming that A-286 and EB-weld will be used.

4.3 Test Program

The three test pieces (No. 1 a separate flange, Nos. 2, 3 a flange + union, together with a nut forming a complete connector) were submitted to the following tests:

Sample 1

1	Superfinish
2	Measure flatness and surface structure

3 Heat treatment test (1325°F, 16 hours in vacuum)
4 Measure flatness and surface structure
5 The warped surface lapped flat at Research and Development Center, Buildings 5 and 37 shops
6 Measure flatness
7 Electron beam weld with Cu-heat shield
8 Measure flatness

Sample 2

1 Superfinish
2 Measure flatness and surface structure
3 TIG-weld (Fusion weld with inert gas protection)
4 Measure flatness and surface structure
5 Stress relieving (1600°F, 1 hour in vacuum)
6 Measure flatness and surface structure

Sample 3

1 Superfinish
2 Measure flatness and surface structure
3 Electron beam weld without Cu-heat shield
4 Measure flatness and surface structure

4.4 Discussion of Test Results

4.4.1 Quality of Superfinished A-286 Surface

All three test samples were superfinished simultaneously and showed similar surface structure and flatness.

The surfaces are shown in Figures 4.1 - 4.4. Except for randomly located pits caused by impurities (carbide precipitation) in the metal, the surface is extremely smooth. No scratches are deep enough to cause displacement of the interference lines (Figure 4.3). The Nomarski photos with higher magnification show very shallow, randomly oriented scratches. The surface finish obtainable for A-286 compares well with the stainless steel 347 samples which were superfinished earlier by Jones Optical Works.

Figure 4.4 shows the flatness of the whole seal surface. It is obvious that the flatness is well within the limit (1 helium band).

It should be noted that in Figure 4.4 and several other figures showing Lapmaster interference photos, many scratch-like marks can be seen in additon to the interference lines. Those are, however, scratches in the optically flat glass disc which is placed on the surface, and have nothing to do with the superfinished surface.

4.4.2 Hardening Heat Treatment of A-286

Test sample No. 1 was machined and superfinished in the soft, annealed condition. The recommended hardening heat treatment is 1325°F for 16 hours. The test sample was so treated in vacuum and allowed to vacuum cool in order to avoid any oxidation.

After the hardening, no changes were visible to the eye. No discoloring of any part was noted. However, the surface, as shown in Figures 4.5 - 4.7, was changed to some degree. Figure 4.5 (interference photo) and Figure 4.6 (Nomarski photo) show that a relocation of crystals has occurred during the hardening. This could have been expected since the hardening involves precipitation of a titanium carbide compound at the crystal boundaries. The maximum relative displacement of the crystals perpendicularly to the surface was measured by an optical interference method and found to be $1.5 - 1.6 \times 10^{-6}$ in (compared with the allowed 0.5×10^{-6} in).

Figure 4.7 shows the change in the surface flatness. Before the heat treatment the surface looked like Figure 4.4, afterwards like Figure 4.7. The latter is a convex surface combined with some rounding off at the seal edges. The degree of convexity is shown in Figure 4.7. Assuming a seal height of 0.10 in, to press two convex seals of this type into full contact with each other would require a seal stress of approximately 6000 lb/in^2 at the inner edge (at the same time as the seal stress is zero at the outer edge).

4.4.3 TIG-welding of Connector to Tubing

Test sample 2 was fusion welded with inert gas protection (TIG-weld) to 316 stainless tubing. The test setup and the weld are shown in Figure 4.8. In order to determine whether cold drawn properties of the tubing can be preserved during such welding, the temperature at point B (Figure 4.7) was monitored. (Compare Section 4.5.2 in the previous quarterly report.) Temperature at point A close to the superfinished surface was also monitored.

Figure 4.9 shows the temperatures at A and B during the welding. Peak temperature at B is approximately 900°F, which is more than the 700°F which is the maximum if the cold drawn strength properties of the tubing are to be preserved.

Figures 4.10 and 4.11 show the seal surface after the welding. Figure 4.11 compares well to Figures 4.1 - 4.2 and shows that no apparent change in suface structure has occurred. However, Figure 4.10 shows a serously warped seal surface, saddle-shaped, with a peak to peak deformation of approximately 140 μin. (Defined as minimum distance between two parallel flat surfaces which can enclose the seal surface.) This is definitely more warping than can be tolerated.

The welded piece was stress relieved (1600°F for 1 hour in vacuum). Figure 4.12 shows the resulting surface. It is still saddle-shaped.

The welding itself could be performed without difficulty and resulted in a very good looking weld. This shows that A-286 and Stainless 316 are compatible.

One way to reduce the varying of the seal surface, as pointed out in the previous quarterly report, Section 4.4.3, is to use a heat shield between the weld and the seal surface. This was tried for the Electron beam weld (next section) with negative results, and is therefore not expected to help the TIG-weld.

4.4.4 Electron Beam Welding of Connector to Tubing

Electron beam welding is a relatively new technique but is now practically available to solve welding problems. The heat is produced by a beam of electrons with energies in the range 10 - 15,000 ev. This beam can be made very narrow ($4\text{-}5\times10^{-3}$ in.) and makes an extremely fast welding technique possible wherein the total heat input necessary to perform a certain weld can be kept very low. The very fast process has also made it possible to weld materials which would not be compatible during welding with conventional means. For example, it has been possible to weld hardened super alloys without producing cracks.

Low total heat input will give small deformations of the welded pieces, which is what we desire to solve the connector welding problem.

Two pieces, test samples 1 and 3, have been welded to tubing by means of electron beam weld (EB-weld). The weld configuration was chosen with regard to the present design of the test pieces, and does not represent the final solution. The calculated sections of the welds are shown in Figure 4.13. The actual appearance of the welded pieces is shown in Figure 4.14.

Test sample 1 was welded first using a copper shield between weld and seal surface. Flatness before and after is shown in Figures 4.15 and 4.16. The surface is warped. However, it is believed that the warping is caused by the cu-collar. The collar was assembled around the connector and tightened before the weld. The engineer who made the weld observed thereafter the interference lines and found them not parallel but similar to Figure 4.10, i.e., the seal surface was saddle-shaped caused by the cu-collar. He then made the weld and later observed the interference lines again, finding an unchanged pattern. The new pattern shown in Figure 4.16 was obtained after removal of the collar.

It is believed that the cu-collar was pressed so hard against the connector (to obtain high thermal conductances) that it warped the surface

approximately 100 μin. elastically, and then during the weld some stress relieving caused the permanent deformation.

Test sample 3 was then welded using a narrower beam to produce less heat, and no cu-collar. Figures 4.17 and 4.18 show the flatness before and after. It is observed that the surface after the weld is flat well within the 1 H-band limit.

The first weld (test sample 1) was made on fully hardened A-286. It shows no cracks observable by microscope at the surface. The test piece has been vacuum checked for leakage and was found tight. It is currently being pressure tested and will thereafter be sectioned.

The second weld (test sample 3) was made on annealed A-286.

There is no risk that the seal surface structure is changed during EB-weld; the seal surface is much cooler than during a TIG-weld.

4.5 Feasibility Study of 4000 psi Convector

In the previous quarterly report it was concluded that a 6000 psi connector with single load path, made of a regular 300-series stainless steel was not feasible.

Since then the double load path alternative has been ruled out because of manufacturing problems. It has therefore now been investigated whether a change from 6000 psi to 4000 psi would make the connector feasible. The study will not be described in detail in that similar calculations were shown in the last quarterly report. Only the result will be mentioned.

1. The change in pressure changes the allowable seal stress variation from 10,000 psi to approximately 13,000 psi if the target 3×10^{-6} atm cc/sec leaves unchanged (compare previous quarterly report, Section 4.6.2).

2. The seal stress variation due to internal pressures and external loads changes. (It is assumed that the external vibration loads are not changed.) Comparing to previous quarterly report Section 4.6.3, the calculation results change in the following way:

F_a:	3829	→	2945 lbs
F_{as}:	807	→	538 lbs
F_n:	F_p + 1314	→	F_p + 1003 lbs
F_3:	F_p - 2481	→	F_p - 1924 lbs
ΔF_3:	2481	→	1924 lbs
$\Delta \sigma_{seal}$:	9530	→	7240 lbs/in^2

The thermal transient calculation does not change.

Since $\Delta\sigma_{seal}$ = 7,240 psi is now considerably below the allowable seal stress variation, 13,000 psi, it is considered that a single load path, regular stainless steel, superfinished seal 3/4 inch connector designed for 4000 psi operating pressure is feasible. However, a design using A-286 or another strong alloy will naturally result in a considerably lighter weight connector. The EB-weld will still have to be used if regular stainless steel is used as connector materials.

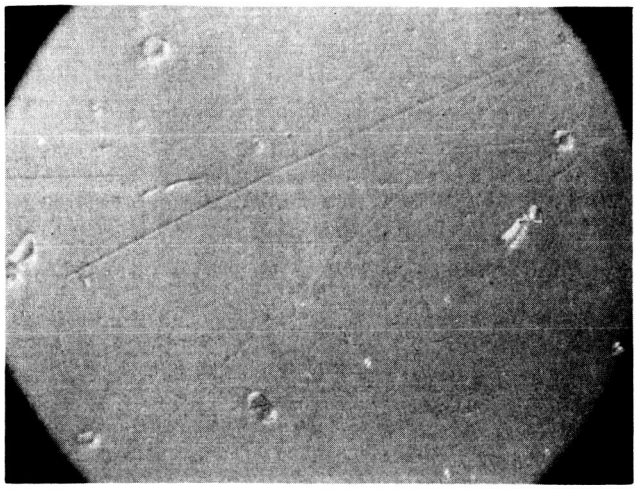

Figure 4.1. Nomarski Micro-photo of Superfinished A-286 Surface (Sample 1) Magnification 460 x.
Finish Made by Jones Optical Works.

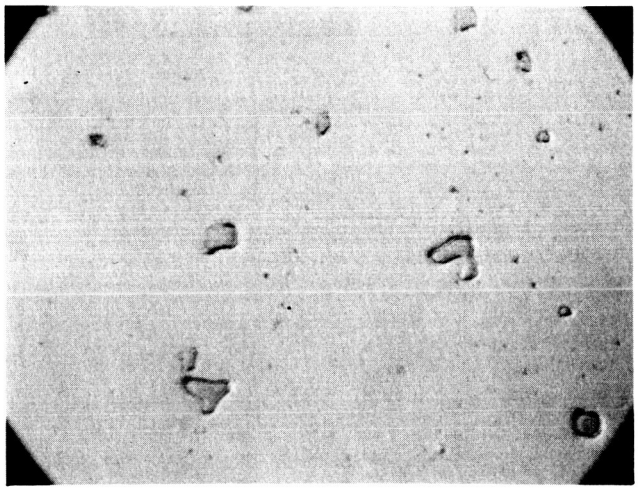

Figure 4.2. Nomarski Micro-photo of Superfinished A-286 Surface (Sample 2) Magnification 460 x.
Finish Made by Jones Optical Works.

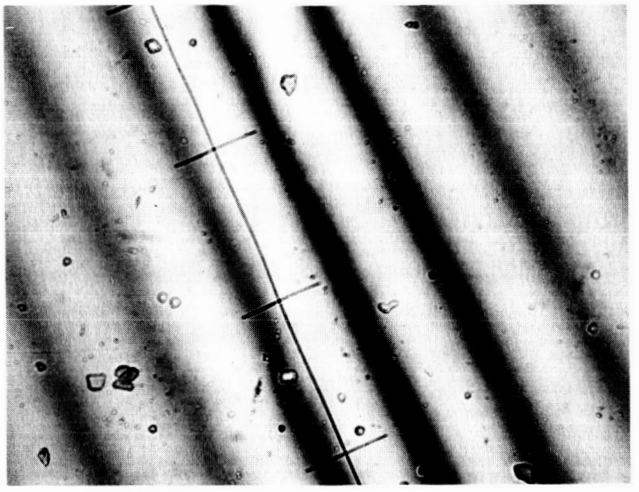

Figure 4.3. Interference Photo (Helium Light) of Superfinished A-286 Surface (Sample 1) Magnification 200 x.

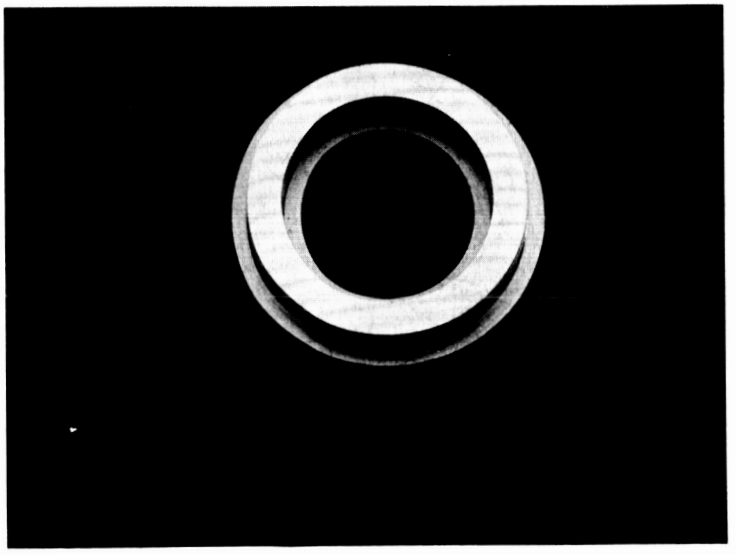

Figure 4.4. Lapmaster Interference Photo (Helium Light) of Superfinished A-286 Surface (Sample 1) 11.8 · 10^{-6} in Between Interference Lines.
Visible Scratches Exist in Lapmaster Glass.

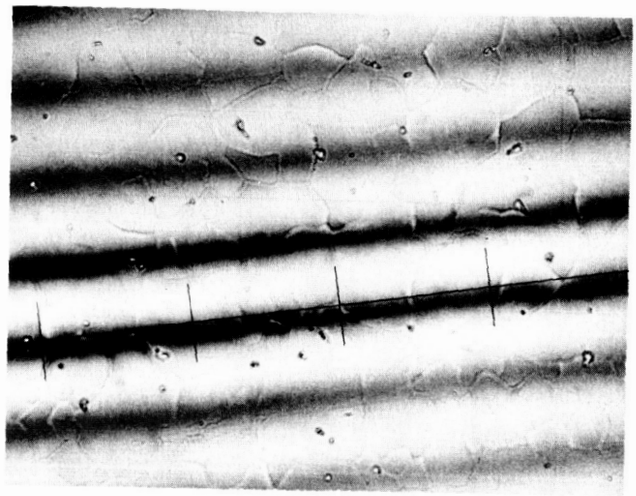

Figure 4.5. Interference Micro-photo (Helium Light) of A-286 Surface After Hardening (Magnification 200 x).

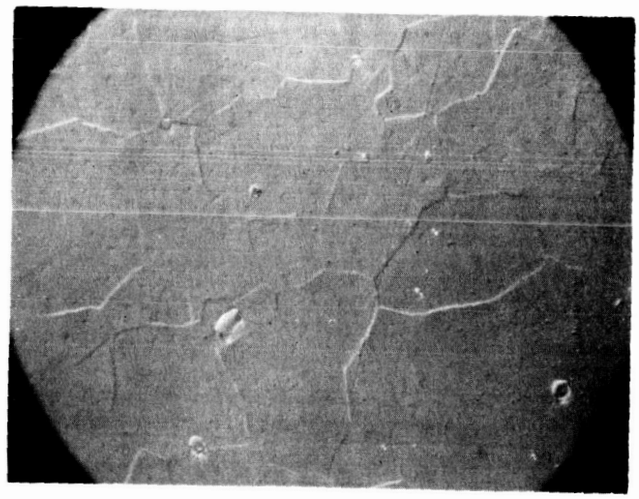

Figure 4.6. Nomarski Micro-photo of A-286 Surface After Hardening (Magnification 460 x).

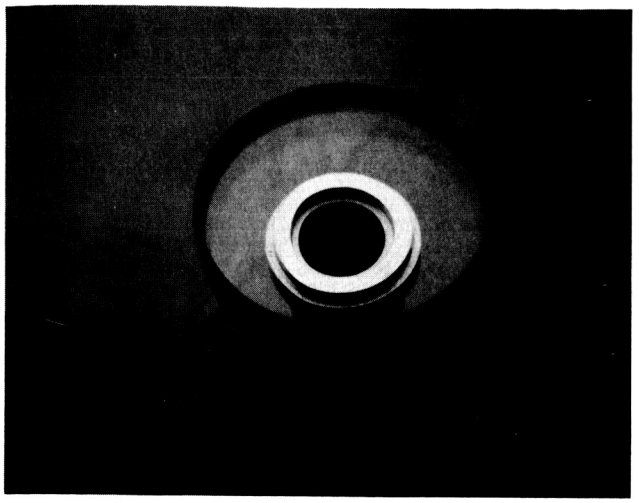

a)

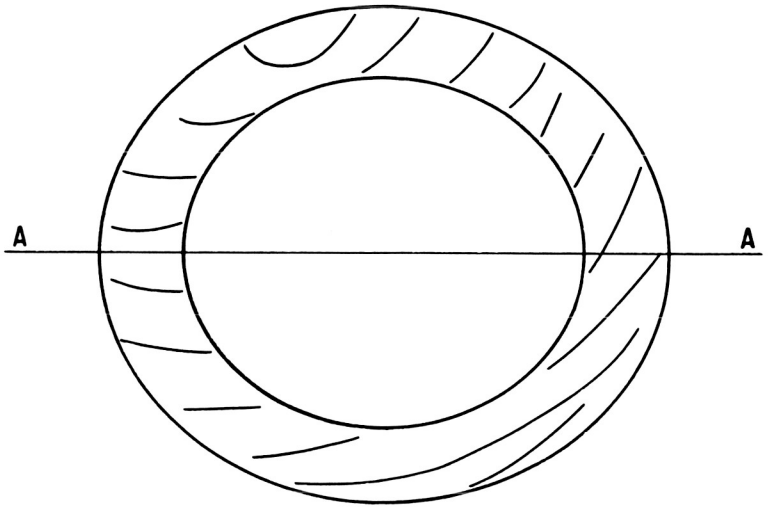

b)

Approximate Array of Lines

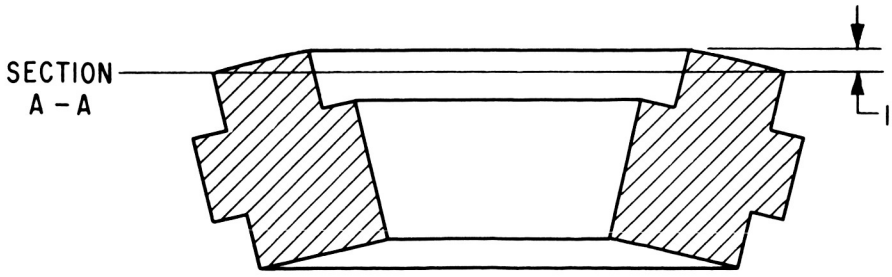

c)

Figure 4.7. A-286 Surface After Hardening.

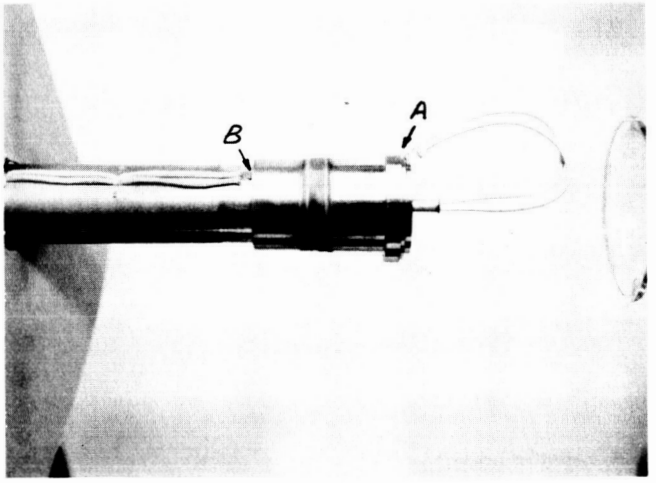

a)

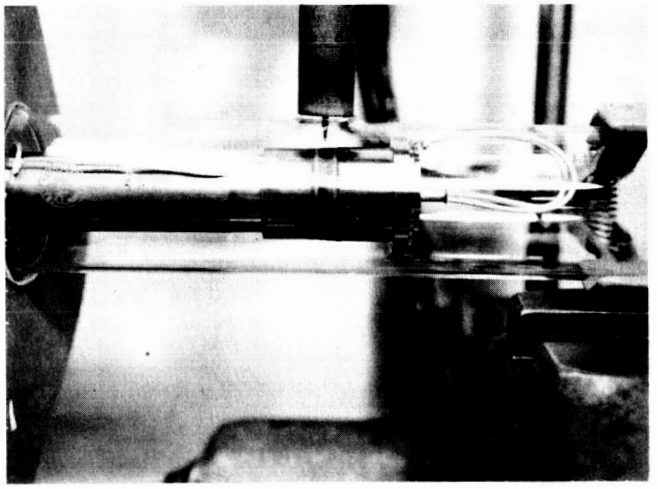

b)

Figure 4.8. TIG - Welding of Connector to Tubing.

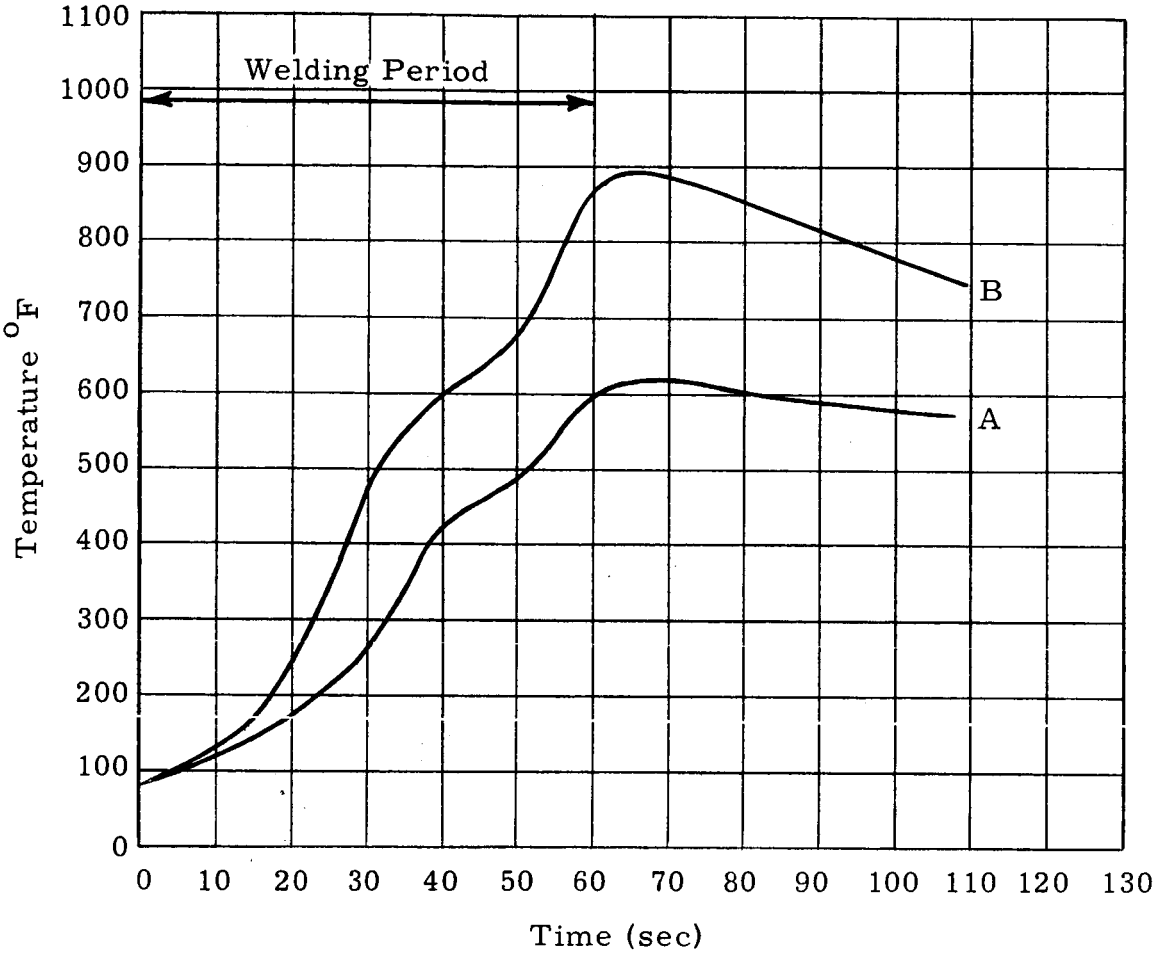

Figure 4.9. Temperatures monitored during TIG-welding of connector to tubing.

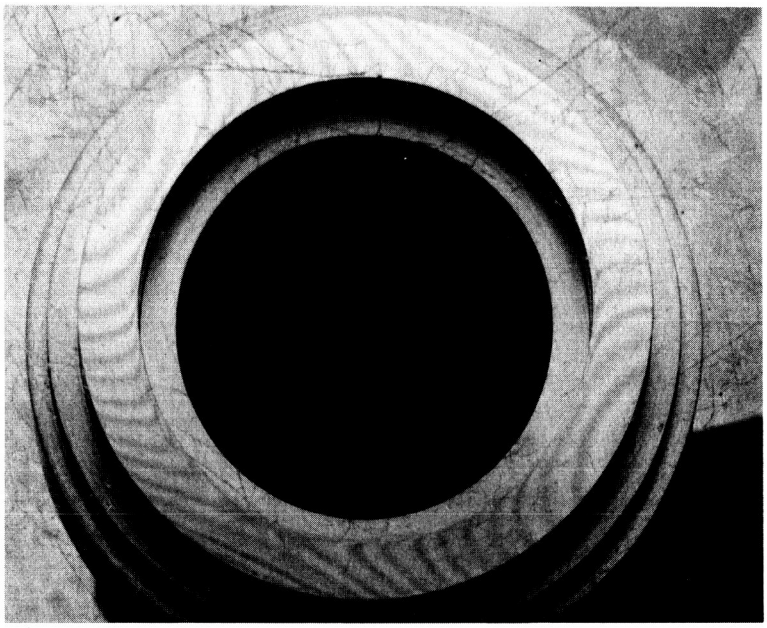

Figure 4.10. Lapmaster Interference Photo of Seal Surface After TIG - Welding of Connector to Tubing.

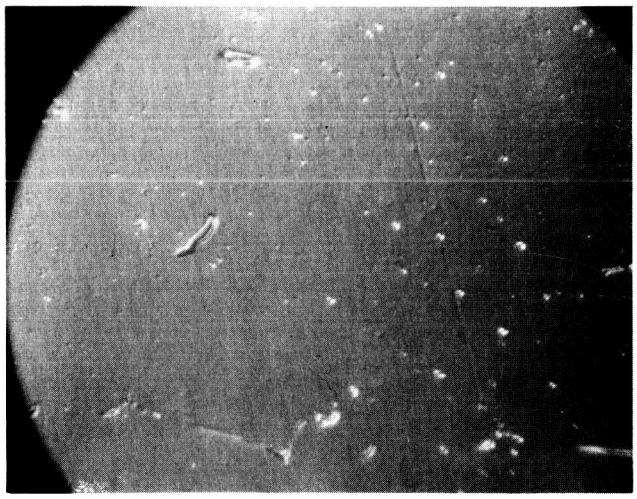

Figure 4.11. Nomarski Micro-photo of Seal Surface in Figure 4.10. (Magnification 460 x).

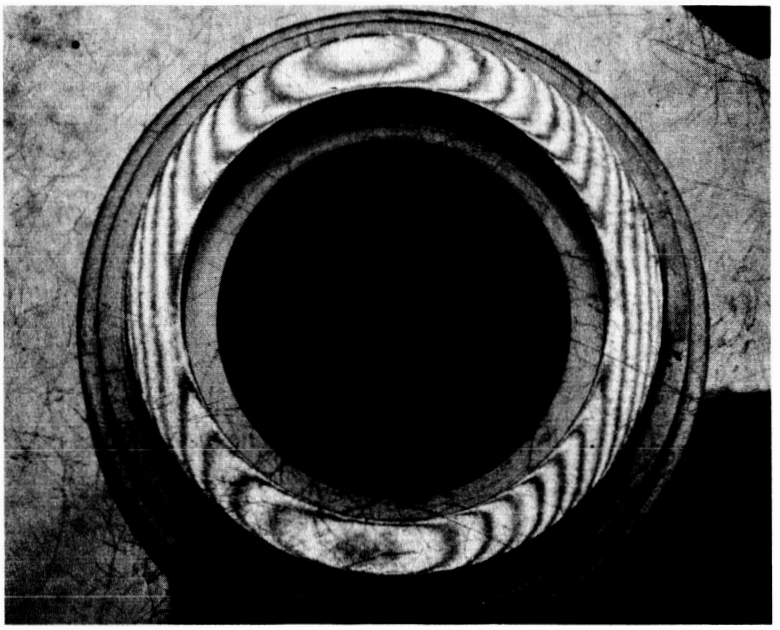

Figure 4.12. Lapmaster Interference Photo of Seal Surface After Welding of Connector to Tubing and Following Stress Relieving.

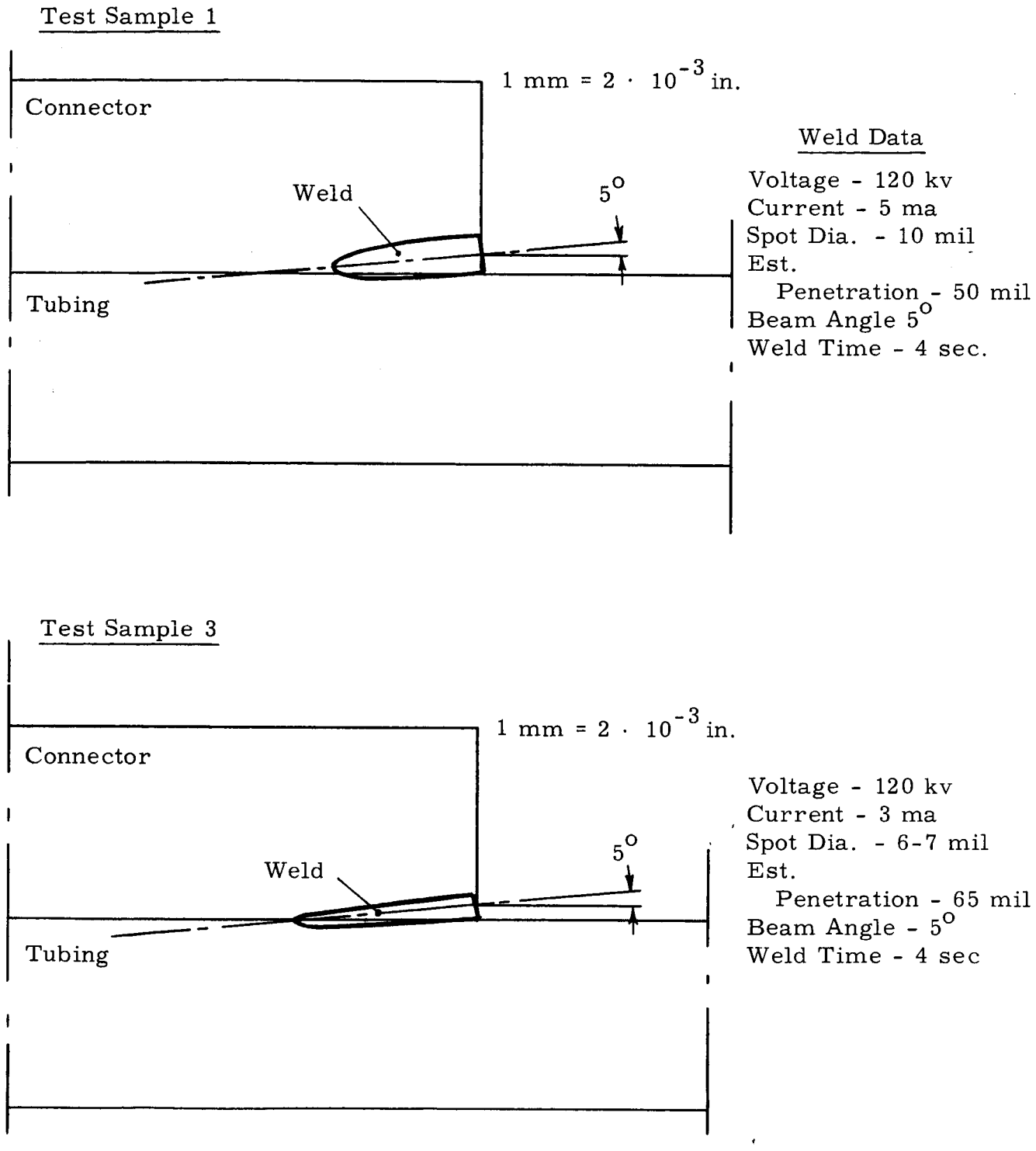

Figure 4.13. Electron beam welds.

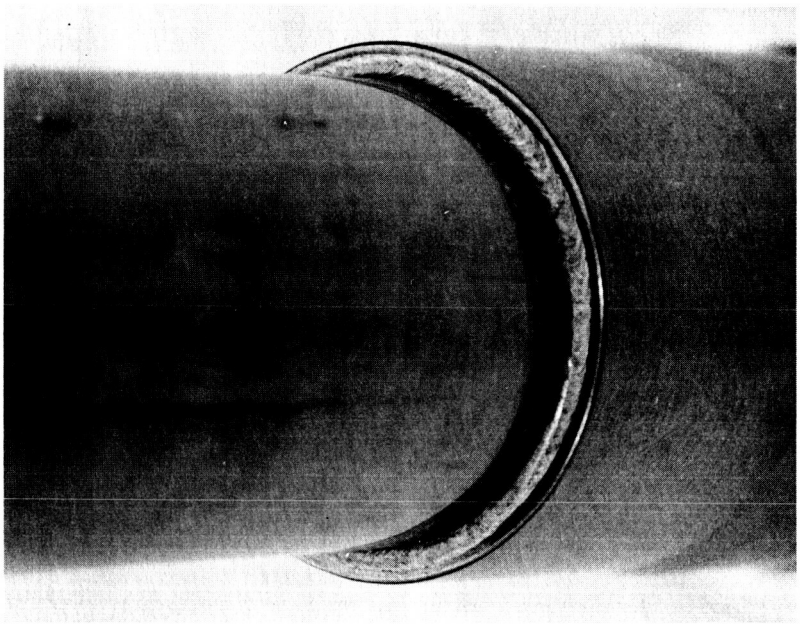

a)

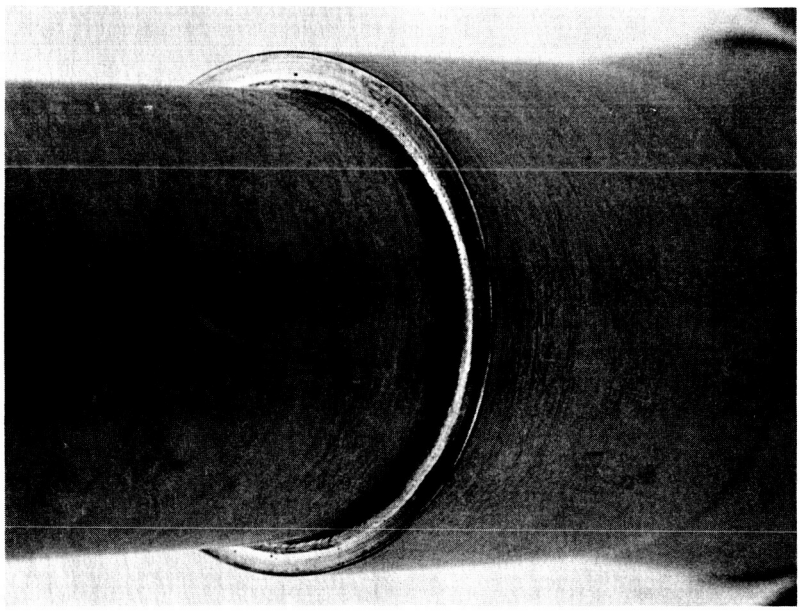

b)

Figure 4.14. Electron Beam Welds on Test Process 1(a) and 3(b).

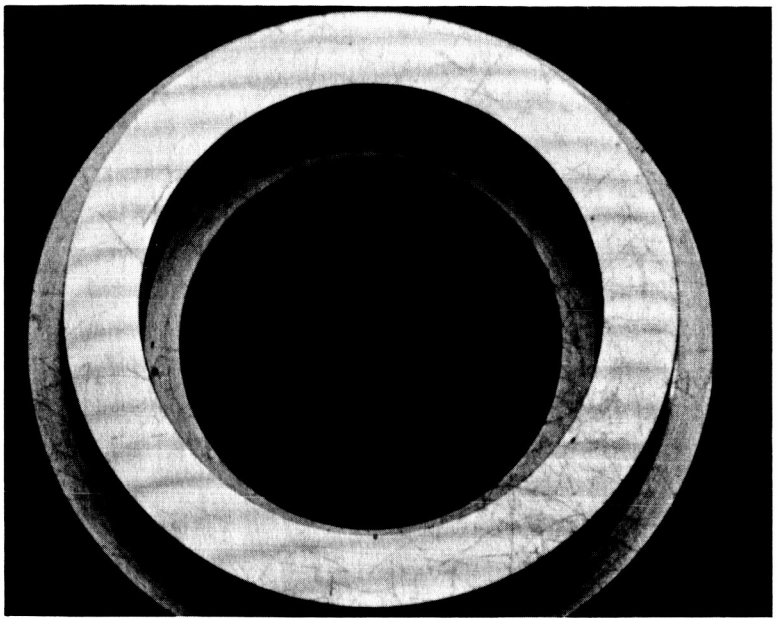

Figure 4.15. Lapmaster Interference Photo of Test Sample 1 Before Electron Beam Weld.

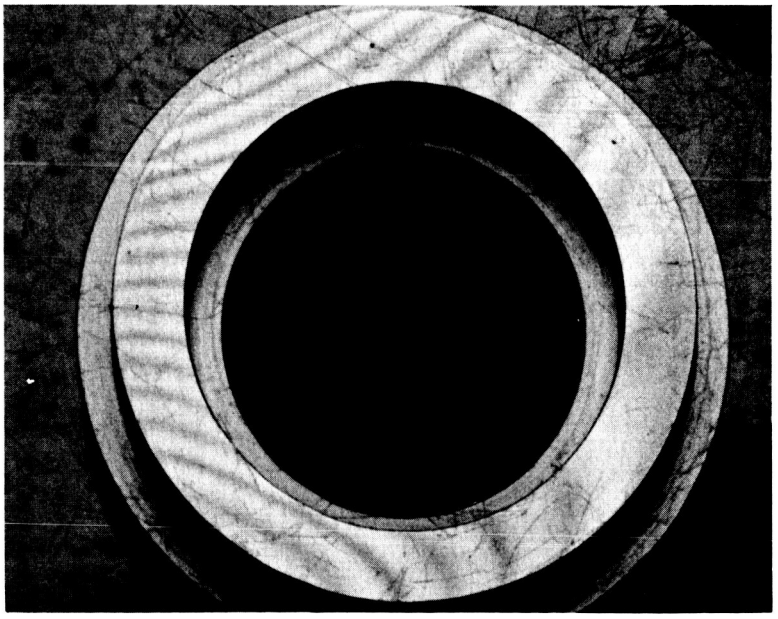

Figure 4.16. Lapmaster Interference Photo of Test Sample 1 After Electron Beam Weld.

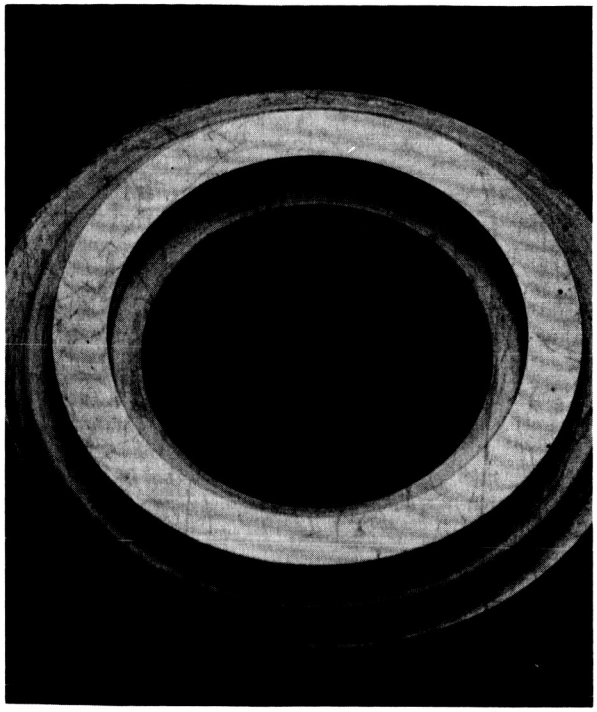

Figure 4.17. Lapmaster Interference Photo of Test Sample 3 Before Electron Beam Weld.

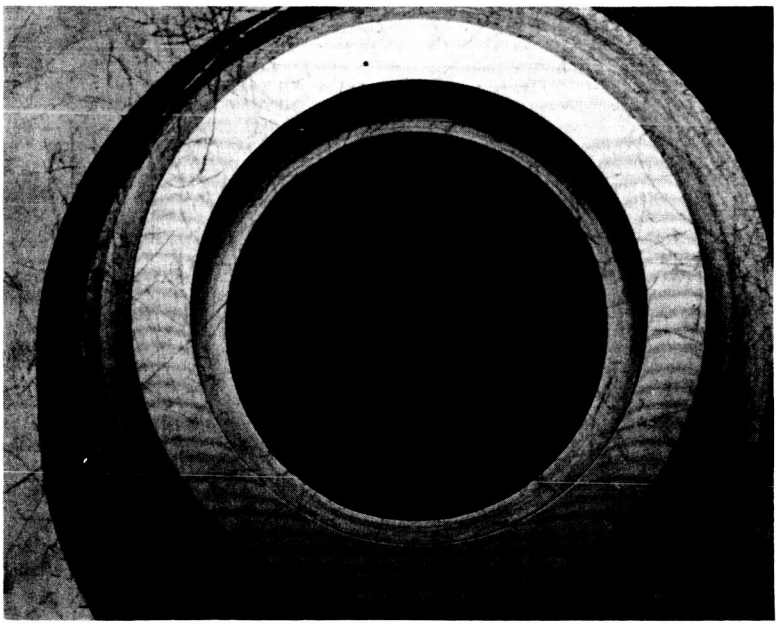

Figure 4.18. Lapmaster Interference Photo of Test Sample 3 After Electron Beam Weld.